Stony Brook University

Two new p53 mutant mouse models display differential gain-of-function effects on tumorigenesis *in vivo*

A Dissertation Presented

by

Walter George Hanel

to

The Graduate School

in Partial Fulfillment of the

Requirements

for the Degree of

Doctor of Philosophy

in

Genetics

Stony Brook University

August 2012

Stony Brook University

The Graduate School

Walter George Hanel

We, the dissertation committee for the above candidate for the

Doctor of Philosophy degree, hereby recommend

acceptance of this dissertation.

Dr. Ute Moll, Professor
Department of Pathology, Dissertation Advisor

Dr. Wei-Xing Zong, Associate Professor
Department of Molecular Genetics and Microbiology
Chairperson of Defense

Dr. Michael Hayman, Professor
Department of Molecular Genetics and Microbiology

Dr. Patrick Hearing, Professor
Department of Molecular Genetics and Microbiology

Dr. Richard Lin, Professor
Department of Medicine and Physiology and Biophysics

This dissertation is accepted by the Graduate School

Charles Taber
Interim Dean of the Graduate School

Abstract of the Dissertation

Two new p53 mutant mouse models display differential gain-of-function effects on tumorigenesis *in vivo*

by

Walter George Hanel

Doctor of Philosophy

in

Genetics

Stony Brook University

2012

p53 is a transcription factor which promotes cell cycle arrest, DNA damage repair, and apoptosis in the presence of DNA damage or oncogenic signaling. It is mutated in more than half of all human cancers demonstrating its clinical significance. Most studies have shown mutation of p53 to be associated with a poor clinical outcome for a broad variety of tumors. Unlike most other tumor suppressors which undergo genomic loss or silencing during tumor progression, p53 undergoes missense mutation within its coding region with retention of expression of the mutated protein in tumors. More importantly, mutant p53 proteins undergo drastic stabilization and accumulate to high levels in neoplastic tissue. These observations led to extensive studies detailing the tumorigenic activities of these mutant proteins in promoting the neoplastic transition and progression of tumors independent of their loss of function of wild type tumor suppressor activity. Study of these gain-of-function (GOF) activities will lead to novel therapeutic interventions for these clinically aggressive neoplasms.

My dissertation studies involved three projects which have each led to important discoveries of mutant p53 GOF. In my first project, phenotyping of two novel mutant p53 knockin mouse models indicates a powerful gain-of-function effect of the specific p53 mutation, R248Q, in the earlier initiation of a wild variety of tumor *in vivo*. In my second project, I identify the presence of enhanced oncogenic signaling in tumors derived from p53 mutant mice as an important gain of function activity. In my third project, I show that mutant p53R248Q results in expansion of the steady state levels of the early stem/progenitor hematopoietic cells, potentially implicating this GOF activity in the increased tumorigenic activity of this p53 mutant. These models add to the growing body of evidence supporting the gain-of-function of p53 mutants and

will serve as useful tools to investigate genotype-phenotype correlations of germline and spontaneous mutant p53 tumors.

Table of contents

List of Figures

List of Abbreviations

TAD: Transcription activation domain

DBD: DNA binding domain

NLS: Nuclear localization sequence

OD: Oligomerization domain

CTD: C-terminal domain

MDM: Mouse double minute

CBP: Core binding protein

L: Loop

APC: Adenomatous Polyposis Coli

ATM: Ataxia Telangiectasia Mutated

MRN: Mre11, Rad51, NBS

NBS: Nijeman Breakage Syndrome

HIF: Hypoxia Inducible Factor

VEGF: Vascular Endothelial Growth Factor

EMT: Epithelial to Mesencymal Transition

MMP: Matrix MetalloProtease

HSC: Hematopoeitic Stem Cell

PTP: Permeability Transition Pore

NMR Nuclear Magnetic Resonance

GOF: Gain-Of-Function

NIN: Nucleotide Instability

MIN: Mismatch instability

CIN: Chromosomal instability

AIN: Amplification instability

SAC: Spindle Assembly Checkpoint

CGH: Comparative Genomic Hybridization

HR: Homologous Recombination

NHEJ: NonHomologous End Joining

CDK1: Cyclin Dependent Kinase 1

ID: Inhibitor of Differentiation

EGFR: Epidermal Growth Factor Receptor

HUPKI: HUmanized P53 KnockIn

ES: Embryonic Stem

Mut: Mutant

MEF: Mouse Embryonic Fibroblast

PI: Propidium Iodide

Q: R248Q

S: G245S

FACS: Fluorescence-Activated Cell Sorting

CD: Cluster of Differentiation

TCR: T-Cell Receptor

PTEN: Phosphatase and Tensin Homolog

LSK: Lin-Sca1+c-Kit+

DN: Double Negative

DP: Double Positive

MSC: Mesencymal Stem Cell

CLP: Common Lymphocyte Progenitor

SCC: Squamous Cell Carcinoma

RAG: Recombination Activation Gene

TORC1: Transducer of Regulation of CREB activity

CREB: cAMP Response Element-Binding

PCR: Polymerase Chain Reaction

MSCV: Mouse Stem Cell Virus

IRES: Internal Ribosome Entry Site

GFP: Green Fluorescent Protein

Acknowledgments

I would like to thank my advisor Dr. Ute Moll for all her guidance and input throughout the course of my Ph.D studies; My committee members Dr. Wei-Xing Zong, Dr. Michael Hayman, Dr. Pat Hearing, and Dr. Richard Lin for their time and support of my Ph.D studies; the Moll lab members, especially Sulan Xu, Dr. Angelina Vaseva, and Dr. Alisha Yallowitz for their contributions to this dissertation and Dr. Oleksi Petrenko for his helpful suggestions; Ingenious Technologies, especially Steve Yu for his work in the generation of the mouse models used in these studies; the SKY/FISH Resource facility a Roswell Park Cancer Institue, especially Leighton Stein for his work and help for SKY cytogenetics, the staff at the Stony Brook Flow Cytometry Laborator, especially Todd, for all their help in acquisition and analysis of FACS data; My family for all their support throughout my Ph.D; My friends, especially Dr. Catherine Salussolia, Dr. Darshan Kothari, and Megan Cosgrove for their help and support; and Genetics Program of Stony Brook University.

Publications

1. **Hanel W**, Xu S, Vaseva AV, Weng W, Yu S, Moll UM. Two novel p53 mutant mouse models display differential effects on spontaneous tumor formation *in vivo*. (in preparation)

2. **Hanel W**, Moll UM. Links between mutant p53 and genomic instability. J Cell Biochem. 2012 Feb;113(2):433-9

3. Onishi RM, Park SJ, **Hanel W**, Ho AW, Maitra A, Gaffen SL. SEF/IL-17R (SEFIR) is not enough: an extended SEFIR domain is required for il-17RA-mediated signal transduction. J Biol Chem. 2010 Oct 22;285(43):32751-9

4. Marchenko ND, **Hanel W**, Li D, Becker K, Reich N, Moll UM. Stress-mediated nuclear stabilization of p53 is regulated by ubiquitination and importin-alpha3 binding. Cell Death Differ. 2010 Feb;17(2):255-67

5. Kramer JM, **Hanel W**, Shen F, Isik N, Malone JP, Maitra A, Sigurdson W, Swart D, Tocker J, Jin T, Gaffen SL. Cutting edge: identification of a pre-ligand assembly domain (PLAD) and ligand binding site in the IL-17 receptor. J Immunol. 2007 Nov 15;179(10):6379-83

6. Maitra A, Shen F, **Hanel W**, Mossman K, Tocker J, Swart D, Gaffen SL. Distinct functional motifs within the IL-17 receptor regulate signal transduction and target gene expression. Proc Natl Acad Sci U S A. 2007 May 1;104(18):7506-11

7. Tanner MJ, **Hanel W**, Gaffen SL, Lin X. CARMA1 coiled-coil domain is involved in the oligomerization and subcellular localization of CARMA1 and is required for T cell receptor-induced NF-kappaB activation. J Biol Chem. 2007 Jun 8;282(23):17141-7

I. Introduction

A. p53 domain architecture

p53 is a transcription factor composed of six distinct domains, each with differing roles in its regulation and function. Starting from the N-terminus and moving towards the C-terminus, these domains are: the transactivation domain (TAD) amino acids (aa) 1-57, the proline rich domain aa 61-92, the DNA binding domain (DBD) aa 102-292, the nuclear localization signal (NLS) domain aa 316-322, the oligomerization domain (OD) aa 323-355, and the C-terminal domain (CTD) aa 356-393.

The TAD is a common element of all transcription factors. The TAD serves to bind to and recruit transcriptional co-activators, such as the p300/CBP complex, to localize them to specific promoter sequences. These transcriptional co-activators in turn recruit the core transcriptional machinery to enhance RNA transcription of downstream sequences. In addition, negative regulators, such as MDM2 and MDM4, can bind to p53's TAD and inhibit transcriptional activity by preventing co-activator recruitment. Not surprisingly, certain mutations in the TAD result in loss of tumor suppressor activity *in vivo* [1, 2]

The proline rich domain plays a role in transcription as well, as cells from mice lacking the polyproline domain are deficient in transcription [3]. p300/CBP was shown to bind to the polyproline domain and directly acetylate p53, enhancing its transcriptional activity [4]. *In vivo*, mice without the polyproline domain were slightly more susceptible to tumor formation, but were much more protected from tumors compared with mice lacking p53, indicating that the polyproline domain is not essential for many of the tumor suppressor activities of p53.

The DBD consists of a well-ordered structure containing two anti-parallel beta sandwiches that have four and five beta strands, respectively [5]. Two loops (L1 and L3) and a

loop-helix-loop motif serve as the interacting surface with DNA, forming contacts at both the minor groove (L3) and major groove (L1 and loop-helix-loop). A core zinc atom binds and coordinates four residues within the two loop regions and is essential for loop stabilization and the overall structure of the DBD. Single point mutations at certain residues within the DBD can result in complete abrogation of all p53 functions. As will be discussed later, this domain contains the vast majority (95%) of p53 mutations found in human cancer.

The NLS domain contains a canonical basic nuclear localization sequence which binds selectively to importin alpha-3, allowing its transport into the nucleus through the nuclear pore complex [6]. Mutating these basic residues leads to loss of nuclear import and transcriptional activity. The OD domain is a dimer of dimers: one helix and a beta sheet organizes with another to form a dimer, which in turn dimerizes with another dimer to form a tetrameric structure [7]. Mutations to eliminate the dimer-dimer interface result in loss of nuclear localization and transcriptional activity. A nuclear export sequence is located within the OD. Oligomerization of p53 serves to shield the nuclear export sequence from the export machinery, trapping p53 in the nucleus when it is in the activated state.

The C-terminus serves as another DNA binding domain, but differs from the DBD in that it binds in a sequence non-specific manner. It is thought to act in a negative auto-regulatory manner by sterically hindering the DBD from DNA binding [8]. Post-translational modifications of multiple types, including ubiquitination, acetylation, and methylation are thought to modulate this inhibition. In addition, two more NLS sequences are located in the extreme C-terminus, although they play less of a role in nuclear export than the NLS domain [9].

B. p53 as a tumor suppressor *in vivo* - a brief historical review

Although presently recognized as a preeminent tumor suppressor, p53 was initially long considered to be an oncogene based on early *in vitro* studies. After the initial discovery of p53 by several independent researchers [10-12], tumor derived p53 gene sequences were used in *in vitro* assays of cellular transformation to classify p53's biological activity as either oncogenic or tumor suppressive [13-15]. These studies indicated that overexpression of p53 with other oncogenes can induce contact independent growth and tumor growth when transplanted into nude mouse hosts. Thus, based on its ability to promote tumor formation in these early assays, p53 was regarded as an oncogene. However, cloning of the p53 allele from normal murine cells indicated that p53 has activities of a tumor suppressor rather than an oncogene [16]. Later studies analyzing genomic DNA isolated from human cancers showed a propensity for point mutations with loss of the opposite p53 locus, definitively establishing its role as a tumor suppressor [17]. It soon became clear that the earlier studies were flawed due to the fact that the cDNA sequences that had been used, which were derived from human tumors, contained mutated versions of the p53 protein, resulting in misinterpretation of the biological activity of the wild type protein.

p53 is now considered to be the most commonly mutated protein in human cancer. Mutations in p53 have been reported in most if not all histological types of cancers. Mutations have typically been associated with later stages of invasive cancer progression. For example, in the traditional model of colon cancer progression, p53 mutation commonly occurs only once tumors acquire invasive capacity and after the mutation of two other genes, APC and k-ras [18]. Like colon cancers, pancreatic carcinomas only contain p53 mutations at a later invasive stage [19]. In the breast, p53 mutations are enriched in larger volume cancers that are at a late clinical

stage by definition, although mutations in *in situ* cancer have been described at a low frequency [20].

In select cases, mutations of p53 have also been known to occur in certain early non-invasive lesions. For example, in colon cancers arising in the context of an inflammatory condition such as ulcerative colitis, p53 mutations can be found in patients in normal non-neoplastic colon cells [21]. In the skin, actinic keratosis, an early lesion which can progress into squamous cell carcinoma, has been shown to contain p53 mutations [22]. Ductal carcinoma-in-situ lesions sometimes possess p53 mutations, although at a low frequency [23]. Thus, p53 mutations have relevance in both pre-cancerous and cancerous cells in a multitude of tissues.

The importance of p53 as a tumor suppressor is underlined by the significantly enhanced cancer susceptibility in patients with a germline mutation in p53. The Li-Fraumeni syndrome is an autosomal dominant disorder characterized by a high incidence and early onset of a variety of tumors due to a germline mutation in one of the two p53 alleles [24]. Sporadic tumors frequently show loss of the second allele [25]. Soft tissue sarcomas, osteosarcomas, brain tumors, breast and adrenal tumors and acute leukemias occur at a much higher incidence than the general population. Some cancers, such as lung cancer and colorectal cancer, have a reduced representation although their incidence is still increased. This syndrome illustrates the drastic consequences which mutation of p53 has in a variety of cell types.

Mice with p53 eliminated in the germline illustrate a pronounced predisposition to tumor formation, verifying its role as a tumor suppressor *in vivo* [26, 27]. The survival and tumor spectrum are quite different in mice with a homozygous loss versus a heterozygous loss, with mostly T-cell lymphomas and sarcomas in homozygous mice and osteosarcomas and carcinomas

in heterozygous mice. Heterozygous mice displayed loss of heterozygosity just like in human tumors. Tissue specific targeting of p53 loss has been used to generate mouse models of many tumor types mimicking many aspects of human disease to a surprising degree [28]. Loss of p53 has also been engineered into the rat germline with a similar tumor spectrum as the mouse but with an exceptionally high rate of metastatic sarcomas, illustrating the importance of p53 in the prevention of metastatic disease [29]. These studies confirmed the importance of p53 as a tumor suppressor in many different tissue types in two different animal species *in vivo.*

C. The molecular biology of the tumor suppressor activities of wild type p53

1. The DNA damage response pathway

Normally in the unstressed cell, p53 is present at very low levels in the cytoplasm. The ubiquitin ligase MDM2 mediates fast turnover of p53 by polyubiquination, followed by proteolysis in the proteasome. Ubiquitination also prevents p53 from undergoing nuclear accumulation by stopping nuclear import and promoting nuclear export [6, 30]. When a DNA double stranded break is created inside a cell, the MRN repair complex, consisting of Mre11, Rad51 and NBS, binds to the free double stranded end of the DNA. This complex recruits the ATM protein to the break, which in turn becomes phosphorylated and activated. ATM then phosphorylates and activates Chk2, and both ATM and Chk2 phosphorylate p53 on multiple sites resulting in its loss of affinity for MDM2. p53 now becomes stabilized and translocates into the nucleus where it carries out its transcriptional effector functions.

p53 binds as a tetramer to two decameric half-sites separated by 0–13 nucleotides (which influence its binding), generically defined by the consensus RRRCWWGYYY (n = 0–13) RRRCWWGYYY (R = purine, C = cytosine, W = any nucleotide, G = guanine, Y = pyridimine). p53 transcribes multiple genes involved in cell cycle arrest, DNA damage repair, and apoptosis, including p21, GADD45, PUMA and NOXA. The phosphorylation sites serine 15 and serine 20, mediated by ATM and Chk2 respectively, increase the DNA binding and transactivation activity of p53 [31, 32]. The extent of DNA damage, presence of other cellular insults, and cellular context determines the final transcriptional outcome of the p53 response and ultimate cellular fate of DNA repair, senescence, or apoptosis. In addition to p53's biological effectors, the

negative regulator MDM2 itself is transcriptionally upregulated by p53 (auto-regulatory feedback loop). MDM2 ubiquinates p53, resulting in its efflux from the nucleus and degradation in the proteasome, effectively shutting off the p53 response.

2. Prevention of Oncogenic signaling

Besides the DNA damage response, p53 also undergoes stabilization by oncogenic stress. For example, high levels of mutant Ras or c-Myc expression potently enhances the stabilization of p53, followed by cell cycle arrest or apoptosis, respectively [33, 34]. High levels of oncogenic stress increase the levels of ARF protein, the main upstream activator of p53. The molecular players of ARF activation remain largely unknown, but are largely independent of the cell cycle regulators E2F1 and E2F2 [35]. ARF sequesters MDM2 into nucleolar sites with concomitant stabilization and activation of p53. High levels of p53 lead to repression of ARF transcription, forming a negative feedback loop [36]. Oncogenic stress also triggers the canonical DNA damage response pathway mediated by ATM and ATR by inducing replicative stress, leading to stalled replication forks that get ‘resolved’ into double strand DNA breaks [37-39]. Thus, parallel pathways converge on p53 to induce a permanent cell cycle response in the face of oncogenic stress.

3. Angiogenesis

Besides cell cycle arrest and apoptosis, additional tumor suppressing transcriptional activities have been described for p53. Angiogenesis is an essential activity necessary to feed an

expanding tumor mass. p53 transcriptional activity produces an environment less permissive for angiogenesis. In particular, p53 transcribes the collagen prolyl hydroxylase gene leading to secretion of the anti-angiogenic factors collagen type 4 and 18 [40]. In addition, p53 mediated upregulation of MDM2 leads to ubiquitination and degradation of HIF-1alpha, a major angiogenic transcription factor important in the upregulation of VEGF [41]. When p53 is lost, this mechanism is inactivated and hypoxia results in VEGF secretion, angiogenesis and tumor growth.

4. Invasion and metastasis

As discussed above, p53 mutation is associated with the transition from non-invasive adenomas to invasive carcinomas in the colon, suggesting that p53 may have a direct role in repressing the invasive behavior of tumor cells. The epithelial to mesenchymal transition (EMT) is a transcriptional program that causes epithelial cells to acquire a motile and invasive phenotype allowing them to travel to distant locations during embryonic development. This program has been implicated in the invasive behavior of carcinomas. The program is mediated by the transcription factors Snail, Slug and Twist by downregulation of the cell adhesion protein E-cadherin and upregulation of motility factors [42]. p53 has been shown to directly interact with Twist to inhibit its transcriptional activity [43]. Also, MDM2 can ubiquinate and degrade Slug to further repress EMT induction [44]. Besides EMT promotion, loss of p53 may also promote extracellular matrix degradation, as p53 has been shown to repress the expression of MMP-1 and MMP-13 [45, 46].

5. Stem cell maintenance

Recently, p53 has been shown to have an important role in stem cell maintenance. The homeostasis of hematopoietic (HSC), neural, and breast stem cells were all shown to be negatively regulated by p53 by limiting self-renewal and favoring quiescence [47-49]. The number of symmetric divisions of each of these stem cell types increases in the absence of p53, resulting in expansion of these stem cell compartments in p53 null mice. The mechanisms behind this function is unclear in neural and breast stem cells. However, in HSCs p53 mediates direct transcription of Gfi-1, a known regulator of HSC maintenance, and of Necdin, a growth suppressor expressed in post-mitotic neurons [47]. Whether these regulators are involved in other stem cell compartments remains to be determined. Stem cells may serve as direct target cells of neoplastic transformation in certain cases. Thus, aberrant expansion of these stem cell compartments may predispose to tumor formation. As breast and brain tumors are prominent tumor types of the Li-Fraumeni syndrome, stem cell compartment expansion mediated by reduced p53 function may be causally involved in this disorder.

6. Transcription-independent apoptosis and necrosis

Transcription independent functions of p53 have also been extensively described by our lab [50]. A fraction of stress-activated stabilized p53 protein translocates to mitochondria and elicits a direct death program by interacting with members of the Bcl family at the outer mitochondrial membrane. Under pro-apoptotic conditions, the ultimate apoptotic effectors Bax and Bak form oligomers and insert into the outer membrane of mitochondria, eliciting release of

cytochrome c leading to caspase activation and apoptosis. The anti-apoptotic family members Bcl2, BclXL and Mcl1 can inactivate Bax and Bak and prevent oligomer formation. p53 can bind to and inactivate both the anti-apoptotic proteins Bcl2 and BclXL and interact with Bax and Bak to promote their oligomer formation.

A novel mechanism has recently been discovered involving p53 and the mitochondrial permeability transition pore (PTP) at the inner mitochondrial membrane. In response to oxidative stress - for example as present in ischemia/reperfusion injury - mitochondrial PT is induced due to high levels of reactive oxygen species (ROS) and calcium which promote sudden opening of the normally closed permeability transition pore (PTP). PTP activation leads to loss of mitochondrial membrane potential, bioenergetic catastrophe due to cessation of ATP production and rupture of mitochondria. This leads to cell necrosis. Cyclophilin D (CypD) in the mitochondrial matrix protects opening of the PT pore and prevents necrosis by this mechanism. Upon oxidative stress and ischemia/reperfusion injury in a stroke model in mice, p53 translocates into the mitochondrial matrix to interact directly with CypD. This interaction promotes opening of the PT pore followed by necrosis induction [51]. Reducing p53 levels in p53+/- mice or using a specific inhibitor of CypD (Cyclosporine A) prevents the destructive p53-CypD complex and is associated with stroke protection [51].

D. Mutations of p53 - origins and structural consequences

Compared with the mutational spectrum of other tumor suppressors, there is an underrepresentation of frameshift and nonsense mutations and a huge overrepresentation of point mutations, representing approximately 75-80% of all p53 mutations [52]. The vast majority of point mutations (95%) fall within the DBD of p53, with the remaining 5% distributed evenly throughout the other domains. In particular, six “hot spot” sites are known to exist, in which most cancer types exhibit a higher frequency of mutation at these codons compared to other codons. Listed in order of highest frequency to lowest frequency, these hot spots are: R248 (9.6%), R273 (8.8%), R175 (6.1%), G245 (6.0%), R249 (5.6%), and R282 (4%).

The structural consequences of p53 mutations in the DBD can vary significantly but have the common effect of loss of DNA binding [53]. All six hot spots are located at or near the DNA contact interface. The R248 (L3) and R273 (loop-helix-loop) form direct contacts with nucleotides in DNA, while R175 (L2), G245 (L3), R249 (L3) and R282 (loop-helix-loop) stabilize the loops responsible for DNA binding. Two classes of mutations have been defined, with R248, R273, and R280 belonging to the “contact” class and most other mutations belonging to the “structural” class [53]. Contact mutations are located at amino acids that directly contact the DNA and typically maintain the overall native structure of the DBD, while structural mutations result in conformational disorder of the DBD [54]. The extent of disorder varies, with R175 mutations being the most disordered due to loss of zinc binding. In general, contact mutations are less sensitive to proteolytic digestion and are found at higher protein levels in cells than structural mutations that tend to expose proteolytic sites [55].

Structural mutants have been shown to bind to a monoclonal antibody (PAb240) directed against an epitope buried inside the beta sheet normally not accessible in the wild type conformation. In addition, structural mutants bind to the hsc70 protein [56], illustrating that disordered p53 may expose new epitopes with physiological relevance. In addition, the disorder of structural mutants may be transmitted to distal parts of the protein outside of the DBD, since a fusion protein consisting of R175H DBD attached to the DNA binding domain of GAL4 was unable to bind to a GAL4 promoter [57]. Recently, it has been shown that ectopic expression of structural mutant proteins results in extensive co-aggregation of p53 with other tumor suppressive transcription factors *in vitro* by exposure of a hydrophobic sequence within amino acids 251-257 not normally exposed in the wild type state [58].

Scanning mutagenesis of the DBD have been undertaken and indicates that most (~90%) of all theoretically possible mutations that result in complete loss of p53 function can be found in a database of p53 mutations in human tumors [59]. However, the frequency spectrum is highly variable among these loss-of-function mutations, as shown by the presence of specific hot spot mutations. The mutational preference can be explained in part by the specific base mutations mediated by carcinogenic agents. One striking example is the extremely high frequency of the 249 mutations in hepatocellular carcinomas, particularly in Asia. This can be explained by the mutagenic properties of metabolites of aflatoxin, a potent carcinogen of the fungus Aspergillus found on grain. These metabolites show a high preference for alkylating the third base of the 249 codon, mediating a G to T transversion. Dietary levels of aflatoxin have shown to correlate with 249 mutations [60]. In the case of lung cancers, a high frequency of G to T transversions are seen at positions 157, 248 and 273, which are commonly mutated sites by the carcinogen benzo(*a*) pyrene in *in vitro* assays [61, 62]. Importantly, these specific transversion mutations are present

at a much higher frequency in lung cancers from smokers, indicating a causative effect of carcinogen on the p53 mutation spectrum.

However, explanation for the frequency spectrum of p53 mutations in most cancers is still lacking. Some proposed that certain mutations are selected for before or during the tumorigenic process because of other activities exhibited by the mutated proteins in addition to their loss of function. These gain-of-function (GOF) activities would confer advantages in the context of tumor formation or progression over other mutations that only exhibit a loss-of-function. However, this theory is not in line with the observation that the frequency distribution of mutations in spontaneous tumors is very similar to that of germline mutations, where tumorigenic selection for mutations is largely absent. It is more likely that mutation preference is more a function of carcinogenic processes mediated by the human environment or tumor microenvironment, similar to the mutation cases discussed above. Carcinogenic screens using a humanized version of the mouse p53 protein are yielding insights into these questions [63]. Further definition of these carcinogenic processes will elucidate more mechanistic information concerning mutation preference.

E. Mutants of p53. The gain-of-function hypothesis

Gain-of-function (GOF) is defined as acquisition of a new function distinct from the function of the wild type protein. Mutant oncogenes are generally considered gain of function proteins while mutant tumor suppressors are considered loss-of-function proteins. As discussed previously, p53 was initially thought to be an oncogene based on early studies using mutant versions of proteins mistakenly thought to be wild type. After analysis of wild type proteins and mutant p53's loss of heterozygosity in tumors, it was rightfully classified as a tumor suppressor. However, studies using cell lines lacking expression of p53 showed that ectopic expression of certain p53 mutants can lead to new oncogenic activities (GOF) in the absence of its dominant negative activity over wild type p53 [64, 65]. Subsequently, many similar studies using ectopic expression in a number of p53 null cell systems supported the notion that certain p53 mutants have GOF properties that may impact tumor progression.

Although provocative, early GOF studies conducted *in vitro* were interpreted with caution since they involved ectopic expression of non-physiological amounts of mutant p53 from heterologous promoters. However, the p53 GOF field then gained significant recognition with the construction of two knockin mouse models with p53 mutations in the germline [66, 67]. These researchers were interested in the impact that two p53 mutations, R172H (a structural mutation) and R270H (a contact mutation), had on spontaneous tumorigenesis compared to the traditional p53 null mouse model. Both groups found an increase in the incidence of a variety of tumors in the mice with p53 point mutations compared to the null mouse. Particularly striking was the rise in carcinoma formation in the point mutant mice, a cancer with very low incidence in the p53 null mouse. Also, metastatic disease was much more prevalent in the R172H/+ and

R270H/+ mice than in the +/- mice, as both osteosarcomas and carcinomas metastasized with a high frequency.

The two p53 mutant KI mice created in Tyler Jacks' lab were engineered with loxP sites flanking an upstream transcriptional stop cassette located between exons 1 and 2. Expression of Cre-recombinase allows removal of the cassette and expression of the p53 mutant. In this manner, mutant p53 expression can be targeted to a particular tissue to study the role of mutant p53 in tumorigenesis within that tissue. Using this strategy, expression of mutant p53 was targeted to breast, pancreas, lung, head & neck, colon and skin epithelium [68-73]. Except for the breast epithelium which utilized the contact mutation R270H, all other studies used the structural mutation R172H to evaluate the GOF of these mutants on carcinoma progression. In the heterozygous state (mutant/+ *vs* -/+), expression of mutant p53 resulted in *earlier onset* of breast, lung, head and neck and skin tumors [68, 70, 71, 73] In the pancreas, R172H/+ resulted in *a higher rate of metastasis* versus -/+ animals [69]. R172H/+ colon tumors underwent much *more frequent invasion* and *transition into carcinomas* compared to -/+ colon tumors [72]. R172H expression in the skin and head & neck had a pronounced impact on tumor initiation relative to no p53 expression [71, 73]. These studies indicate that p53 mutants have a distinct set of activities not present in the p53 null state and that these effects are present in multiple tissues, illustrating the widespread importance of mutant p53 GOF in cancer.

F. Mechanisms of mutp53 GOF

Given mutant p53's pervasive GOF activity in multiple tissues, it is not surprising that many mutant p53 GOF activities have been discovered. Mechanistically, these tumor promoting abilities can be carried out by one of the following three molecular mechanisms that are not mutually exclusive: 1) direct binding and inactivation of cytoplasmic proteins or nuclear transcription factors with tumor suppressor activities; 2) binding and activation of oncogenic proteins; and 3) transcription of proteins with tumor promoting capabilities by binding to their respective canonical transcription factors and modulating their activity. Mutant p53 has been shown to promote genomic instability, apoptosis resistance, angiogenesis, invasion and metastasis, all hallmarks of human tumors [74].

1. Genomic instability

Genomic instability is defined as an increase in the rate of DNA alterations compared to normal cells. Over time, genomic instability is thought to give rise to clonal evolution of tumor cells that harbor advantageous variants and combinations of genes. There are four types of genomic instability (IN): subtle sequence instabilities at the nucleotide (NIN) and mismatch (MIN) level, chromosomal instability (CIN), and amplification instability (AIN) [75]. Wild-type p53 has been implicated either directly or indirectly in suppression of each type of instability. Concerning mutant p53 GOF, most studies have focused on the ability of p53 mutants to promote CIN.

CIN can be divided into aneuploidy (the numerical gain or loss of whole chromosomes)

and structural changes (i.e. translocations and deletions). Mouse models of mammary tumors, pancreatic tumors and squamous cell carcinomas of the skin expressing mutp53R172H all displayed extensive aneuploidy and centrosome amplification, demonstrating the relevance of mechanistic *in vitro* findings [76-78]. Two well known chromosome-numerical checkpoints exist in the cell cycle: the mitotic spindle assembly checkpoint (SAC) in M-phase and the tetraploidy checkpoint at G1/S. Mounting evidence suggests that p53-null cells have disrupted only the tetraploidy G1/S checkpoint, while mutp53 harboring cells have disrupted both the G1/S and M checkpoints. For example, fibroblasts cultured from Li-Fraumeni patients harboring p53 missense mutations including R175H were able to undergo S-phase reentry and polyploidization after disruption of their mitotic spindles by depolymerizing agents, while cells expressing a truncated p53 protein (equivalent to no p53) were blocked from re-entry of S-phase. This suggests that p53 mutant cells can actively disrupt or at least bypass the mitotic checkpoint and exit as tetraploid cells, while p53 null cells get stopped by this checkpoint. The transcriptional activation function of p53 is not required for this mutant GOF behavior [79]. Ectopic expression of mutp53 R172H in p53-null primary mouse mammary epithelial cells resulted in aberrant centrosome amplification, multipolar mitoses, and consequently increased numbers of chromosomes [80]. Interestingly, the p53 R172H mutant protein was found to directly bind to centrosomes potentially causing their dysregulation [81]. Besides this, mutp53 can bind to and inactivate TAp73, a key regulator of SAC [82].

Structural chromosomal changes are also a common finding in mutp53 human cancers. Several studies investigating the genomic complexity of a variety of human primary tumors have generally shown an increase in genomic aberrations present in mutp53 samples versus wild-type p53 samples. Breast tumors with p53 mutations have a higher average number of comparative

genomic hybridization (CGH) alterations compared to p53 wild-type tumors [83, 84]. Soft tissue sarcomas with highly complex, unbalanced karyotypes correlate with mutant p53 status, while the ones with simpler karyotypes typically have a wild-type p53 status [85]. Importantly, Mdm2-amplified mutant p53 osteosarcomas had a lower degree of genomic instability compared to Mdm2-nonamplified osteosarcomas, suggesting that high levels of mutp53 protein are important for maintaining high levels of genomic instability in human cancers [86].

The fidelity of DNA double strand break repair plays a central role in preventing translocations. In response to DNA double strand breaks, cells invoke two distinct repair pathways: high fidelity homologous recombination (HR) and error-prone nonhomologous end joining (NHEJ) [87]. The choice between these pathways involves multiple factors, including the cell-cycle stage, tissue type (somatic vs. germ cells), and the integrity of the two pathways [88, 89]. Mre11 is a DNA binding protein with roles in both HR and NHEJ [90]. Several mutp53 proteins were proposed to bind and sequester Mre11 away from double stranded DNA breaks [91]. Loss of functional Mre11 would be predicted to increase the amount of spontaneous chromosome and chromatid breaks and translocations, which occurs in Mre11 null cells [92]. Abrogation of Mre11 function limits the phosphorylation and activation of ATM, the major double strand break sensor in cells, resulting in bypass of the G2/M DNA damage checkpoint. Loss of this checkpoint with expression of p53 mutants severely reduces the ability for efficient HR, resulting in less conservation of genetic information [91]. Overall, studies suggest that mutant forms of p53 proteins, through interactions which inactivate multiple genome caretaker proteins, lead to inactivation of the residual genome-stabilizing mechanisms that are still present in the absence of wild type p53 function.

2. Resistance to cell death

Deficient repair in the face of increased levels of DNA damage has devastating consequences on the viability of cells, even in the absence of p53 [93, 94]. However, mutp53 cells, instead of being more sensitive, frequently have been found to be as viable and sometimes even more resistant to DNA damage than p53 null cells [95-97]. This apparent paradox is explained by numerous studies detailing the active inhibition of many cell death and checkpoint functions by mutp53. Mutp53 protein associates with the trimeric transcription factor complex NF-Y at promoters of genes involved in cell-cycle regulation [97]. Upon DNA damage, mutp53 recruits the acetyltransferase p300 to NF-Y target genes such as cyclin A, cyclin B2, CDK1 and cdc25 and upregulates their transcription. This abnormal upregulation of cell-cycle promoting genes leads to increased DNA synthesis and proliferation instead of the normal cell-cycle checkpoint response mediated by wild-type p53.

Direct binding and inactivation of TAp63 and TAp73 has surfaced as another GOF activity of mutant p53 proteins [98, 99]. p63 and p73 can transcribe similar DNA stress response and apoptotic genes as wild-type p53 [100-102]. With the p53-independent apoptotic pathways of TAp63 and TAp73 inactivated, the threshold for apoptosis after DNA damage increases further. Accordingly, chemoresistance to apoptosis mediated by mutp53 is correlated with its ability to bind p73 [103-105].

3. Angiogenesis

Angiogenesis is essential for tumor growth. An expanding tumor eventually requires a blood supply as diffusion of oxygen and nutrients will become insufficient to support its further growth. The tumor must undergo an angiogenic “switch” to induce new vasculature necessary

for further tumor growth [106]. The switch occurs when pro-angiogenic factors such as VEGF outnumber anti-angiogenic factors, such as thrombospondin. Importantly, in human tumors, mutant p53 has been shown to correlate with increased expression of VEGF and reduced expression of thrombospondin [107, 108]. Evidence that mutp53 may promote this switch by a GOF mechanism has been elucidated by the finding of a trimolecular transcription complex involving mutp53 with E2F1 and p300 [109]. This complex directly transcribes ID4, which promotes the translation of IL-8 and GROalpha by direct binding to mRNAs encoding these proteins.

4. Invasion and metastasis

As discussed previously, invasion and metastasis was a prominent phenotype of mouse models expressing mutp53 in the germline [66, 67], paving the way for many mechanistic studies to identify the molecular mechanisms behind these observations. Several studies have shed light on the pro-invasive and metastatic properties of mutp53. The first key study demonstrated that mutp53 was able to produce an increase in cell scattering [72]. Cells expressing mutp53 showed enhanced random motility, which was thought to contribute to the invasive nature of mutp53 tumors. Mutp53 was found to bind to the Rab coupling protein, an integrin and EGFR membrane recycling protein, resulting in increased turnover and expression of integrins and EGFR on the membrane. This recycling effect led to enhanced cell motility and oncogenic signaling. A second study showed that mutp53 can inactivate TAp63 in the presence of TGF-beta signaling, resulting in higher metastatic potential since p63 acts as an anti-metastatic transcription factor [110]. Another study also illustrated the importance of inactivation of p63's transcriptional program as

an important part of mutp53 induced migration and metastasis and identified Pin1 as being crucial for this inhibition of p63 [111].

Although the results establishing multiple GOF functions of mutp53 are compelling, the vast majority of results concerning the *in vivo* impact of mutp53 GOF derive from studying only two mouse models with the p53 point mutations R172H and R270H which may not be representative of other p53 point mutations. In my dissertation studies, I used two novel p53 knockin mouse models which each contain a hot spot point mutation within the p53 DBD, as research tools to study whether or not these mutations also exert GOF activities *in vivo*. In my first project, I evaluated the impact of these two point mutations, R248Q and G245S, on spontaneous tumorigenesis. I found that expression of the R248Q mutation in the germline of mice results in *reduced tumor latency and earlier death* compared to complete loss of expression of p53, a phenotype not present in any of the other mutp53 mouse models studied to date. This result correlated nicely with data from human Li-Fraumeni patients and thus suggests that mutp53 GOF may indeed play a role in humans and impact the mutp53 genotype-phenotype correlations in human patients.

In my second project, I evaluated whether expression of the R248Q and G245S mutants in tumors impacts the chromosomal stability and oncogenic signaling pathways compared to tumors without p53 expression. I discovered that tumors expressing either point mutation show enhanced oncogenic signaling. Specifically, out of numerous signaling pathways evaluated, I identified the Akt signaling pathway as being uniquely upregulated by tumors containing p53 mutations. This result may partially explain the enhanced aggressiveness of lymphomas arising in the R248Q mouse model.

In my third project, I performed a detailed analysis of the impact of R248Q and G245S on the development and differentiation of hematopoietic and mesenchymal cells *in vivo*. I show that mutant R248Q results in expansion of both the hematopoietic and mesenchymal stem cell pools, while having little effect on the differentiation of cells downstream of these stem cells.

II. Results

A. Expression of p53 R248Q results in enhanced tumorigenesis in vivo in both mouse and human

Construction of p53HUPKI mutant mice. We wanted to investigate common and novel mutp53 gain-of-function phenotypes *in vivo* with two new p53 mutant mouse models. Since it is unknown whether mouse p53 sequence mutated at the homologous amino acids in human p53 sequence would produce similar structural alterations as in the human protein, we wished to evaluate *human* p53 mutant sequence in the *in vivo* context of the mouse. In support, it is known that other sequences within p53, such as the well-known proline/arginine sequence polymorphism at codon 72 not present in mouse sequence, can influence GOF behavior of p53 mutants [112]. To achieve this, we chose the HUPKI (HUmanized p53 Knock-In) approach [113] in which exons 4-9 of mouse genomic p53 sequence are swapped with human p53 genomic sequences (Figure 1A). This leads to creation of a chimeric p53 protein containing mouse sequences at amino acids 1-32, human at 33-332, and mouse at 333-390 (Fig. 1B). Swapping of only the DBD and poly-proline domain is necessary since complete replacement of human p53 with mouse p53 leads to a high level of interaction of mouse MDM2 with the N-terminal of human p53 [114]. Our humanized allele contains a proline at position 72.

We chose to evaluate R248Q and G245S, two p53 hot spot mutations which have not been characterized yet *in vivo*. Both mutations are located within the L3 loop of p53 [5]. The R248 residue is in direct physical contact with the minor groove of DNA and has been traditionally called a ‘contact’ mutation. Mutations in G245 result in significant disruption of the structure of the L3 DNA binding loop and is thus classified as a ‘structural’ mutation [53]. Each mutation was introduced into a common targeting construct (Fig. 2A) and electroporated into ES

cells. Integration of the construct in ES cells was verified by Southern blot analysis with probes directed against the 5' and 3' ends of the targeting construct and mutations were confirmed by sequencing of genomic DNA (Fig.2B and data not shown). The neomycin resistance cassette was effectively removed by transfection of the flp recombinase into ES cells. Chimeric mice were mated to wild type mice and offspring from these crosses were genotyped to confirm germline transmission of each mutation.

Primary cells from R248Q/- and G245S/- mice show complete loss of wild type p53 activity. We wanted to study the functional impact of both endogenous p53 point mutations in primary cells. To this end, we isolated MEFs from p53 +/+, -/-, R248Q/- (Q/-) and G245S/- (S/-) mice to investigate the impact that these p53 mutations had on p53 protein levels, DNA damage response and growth properties in MEFs (Fig. 3). An antibody directed against a peptide surrounding serine 20 (1C12) which is present as mouse sequence in both the wild type (wt) and HUPKI configurations was used to allow for comparison of levels between the mouse wtp53 and mut HUPKI proteins. Consistent with previous findings [26, 67, 91, 115], both mutations led to accumulation of p53 protein in cultured MEFs (Fig. 3A), with the two mutations displaying similar levels of mutant protein in culture. There is a slight upward shift in mobility of the HUPKI proteins, most likely due to their slightly higher molecular weight of the chimeric protein. Treatment with the DNA damage agent Doxorubicin increased these high mutant levels even further (Fig. 3A). As expected, despite activation in response to DNA damage, neither mutant was transcriptionally active, as both mutants had low levels of p21 mRNA and protein at baseline and upon DNA damage (Fig. 3A).

We also tested for differences in proliferation of MEFs upon expression of mutp53 protein. Replicative senescence is a process by which cells undergo an irreversible cell cycle arrest after undergoing a set amount of cell doublings. Loss of p53 results in bypass of this process and immortalization. We found that, like p53 null MEFs, both Q/- and S/- MEF populations were immortal and their growth rates were comparable with null MEFs, while wild type cells underwent senescence after two weeks in culture (Fig. 3B).

To test the apoptotic response of cells containing the point mutants, we irradiated thymoctyes from 4 week old p53 +/+, -/-, Q/- and S/- mice and assessed their apoptosis as a function of time using Annexin V staining and Parp cleavage. As shown in Fig. 4C, wild type and both mutants displayed similar kinetics and levels of upregulation of mutp53 protein upon irradiation. Where +/+ thymocytes displayed a high degree of apoptosis and cleaved caspase upon irradiation over the course of 24 hours, -/-, Q/- and S/- all showed significant resistance (Fig. 4A, C). In agreement with the MEF data, Q/- and S/- showed a complete lack of upregulation of p21 and PUMA at both the transcriptional and protein levels (Fig. 4B, C). Overall, these results indicate that cells containing both p53 mutants show a complete loss of wild type p53 activity in several *in vitro* assays of p53 function.

R248Q mice display more rapid onset of tumors compared to p53 null mice. To study the gain of function effects of these two mutations in vivo, we bred six different cohorts of mice and compared their survival, tumor spectrum, and tumor latency. The breeding scheme to obtain these cohorts is shown in Fig. 5. We evaluated each mutation in both the heterogygous (mutant/-) or homozygous (mutant/mutant) configuration, since it was recently shown that a homozygous

vs heterozygous configuration may impact tumor spectrum, at least with the R270H allele [116]. Although it was already previously shown that wtHUPKI can act as a fully functional tumor suppressor *in vivo*[115], we also bred a homozygous wtHUPKI control cohort to confirm wtHUPKI's ability to act as a tumor suppressor under our experimental conditions.

Expression of the R248Q allele resulted in a sharp reduction in survival compared to the null allele (Fig. 6A). Gene dosage did not have any effect on further exacerbating this phenotype, as both R248Q homozygous and heterozygous mice had similar survival and tumor latencies (Fig. 6A). The survival difference in mice expressing the R248Q mutation was due to an accelerated onset of all tumors compared to null mice (Fig. 6B). There was a slight broadening of the histological tumor spectrum within our R248Q groups, with mutant mice showing more diverse sarcoma subtypes and carcinomas compared to null mice (Fig. 7A, 8, 9). With regard to solid tumors, only two animals, one in the Q/- and one in the -/- groups, died with metastatic sarcoma to the lungs (Fig. 9 bottom). Thus, mutant R248Q has a gain-of- function (GOF) effect of decreasing the latency of spontaneous tumor onset compared to p53 null mice. Interestingly, this phenotype of decreased survival has not been previously reported in the existing germline mutp53 knock-in models [66, 67, 91, 115], illustrating a unique GOF role for the p53R248Q mutation.

Mice expressing mutp53 G245S show no difference in spontaneous tumor formation compared to null mice. In contrast to the R248Q allele, the G245S allele did not display statistically significant differences with regard to survival, tumor latency, or tumor spectrum compared to null mice (Figs. 7B, 9, 10). There were slightly more carcinoma formation in

G245S mice (Fig. 7B). Beyond 230 days, there was a trend towards extension in survival of G245S mice compared to nulls, most likely due to a potential reduction in B-lymphoma frequency within G245S mice (Fig. 4B). Thus, although the hot spot mutations R248Q and G245S display a similar loss of wt p53 function in *in vitro* assays (Figs. 3, 4), they display strong phenotypic differences *in vivo* with regard to tumor latency.

Consistent with the mouse models, persons with germline mutations in R248Q display earlier onset tumor formation compared to null and G245S mutations. Individuals with p53 germline mutations are prone to the Li-Fraumeni syndrome, a familial cancer pre-disposition syndrome characterized by multiple sporadic tumors developing at an early age [24]. It is becoming increasingly clear that the specific type of germline p53 mutation plays a critical role in determining time of onset of tumor formation, with the presence of missense mutations in Ex 4-9 accelerating the onset of first tumor formation [117, 118].

To validate the findings of our mouse model, we wanted to evaluate whether or not genotype-phenotype differences exists in human persons with p53 mutations at codons 248, codon 245, and complete loss of p53 with regards to earlier tumor onset. To this end, we used the latest p53 IARC database, version R15, which contains an extensive collection of clinical information regarding tumor onset in carriers of p53 germ line mutations [119]. Patients with large deletions, nonsense, and frameshift mutations eliminating the DNA-binding domain were considered ‘null’ in this analysis. Indeed, mutations in human codon 248 led to a trend towards earlier onset of first tumor presentation compared to patients with null or codon 245 germline mutations (Fig. 11A), with R248 compared to null approaching statistical significance (Fig. 11A

right). In addition, the total number of tumors reported was also higher within the codon 248 group (Fig. 11B). In contrast, null and codon 245 mutations were similar with regard to first tumor onset and total number of tumors.

Taken together, these data indicate that: 1) mutant p53 R248Q predisposes to earlier tumor formation compared to G245S and loss of p53; 2) all tumor types (T-lymphoma, B-lymphoma, and solid tumors) were effected by R248Q's GOF activity; 3) gene dosage of the mutation did not have any impact on phenotype, as both heterozygous mut/- and homozygous mut/mut dispayed essentially the same phenotype; and, 4) human Li-Fraumeni populations display a similar genotype-phenotype correlation, as persons having R248Q/+ in their germline show an earlier onset of tumor formation compared to G245S/+ or -/+ persons, establishing the relevance of our model to human populations.

B. Tumors expressing p53 mutants display enhanced oncogenic signaling through the Akt signaling pathway.

R248Q and null T-lymphomas display similar surface phenotype. We next compared tumors between mutant and null mice to gain a better understanding for the basis of the GOF phenotype exhibited by mutant p53. We focused on T-lymphomas since they represent the most frequent tumor type present within this model. We investigated the surface phenotypes of T-cell lymphomas from each mouse genotype to study the cell of origin of the T-cell lymphomas. Each T-lymphoma from each genotype consisted of either CD4+CD8+ or a mix of CD4+CD8+ and CD8+ cells with surface expression of both CD3 and TCRbeta (Fig. 12A and data not shown),

indicating a differentiation state after TCR recombination but prior to negative selection. Most B-lymphomas were of a CD19+B220^{low} surface phenotype, with no clear distinction between null and mutant groups (Fig. 12B). Thus, we could not identify differences in the cell or origin of null and R248Q lymphomas based on surface phenotype analysis.

Chromosomes from R248Q and null T-lymphomas display similar qualitative and quantitative characteristics. Chromosomal instability at the level of aneuploidy brought on by the loss of mitotic checkpoint proteins such as Bub1 and Cdc20 can result in drastic acceleration of tumorigenesis in p53 null mice with tumors containing extensive aneuploidy [120]. Similarly, deficiency of double stranded DNA breakage repair proteins such as ATM and H2AX result in accelerated tumorigenesis in p53 null mice with tumors containing many clonal translocations [121, 122] As discussed previously, many studies have shown that expression of certain p53 mutants may enhance the genomic instability of cells primarily at the level of CIN, primarily by inactivating the chromosome segregation and double stranded DNA damage checkpoints [123]. Thus, we wanted to determine whether CIN was enhanced in R248Q mutant tumors by comparing the cytogenetics of tumors expressing mutp53R248Q and no p53.

To this end, we analyzed the cytogenetics from two null, two Q/-, and one Q/Q early passage T-lymphoma lines (Figs. 13, 14). As shown in Figure 14A, the aneuploidy profile between the lymphomas appeared similar, with frequent gains in chromosomes 1, 4, 5, 6, 11, 14, and 15, with no frequent losses of any chromosomes. Each lymphoma had at least one clonal chromosomal translocation present in the majority of cells, with both nulls and one Q/- lymphoma having two clonal translocations (Fig. 14B), indicated that chromosomal instability at

the level of both aneuploidy and translocations may be an important driver of tumorigenesis in these mouse models. However, we could not establish an enhanced amount of CIN in mutp53R248Q T-lymphomas since tumors arising from null and R248Q mice were qualitatively similar.

R248Q T-lymphomas show enhanced proliferation and signaling through the Akt pathway *in vivo* compared to null T-lymphomas. Next, we looked at the proliferation and apoptotic rates of T-cell lymphomas *in vivo*. Figure 15 shows that Q/- lymphomas had a two fold increase in the number of proliferating cells *in vivo,* as indicated by phospho-H3 staining of tumors, as compared to null or S/- lymphomas. In contrast, the rate of apoptosis *in vivo* was not significantly different between the three genotypes, overall illustrating that proliferation was probably a contributing factor to the earlier presentation of Q/- lymphomas.

To get an idea for the reason behind enhanced proliferation of Q/- lymphomas, we evaluated a number of signaling pathways involved in the cell cycle deregulation and malignant progression of lymphoma cells, including Notch1, Akt, c-Myc, and Aurora Kinase A. Importantly, these four key effectors have been implicated in the progression of mouse or human mutant p53 tumors *in vivo* [72, 116, 124]. As shown in Figure 16A, c-myc, cleaved Notch1, and p-Akt were increased in lymphomas of both genotypes compared to pre-malignant thymocytes. Importantly, dramatically increased phosphorylation of Akt was present in Q/- lymphomas compared to -/- lymphomas. In addition, the downstream target S6 displayed increased levels of phosphorylation, confirming that mutant Q/- lymphomas have enhanced signaling through the Akt pathway. Although loss of PTEN was observed in two Q/- lymphomas and one -/-

lymphoma, this result could not explain the widespread effect of Akt activation in Q/- lymphomas. We also seen high p-Akt levels in S/- T-lymphomas comparable to Q/- T-lymphomas (Fig. 16B). This gain-of-function mechanism is relevant to human tumors, since p-Akt have been shown to have a strong association with mutant p53 IHC in human tumors [72]. These results suggest that signaling through the p-Akt pathway is a common GOF in mutant p53 lymphomas arising in this model and may be a contributing factor to the earlier presentation of Q/- lymphomas.

Cell lines derived from Q/- mice develop into highly aggressive leukemias when injected into mice in vivo. We established cell lines from null and Q/- T-lymphomas and compared their growth rates and apoptosis. All three Q/- cell lines showed faster growth rates compared to the two null lines (Figure 17A), consistent with the enhanced proliferation *in vivo*. Upon serum deprivation, the apoptosis of null cell lines was higher than that of mutant lines (Figure 17B). Importantly, two cell lines derived from Q/- T-lymphomas produced more aggressive leukemias than null cell lines when injected into the circulation of nude mice, producing very rapid colonization of bone marrow, liver, and kidneys (Fig. 18).

We investigated whether mutp53 R248Q could induce the GOF effects directly by expression in p53 null lymphoma cells. Retroviral ectopic expression of the HUPKI R248Q, but not G245S, protein in null cell lines could enhance growth rate of p53 null T-lymphoma cells (Fig. 19A) identifying a direct role for the R248Q protein in the GOF of growth of T-cell lymphomas. We further confirmed this result by competition assays (Fig. 19B), as null lymphomas ectopically expressing R248Q were able to effectively outcompete the original non-

infected null lymphoma cells over time, while vector infected null cells was unable to do so. These results also agree with a previous study in a p53 null *human* T-ALL line where ectopic expression of R248Q was capable of enhancing their growth [125].

We next looked at signaling through the Akt pathway in our tissue culture system. We were unable to see significant differences in Akt signaling between null and mutant Q/- T-lymphomas in tissue culture and after injection into nude mice (Fig. 20). This result suggests that mutant p53 inducded Akt signaling is most likely not a cell intrinsic process and relies on external cues from the tumor microenvironment to mediate this signaling.

Overall, these results indicate that: 1) there was no evidence of an increase in CIN in mutp53R248Q T-lymphomas compared to null T-lymphomas based on karyotype analysis; 2) both R248Q and G245S T-lymphomas display enhanced Akt signaling which may largely depend on the primary tumor microenvironment; and, 3) R248Q can directly produce an increase in growth in p53 null cells in the context of T-cell lymphomas.

C. Expression of R248Q expands hematopoetic and mesenchymal stem cell populations with normal T-cell, B-cell, and mesenchymal cell differentiaton.

Perturbation in pre-tumor cell populations and their differentiation can have drastic consequences on their potential for neoplastic transformation, especially in the absence of a functional p53 pathway [126]. To date, a detailed study analyzing the impact of mutant p53 on pre-tumor hematopoetic, lymphocyte, and mesenchymal cell populations has not been conducted. We wished to determine whether or not mutp53 induced a perturbation of T-cell, B cell, or mesenchymal cell subpopulations in 4-5 week old mice, and if so, what the consequences

of this perturbation are on accelerated tumorigenesis. As shown previously [47], there was an increase in the number of Lin-Sca1+c-kit+(LSK) progenitor cells upon loss of wild type p53 (Fig. 21B). Importantly, this population was further expanded in mice expressing R248Q, showing a statistically significant difference between both null and wild type mice. There was a slight trend towards an increase in LSK cells in the G245S mice as well, but it was not statistically significant. T cell and B-cell differentiation was not altered to a significant extent in either p53 mutant mouse (Fig. 21B and Fig. 22). There was a slight but not statistically significant decrease in the DN4 subset of thymocyte differentiation when comparing R248Q thymocytes to the other two subsets.

MSCs have been suggested to be the cell of origin of a diverse range of histological subtypes of sarcomas in both mouse and humans [127]. Since R248Q mice are predisposed to earlier onset of sarcomas in this model, we also derived the mesenchymal stem cell population from the bone marrow of +/+, -/-, and Q/- mice. Consistent with the findings of the LSK cells, we found a similar expansion of MSCs in the presence of mutp53R248Q (Fig. 23A). Surface marker analysis of both -/- and Q/- MSC populations shown expression of CD44, CD29, and Sca1 and lack of CD45 and CD11b, consistent with a MSC surface phenotype (Fig. 23B). -/- and Q/- populations were capable of differentiating into adipocytes and osteoblasts indicating no perturbation in the differentiation of these cells by the expression of R248Q (Fig. 24). Overall, these results show that R248Q expands early LSK progenitor cells and MSCs in the bone marrow but has no significant effects on later stages of T cell, B cell, or mesenchymal development, at least among the cell populations analyzed in this study.

When the stability of mutant p53 R172H protein is enhanced in mouse pre-tumor cells by loss of Mdm2, a marked decrease in survival and earlier onset of tumor formation is seen [128].

We wanted to know if any normal populations of cells shown enhanced stabilization of mutp53, suggesting a higher likelihood of GOF effects in these specific cell populations. As shown in Fig. 25, no staining of p53 was seen in any of the normal tissues analyzed from +/+, Q/-, and S/- mice, indicating a lack of mutp53 stabilization. This was in contrast to the extensive mutp53 stabilization seen in all tumor types present in p53 mutant animals. We also looked at the expression of R248Q in individual cell populations by FACS analysis. In support of our IHC findings, we were not able to detect large amounts of p53 in normal lymphocyte populations from Q/- mice, while p53 was readily detectable in a Q/- T-lymphoma cell line (Fig. 26). Thus, like the R172H protein, neither the R248Q nor the G245S proteins show stabilization in *normal tissues*. This excludes that generalized aberrant stabilization in normal tissues is a determinant for earlier tumor formation in the R248Q model.

The results from our developmental studies suggest that mutp53 R248Q exhibits a GOF in LSK cells. The importance of perturbation of hematopoietic stem cells in the tumorigenesis of mature lymphoid populations has recently been recognized [129]. We wished to evaluate whether or not mutp53 R248Q GOF effects in the LSK cell population plays a role in the accelerated onset of spontaneous T and B-cell lymphomas arising in R248Q mice. To determine this, a mouse model is required in which expression of mutp53 R248Q occurs within the LSK cell population and mutp53 R248Q is removed in differentiating T and B cells. This can be achieved with a combination of two mouse models, which will be discussed below.

Recently, our lab has created a floxed R248Q mouse model in which loxP sites flank exons 2 and 10 of p53, a similar design to the wild type p53 floxed mouse model (Fig. 27A) [28]. Upon expression of Cre, R248Q is effectively deleted from cells, resulting in loss of expression of mutant p53R248Q protein from cells (Fig. 27B). A second mouse model, the CD2-Cre

model, expresses Cre under the regulation of the CD2 locus control region. CD2 begins expression at the level of the common lymphocyte progenitor (CLP) [130], which gives rise to both T and B cells. Crossing of our floxed R248Q mice with the CD2-Cre model results in mice with loss of mutp53 R248Q in all T and B cell populations and retention in their LSK population (Fig. 28). Thus, GOF effects in normal T and B cell populations and tumors arising from these populations can be experimentally eliminated and the GOF effects in the LSK population that contribute to T and B cell lymphomas can be selectively evaluated.

To summarize the key findings of my dissertation study, my results strongly support the notion that different p53 mutant alleles have differential impacts on the onset and progression of spontaneous tumors in both mouse and human. In particular, expression of the R248Q mutant results in more rapid tumor formation compared to null and G245S mice. p53 R248Q GOF effects may play an important role in the earlier onset of tumor formation in Li-Fraumeni patients carrying germline R248Q mutations. On the other hand, both R248Q and G245S were capable of enhancing Akt signaling, at least in primary tumors. We define the first GOF in normal cells, in that R248Q was capable of expanding normal LSK and MSCs *in vivo.* We are currently investigating whether or not a GOF effect in the LSK stem cell population plays a role in the *in vivo* lymphoma formation within this model using Cre-lox technology.

III. Discussion

p53 mutants display genotype-phenotype differences in spontaneous tumorigenesis.

In my dissertation study, I showed that expression of humanized mutant p53R248Q protein in the mouse germline results in earlier tumor onset and decreased survival compared with mice containing a p53 deletion or mutp53G245S. All tumor types in the p53R248Q model have an earlier onset compared to null and G245S mice, showing the widespread and strong gain of function of this particular mutation. We anticipate that the Li-Fraumeni syndrome model R248Q/+ mice will also exhibit a decrease in survival compared to +/- mice. Human Li-Fraumeni persons with mutations in the codon 248 also showed earlier onset of tumors (approaching statistical significance) compared to p53 deletion or mutation in codon 245, illustrating the relevance of mutp53 GOF in *human* tumorigenesis. During tumor progression in Li-Fraumeni patients, the remaining p53 wild type allele is lost in the majority of cases, further indicating that GOF mechanisms may be relevant in the pathogenesis of cancers arising in this population [25]. Moreover, our mouse model suggests that GOF mechanisms may account for some of the genotype-phenotype differences between R248 patients and other mutations.

Interestingly, the strong *in vivo* GOF of R248Q contrasts with the previously reported weaker *in vivo* GOF of R248W which caused a broader tumor spectrum but did not cause shorter latency or accelerated death [91]. This is despite the fact that in both KI models, the two different codon 248 mutations were expressed from the identical genetic context (p53 HUPKI). An attractive explanation for these biological differences is that different structural consequences of these two 248 mutations may lead to differential functions that affect their GOF properties. A recent biochemical study demonstrated that structural distortion mediated by certain p53

mutations including R248Q results in co-aggregation of mutant p53 proteins with other tumor suppressor transcription factors, such as p63 and p73 [58]. Of note, R248W was not able to co-aggregate [58]. In agreement, ectopic expression of R248Q but not R248W showed enhanced invasion in H1299 xenografts *in vivo* [131], confirming allele- specific differences in GOF properties.

No evidence of enhanced CIN in R248Q T-lymphomas.

Previous studies have shown that extensive structural and numerical chromosomal abnormalities are present in carcinomas of mice containing tissue-specific K-rasG12D and mutp53 R172H [73, 78]. Skin squamous cell carcinomas (SCCs) expressing R172H show a higher rate of chromosomal gains and deletions compared to SCCs lacking p53 [132]. Importantly, genomic instability was an important step in cancer progression, as late stage tumors expressing R172H have high rates of c-myc and K-rasG12D amplifications. In our study, we addressed whether or not GOF-mediated genomic instability was important in tumor progression by comparing T-lymphomas between null and R248Q mice at the karyotype level. This analysis showed no differences in the aneuploidy profile or number of translocations between null and R248Q T-lymphomas. In past studies, T-lymphomas arising in p53 null mice have been reported to contain aneuploidy with infrequent translocations [122, 133]. This is in contrast to our study, in which the two p53 null T-lymphomas each contained two clonal translocations. A previous study conducted in our lab has also illustrated frequent translocations present in p53 null T-lymphomas, illustrating that structural abnormalities are actually a common event in p53 null T-lymphomas arising under our experimental conditions [134]. In this study,

the number of tumor samples analyzed was small, so it is possible that differences would have been revealed by a larger sample size. In addition, finer mapping of genomic gains and losses by array CGH analysis may have also yielded genomic differences between p53 genotypes, as were seen in SCCs expressing R172H compared to null SCCs.

The homozygous R248Q lymphoma had a translocation involving chrom 12 which contains the IgH locus, possibly implicating RAG-mediated recombination in the pathogenesis of this lymphoma, although this would have to be confirmed by a finer mapping of this translocation. R248Q mice showed a slight decrease in the progression to the DN4 stage of thymocyte development, a stage that requires appropriate RAG recombination. However, in our study aberrant TCR recombination was a rare event in pre-tumor thymocytes derived from null and R248Q/- mice, as assessed by inappropriate TCRbeta to TCRgamma junctions (data not shown), in contrast to a previous study in which thymoctes isolated from 78% of R248W mice had inappropriate TCR junctions [91]. Thus, overall, aberrant RAG recombination is most likely not an important general contributing factor to earlier onset of T-cell lymphomas in R248Q mice.

Mutp53 tumors display enhanced Akt signaling in primary T-lymphomas.

Both R248Q and G245S p53 mutant tumors exhibited higher levels of p-Akt signaling *in vivo*, consistent with studies found in human tumors [72]. We could not see enhanced p-Akt signaling *in vitro* in cell lines derived from tumors or when these cell lines were later propagated again as allografts, indicating either that: 1) tumor cell extrinsic factors in the tumor microenvironment are responsible for this signaling, which is lost upon removal of tumor cells from this environment; or, 2) forced adaptation into tissue culture produces conditions which

result in loss of p-Akt signaling. Direct propagation of primary tumor cells into a secondary mouse host with assessment of the p-Akt signaling pathway would distinguish between these two possibilities.

The mechanism of enhanced Akt signaling is unknown at the present time, but reduced levels of PTEN by gene loss or downregulation is unlikely the generic principle, since PTEN was retained in most tumors with high levels of p-Akt. Mutant p53 has been shown to sensitize cells to growth factors by increasing the recycling of growth factor receptors such as EGFR and integrins to the cell surface [72]. Further work would be needed to identify if receptor recycling is playing a role in this model by identifying higher levels of surface expression of growth factor receptors of mutant p53 primary lymphoma cells.

Although p-Akt was elevated in G245S/- to comparable levels as R248Q/- lymphomas, we did not observe a difference in T-lymphoma latency or proliferation rate in this group of lymphomas to null mice. These results suggest that the mutant p53 G245S may still have retention of certain p53 tumor suppressor functions and this may counteract the GOF effect of increased p-Akt. Of note, both groups of G245S mice did have a trend towards reduced B-lymphoma and increased survival but did not reach statistical significance, possibly due to insufficient mouse numbers to detect these differences. Analysis of growth and DNA damage induced transcription of p53 growth arrest and apoptosis targets shown no difference between -/- and G245S/- MEFs and thymocytes. A recent study has suggested that p53 has tumor suppressor functions that can be dissociated from its ability to induce a transcriptional response [135]. In particular, ablation of three acetylation sites in p53 that resulted in loss of DNA damage induced transcriptional responses was still capable of producing a partially functional tumor suppressor by retention of other functions related to metabolic function and antioxidant regulation. In

addition, as discussed previously, our lab has recently demonstrated a novel function of p53 in the opening of the mitochondrial PTP pore, an activity unrelated to its transcriptional ability. It is possible that certain p53 mutants like G245S retain these wild type activities along with GOF activities, giving a proliferation phenotype in the T-lymphomas closer to null T-lymphoma cells. In any event, eliminating the downstream growth promoting effects of p-Akt signaling in either mutant p53R248Q or G245S lymphoma cells would be predicted to have a beneficial impact on survival by limiting the growth of mutant lymphomas to a greater extent compared to null lymphomas. To test this hypothesis, we are currently in the process of treating each mouse genotype with rapamycin, an inhibitor of the TORC1 complex which is responsible for phosphorylating p-S6K which in turn phosphorylates the ribosomal protein S6 to promote translation and growth. These experiments will establish the importance of elevated p-Akt signaling in mutant p53 tumors and suggest a novel treatment strategy for mutant p53 cancers in general.

p53 R248Q expands early stem cell populations with no effect on differentiation.

Expression of R248Q led to marked expansion of the hematopoietic LSK progenitor and mesenchymal stem cell niches. Studies evaluating wild type p53 in stem cell niches has led to important insights in its regulation of survival and self-renewal in hematopoietic, neural, and breast epithelium [48, 49, 115] Extensive studies concerning mutant p53's effects on early stem cell compartments have not been conducted to date. In ES cells, mutant p53 expression in these cells has been shown to lead to significant dominant negative activity in the +/mutant configuration [136, 137]. The importance of perturbation of early progenitor populations in the

tumorigenesis of downstream differentiated cell populations is becoming increasingly recognized [129]. We are currently investigating whether this is the case for mutant p53 expression in this mouse model. In particular, given mutant p53's known role of inducing higher levels of genomic instability [123], p53 mutants may allow more rapid acquisition of oncogenic lesions in early progenitor cells, allowing rapid transformation of differentiated cells harboring these lesions and a significantly decreased tumor latency of many cell types, as seen in the R248Q expressing mice.

In conclusion, this dissertation provides strong support for the gain-of-function hypothesis of the R248Q mutation in spontaneous tumor formation and both R248Q and G245S in enhanced oncogenic signaling. The future experiments outlined above will allow elucidation of the importance of p-Akt signaling and GOF effects present in the LSK cell population to the contribution of lymphomagenesis in this model. These experiments as well as further characterization of these mice will shed light on mechanistic explanations for genotype-phenotype correlations seen in people with Li-Fraumeni syndrome, as well as uncover important insights in GOF mechanisms in spontaneous tumors expressing p53 mutations.

IV. Material and Methods

Ethics Statement. All research involving animals has been conducted according to national and international guidelines with respect to husbandry, experimentation and welfare as part of this project. All animal studies were approved by the Institutional Animal Care and Use Committee at Stony Brook University.

Mice. Targeted iTL BA1 (C57BL/6 x 129/SvEv) hybrid embryonic stem cells were microinjected into C57BL/6 blastocysts. Resulting chimeras with a high percentage agouti coat color were mated to wild-type C57BL/6 mice to generate F1 heterozygous offspring. Tail DNA was genotyped to confirm germline transmission. For tumorigenesis studies, mice were initially crossed with p53-/- mice [26] to generate heterozygous R248Q/- mice which were then interbred to obtain -/-, R248Q/-, and R248Q/R248Q mice. A similar approach was used for the G245S mutation. -/- mice from both breeding strategies had overlapping survivals and tumor spectrum and were combined for all analyses. All mice were of a mixed 129Sv/C57BL6 background. Mice were monitored regularly and euthanized upon becoming moribund. Tumors and major organs were collected, fixed in 10% formalin, embedded in paraffin and sectioned at 4 um tissue sections for histopathologic analysis. Cell suspensions were prepared from lymphoma samples as described below for FACS analysis and identified using T-cell, B-cell, or myeloid surface markers [138, 139].

MEFs and thymocyte treatments. MEFs were isolated from 12.5 day old embryos. Briefly, embryos were dissected out of gravid mice and placed in 10 cm dishes and washed in PBS. The

head and liver were removed and the embryo was finely minced with a scalpel. 0.025% trypsin was added for 15 minutes at 37 degrees. Embryo fragments were collected and spun down to remove trypsin and plated in DMEM + 10% FBS. After one day, cell were trypsinized, run through a 40 um cell strainer and used for studies. For DNA damage studies, cells were treated with 250 nM of doxorubicin for 24 hours. For 3T3 assays, cells were plated at a density of 5.0 X 10^5 cells/ 10 cm dish. Cells were trypsinized every three days, enumerated, and the number of cell generations was determined by the equation (# of cells) = (5.0 X 10^5 cells X 2^n) where n is the number of cell generations. For irradiation experiments, thymi were isolated from 4 week old mice, resuspended in red blood cell lysis buffer (8.26g NH4Cl, 1g KHCO3, 0.037g EDTA in 1L H20), filtered through a 40um filter and resuspended in lymphoma media (225 mL DMEM, 225 IMDM, 10mL 200mM L-glutamine, 5 mL Pen/Strep, 500 ul 55mM Beta-Mercaptoethanol). Thymocytes were seeded at 1 million cells/mL and gamma-irradiated at a dose of 5 Grays. Cells were collected at indicated time points and assessed for viability by staining for Annexin V (Roche) and PI (Sigma) using the manufacturers protocol by staining 2 X 10^5 cells in 150 ul with 7.5 ul of Annexin V antibody and 15 ul of 50 ug/mL stock PI . RNA was prepared with the RNeasy kit (Qiagen) with on column DNA digestion, reverse transcribed using Superscript II (Invitrogen) according to the manufacturers protocol, and cDNA was used in Quantitative PCR reactions using the SYBR green kit (Qiagen). A listing of the primers is shown in Fig. 29. Relative expression of the target genes was calculated using the ΔΔCT method.

Hematopoetic Development Experiments. Thymi, spleen, and bone marrow cells were isolated and suspended in red blood cell lysis buffer and filtered through a 40um filter. Cells were suspended in incubation buffer (PBS, 1% BSA) and 2 X 10^6 cells were stained for the indicated

surface markers (Figure 30) at a volume of 1 mL using 0.5 ul of each of the indicated antibodies. For intracellular stainings for p53, cells were stained for surface markers as above but followed by resuspension in FACS lyse (BD Biosciences) for 15 minutes, washed two times, resuspended in incubation buffer and stained for p53 (IC12, Cell Signaling). Cells were then washed two times with incubation buffer, resuspended and analyzed by gating on forward and side scatter properties and then gated for the indicated flurophores in figure 30.

Mesenchymal Stem Cell Isolation and Differentiation. MSCs were isolated in a similar manner as hematopoietic cells but without red blood cell lysis. A portion of the bone marrow suspension was removed and resuspended in red blood cell lysis buffer to determine the amount of nucleated cells. 1 X 10^6 nucleated cells were plated per well in 6 well plates in mesencymal stem cell media (R&D). Media was exchanged after 4 hours of plating and then every 12 hours. Two weeks later, plates were fixed with 10 % formalin and stained with Giemsa to enumerate colonies. Colonies were also trysinized briefly (2 minutes with 0.5 % trypsin) and plated in 10 cm dishes. After three days, cells were trypsinzed and expanded into three plates. For FACS stainings, cells were treated with accutase (Sigma) for 5 minutes and resuspended in incubation buffer, followed by staining with CD45-FITC, CD11b-PE, Sca1-FITC, CD44-PE, or CD29-PE. For differentiation into adipocytes and osteocytes, cells were plated at subconfluency into 6 well dishes. When confluent, MSC media was replaced with adipocyte or osteocyte differentiation media (Stem Cell Technologies) or left in MSC media for undifferentiated cells, with media replacement every three days. After 2 weeks, cells were fixed in 10% formalin. For Oil Red O staining, cells were incubated in 60% isopropanol for 5 min at RT. Cells were dried, and then incubated in Oil Red O working solution (2:3 mixture of filtered distilled water:Oil Red O stock

(0.35g Oil Red O in 100mL isopropanol)) with shaking. Cells were then washed four times for 5 minutes and imaged with the microscope. For Alizarin Red S stainings, cells were washed with dH_2O and incubated in 40 mM Alizarin Red S (pH 4.1) for 20 minutes with shaking. Cells were then washed four times for 5 minutes and imaged with the microscope.

T-lymphoma cell lines. Cell lines were prepared by culturing suspension from T-cell lymphomas into lymphoma media. NIH 3T3 cells were used as feeders for the first 2 passages, after which lymphoma cells were removed from feeders and used for assays. For SKY analysis, passage 3-5 cells from two -/-, two R248Q/-, and R248Q/R248Q were frozen in FBS + 10% DMSO and shipped to Roswell Park Cancer Institute. Briefly, cells were incubated in colcemid at 0.045 ug/mL for 2 hours, collected and resuspended in cancer hypotonic solution (3.0 g KCl, 4.8 g HEPES, 0.2 g EGTA, 0.36 g NaOH in 1 L H_2O). Nuclei were incubated in 10 mL of CHS at 37 degrees for 45 minutes. One mL of fixing solution (1:3 solution of glacial acetic acid to methanol) was then added, nuclei were spun down and washed in fixing solution, and spun down and resuspended again in fixing solution. SKY was performed on chromosomes using earlier protocols [140].

Immunohistochemistry and Western blots. For immunohistochemical staining, 4 um paraffin sections were cut onto slides. Slides were deparaffinized. For antigen retrieval, slides were cooked in citrate buffer (10mM, pH 6.0) for 20 minutes, left for 10 minutes, followed by two rinses in water. 3% H_2O_2 was added for 10 minutes, followed by two rinses in water. Slides were then blocked in 1% goat serum for 1 hour, followed by staining with anti-histone H3 (phosphor S28)(Cell signaling), anti-p53(FL393) (Santa Cruz), or p-Akt (XP-Cell Signaling) at a 1:100

dilution in 1% goat serum. The following day, slides were washed two times with PBS and 2 drops of biotinylated secondary antibody were added and incubated for 20 minutes. Slides were washed two more times and 2 drops of enzyme conjugate were added per slide for 15 minutes, washed with PBS+tween20 twice and with PBS twice. DAB was added for 5 minutes, put into water, counterstained with hematoxylin for 5 minutes and mounted for viewing. For TUNEL staining, the in Situ cell Death and Detection kit (ROCHE) was used according to the manufacturer's instructions. Slides were initially prepared as they were for IHC, but after 3% H_2O_2 addition, slides were permeabilized in 0.1% Trition X-100 in sodium citrate buffer for 10 minutes at 37 degrees. Slides were then blocked in goat serum 2% for 1 hour, and incubated O/N with enzyme solution: labeling solution. Sections were washed the following day with PBS, and 2 drops of POD were added for 3 minutes. Slides were washed three times and DAB (Invitrogen) was applied for 2 minutes, washed, counterstained with hematoxylin, mounted and viewed as described above.

Western blotting. Protein lysates were prepared by suspending pelleted cells in lysis buffer (2.5 mL 1 M Tris pH 7.5, 7.5 mL 5 M NaCl, 0.5 mL 0.5 M EDTA, 2.5 mL Triton X-100, 2.5 mL glycerol, 0.1 % SDS in 250 mL of water). 40 ug of protein were loaded onto 10 % polyacrylamide gels and Western blots were carried out using standard protocol. Antibodies used are as follows: IC12 for p53 (Cell Signaling), p21 (BD Pharmingen), ERK1/2 (Millipore), PUMA (Cell Signaling), Cleaved Casp (Cell Signaling), c-Myc (Santa Cruz), cleaved Notch (Cell Signaling), Aurora A, p-Akt (Cell Signaling), Akt (Cell Signaling), p-S6K (Cell Signaling), p-S6 (Cell Signaling), PTEN (Cell Signaling). Each antibody was used at a 1:1000 dilution.

Cloning and retroviral infection. HUPKI R248Q and G245S p53 cDNAs were prepared from mRNA derived from MEFs of R248Q/- and G245S/- embryos. The open reading frame was PCR amplified with primers complementary to the 5' (CTCTCGAATTCATGACTGCCATGGAGGA GTCACAGTCGG) and 3' (TGGGCGGCCGCTCAGTCTGAGTCAGGCCCCACTTT) ends of the mouse p53 gene with flanking EcoR1(5') and Not1(3') restriction sites (underlined). PCR products were subcloned into the pBluescript vector, sequenced confirmed, and subcloned into the REBNA-puro and MSCV-IRES-GFP vectors [141]. For retroviral infection, plasmids were transfected into Phoenix E packaging cells. 24-48 hours later, supernatants were collected. Lymphoma cells were suspended in virus media and spinoculated for 45 minutes at 1,000 rpms. This process was repeated 3 times at 4 hour intervals. Two days later, cells were selected in puromycin for 2 days. For infections with MSCV-IRES-GFP, cells were FACS sorted for GFP selection 2 days after infection.

Statistics. For survival analysis, p-values were determined by log-rank analysis. P-values for tables in Fig. 6C and 10C was determined by two-tailed student's t-test. P-values in the table in Fig. 11A were determined by ranked sum test. All other statistical tests were performed by two-tailed student's t-test.

References

1. Gaidarenko, O. and Y. Xu, *Transcription activity is required for p53-dependent tumor suppression.* Oncogene, 2009. **28**(49): p. 4397-401.

2. Brady, C.A., et al., *Distinct p53 transcriptional programs dictate acute DNA-damage responses and tumor suppression.* Cell, 2011. **145**(4): p. 571-83.

3. Toledo, F., et al., *A mouse p53 mutant lacking the proline-rich domain rescues Mdm4 deficiency and provides insight into the Mdm2-Mdm4-p53 regulatory network.* Cancer Cell, 2006. **9**(4): p. 273-85.

4. Dornan, D., et al., *The proline repeat domain of p53 binds directly to the transcriptional coactivator p300 and allosterically controls DNA-dependent acetylation of p53.* Mol Cell Biol, 2003. **23**(23): p. 8846-61.

5. Cho, Y., et al., *Crystal structure of a p53 tumor suppressor-DNA complex: understanding tumorigenic mutations.* Science, 1994. **265**(5170): p. 346-55.

6. Marchenko, N.D., et al., *Stress-mediated nuclear stabilization of p53 is regulated by ubiquitination and importin-alpha3 binding.* Cell Death Differ, 2010. **17**(2): p. 255-67.

7. Clore, G.M., et al., *High-resolution structure of the oligomerization domain of p53 by multidimensional NMR.* Science, 1994. **265**(5170): p. 386-91.

8. Ayed, A., et al., *Latent and active p53 are identical in conformation.* Nat Struct Biol, 2001. **8**(9): p. 756-60.

9. Shaulsky, G., et al., *Nuclear accumulation of p53 protein is mediated by several nuclear localization signals and plays a role in tumorigenesis.* Mol Cell Biol, 1990. **10**(12): p. 6565-77.

10. Lane, D.P. and L.V. Crawford, *T antigen is bound to a host protein in SV40-transformed cells.* Nature, 1979. **278**(5701): p. 261-3.

11. Linzer, D.I. and A.J. Levine, *Characterization of a 54K dalton cellular SV40 tumor antigen present in SV40-transformed cells and uninfected embryonal carcinoma cells.* Cell, 1979. **17**(1): p. 43-52.

12. Crawford, L., *The 53,000-dalton cellular protein and its role in transformation.* Int Rev Exp Pathol, 1983. **25**: p. 1-50.

13. Eliyahu, D., et al., *Participation of p53 cellular tumour antigen in transformation of normal embryonic cells.* Nature, 1984. **312**(5995): p. 646-9.

14. Jenkins, J.R., K. Rudge, and G.A. Currie, *Cellular immortalization by a cDNA clone encoding the transformation-associated phosphoprotein p53.* Nature, 1984. **312**(5995): p. 651-4.

15. Parada, L.F., et al., *Cooperation between gene encoding p53 tumour antigen and ras in cellular transformation.* Nature, 1984. **312**(5995): p. 649-51.

16. Finlay, C.A., P.W. Hinds, and A.J. Levine, *The p53 proto-oncogene can act as a suppressor of transformation.* Cell, 1989. **57**(7): p. 1083-93.

17. Baker, S.J., et al., *Chromosome 17 deletions and p53 gene mutations in colorectal carcinomas.* Science, 1989. **244**(4901): p. 217-21.

18. Fearon, E.R. and B. Vogelstein, *A genetic model for colorectal tumorigenesis.* Cell, 1990. **61**(5): p. 759-67.

19. Hruban, R.H., et al., *Progression model for pancreatic cancer.* Clin Cancer Res, 2000. **6**(8): p. 2969-72.

20. Olivier, M., et al., *The clinical value of somatic TP53 gene mutations in 1,794 patients with breast cancer.* Clin Cancer Res, 2006. **12**(4): p. 1157-67.

21. Hussain, S.P., et al., *Increased p53 mutation load in noncancerous colon tissue from ulcerative colitis: a cancer-prone chronic inflammatory disease.* Cancer Res, 2000. **60**(13): p. 3333-7.

22. Ortonne, J.P., *From actinic keratosis to squamous cell carcinoma.* Br J Dermatol, 2002. **146 Suppl 61**: p. 20-3.

23. Aubele, M., M. Werner, and H. Hofler, *Genetic alterations in presumptive precursor lesions of breast carcinomas.* Anal Cell Pathol, 2002. **24**(2-3): p. 69-76.

24. Kleihues, P., et al., *Tumors associated with p53 germline mutations: a synopsis of 91 families.* Am J Pathol, 1997. **150**(1): p. 1-13.

25. Trkova, M., et al., *A Li-Fraumeni syndrome family with retained heterozygosity for a germline TP53 mutation in two tumors.* Cancer Genet Cytogenet, 2003. **145**(1): p. 60-4.

26. Jacks, T., et al., *Tumor spectrum analysis in p53-mutant mice.* Curr Biol, 1994. **4**(1): p. 1-7.

27. Donehower, L.A., et al., *Mice deficient for p53 are developmentally normal but susceptible to spontaneous tumours.* Nature, 1992. **356**(6366): p. 215-21.

28. Jonkers, J., et al., *Synergistic tumor suppressor activity of BRCA2 and p53 in a conditional mouse model for breast cancer.* Nat Genet, 2001. **29**(4): p. 418-25.

29. van Boxtel, R., et al., *Homozygous and heterozygous p53 knockout rats develop metastasizing sarcomas with high frequency.* Am J Pathol, 2011. **179**(4): p. 1616-22.

30. Lohrum, M.A., et al., *C-terminal ubiquitination of p53 contributes to nuclear export.* Mol Cell Biol, 2001. **21**(24): p. 8521-32.

31. Dumaz, N. and D.W. Meek, *Serine15 phosphorylation stimulates p53 transactivation but does not directly influence interaction with HDM2.* EMBO J, 1999. **18**(24): p. 7002-10.

32. Jabbur, J.R., P. Huang, and W. Zhang, *DNA damage-induced phosphorylation of p53 at serine 20 correlates with p21 and Mdm-2 induction in vivo.* Oncogene, 2000. **19**(54): p. 6203-8.

33. Serrano, M., et al., *Oncogenic ras provokes premature cell senescence associated with accumulation of p53 and p16INK4a.* Cell, 1997. **88**(5): p. 593-602.

34. Hermeking, H. and D. Eick, *Mediation of c-Myc-induced apoptosis by p53.* Science, 1994. **265**(5181): p. 2091-3.

35. Palmero, I., et al., *Activation of ARF by oncogenic stress in mouse fibroblasts is independent of E2F1 and E2F2.* Oncogene, 2002. **21**(19): p. 2939-47.

36. Zeng, Y., et al., *p53 binds to and is required for the repression of Arf tumor suppressor by HDAC and polycomb.* Cancer Res, 2011. **71**(7): p. 2781-92.

37. Di Micco, R., et al., *Oncogene-induced senescence is a DNA damage response triggered by DNA hyper-replication.* Nature, 2006. **444**(7119): p. 638-42.

38. Bartkova, J., et al., *Oncogene-induced senescence is part of the tumorigenesis barrier imposed by DNA damage checkpoints.* Nature, 2006. **444**(7119): p. 633-7.

39. Mallette, F.A., M.F. Gaumont-Leclerc, and G. Ferbeyre, *The DNA damage signaling pathway is a critical mediator of oncogene-induced senescence.* Genes Dev, 2007. **21**(1): p. 43-8.

40. Teodoro, J.G., et al., *p53-mediated inhibition of angiogenesis through up-regulation of a collagen prolyl hydroxylase.* Science, 2006. **313**(5789): p. 968-71.

41. Ravi, R., et al., *Regulation of tumor angiogenesis by p53-induced degradation of hypoxia-inducible factor 1alpha.* Genes Dev, 2000. **14**(1): p. 34-44.

42. Bolos, V., et al., *The transcription factor Slug represses E-cadherin expression and induces epithelial to mesenchymal transitions: a comparison with Snail and E47 repressors.* J Cell Sci, 2003. **116**(Pt 3): p. 499-511.

43. Shiota, M., et al., *Twist and p53 reciprocally regulate target genes via direct interaction.* Oncogene, 2008. **27**(42): p. 5543-53.

44. Wang, S.P., et al., *p53 controls cancer cell invasion by inducing the MDM2-mediated degradation of Slug.* Nat Cell Biol, 2009. **11**(6): p. 694-704.

45. Sun, Y., et al., *p53 down-regulates human matrix metalloproteinase-1 (Collagenase-1) gene expression.* J Biol Chem, 1999. **274**(17): p. 11535-40.

46. Ala-aho, R., et al., *Adenoviral delivery of p53 gene suppresses expression of collagenase-3 (MMP-13) in squamous carcinoma cells.* Oncogene, 2002. **21**(8): p. 1187-95.

47. Liu, Y., et al., *p53 regulates hematopoietic stem cell quiescence.* Cell Stem Cell, 2009. **4**(1): p. 37-48.

48. Cicalese, A., et al., *The tumor suppressor p53 regulates polarity of self-renewing divisions in mammary stem cells.* Cell, 2009. **138**(6): p. 1083-95.

49. Meletis, K., et al., *p53 suppresses the self-renewal of adult neural stem cells.* Development, 2006. **133**(2): p. 363-9.

50. Vaseva, A.V. and U.M. Moll, *The mitochondrial p53 pathway.* Biochim Biophys Acta, 2009. **1787**(5): p. 414-20.

51. Vaseva, A.V., et al., *p53 Opens the Mitochondrial Permeability Transition Pore to Trigger Necrosis.* Cell, 2012. **149**(7): p. 1536-48.

52. Hollstein, M., et al., *p53 mutations in human cancers.* Science, 1991. **253**(5015): p. 49-53.

53. Bullock, A.N. and A.R. Fersht, *Rescuing the function of mutant p53.* Nat Rev Cancer, 2001. **1**(1): p. 68-76.

54. Wong, K.B., et al., *Hot-spot mutants of p53 core domain evince characteristic local structural changes.* Proc Natl Acad Sci U S A, 1999. **96**(15): p. 8438-42.

55. Bargonetti, J., et al., *A proteolytic fragment from the central region of p53 has marked sequence-specific DNA-binding activity when generated from wild-type but not from oncogenic mutant p53 protein.* Genes Dev, 1993. **7**(12B): p. 2565-74.

56. Finlay, C.A., et al., *Activating mutations for transformation by p53 produce a gene product that forms an hsc70-p53 complex with an altered half-life.* Mol Cell Biol, 1988. **8**(2): p. 531-9.

57. Raycroft, L., et al., *Analysis of p53 mutants for transcriptional activity.* Mol Cell Biol, 1991. **11**(12): p. 6067-74.

58. Xu, J., et al., *Gain of function of mutant p53 by coaggregation with multiple tumor suppressors.* Nat Chem Biol, 2011. **7**(5): p. 285-95.

59. Kato, S., et al., *Understanding the function-structure and function-mutation relationships of p53 tumor suppressor protein by high-resolution missense mutation analysis.* Proc Natl Acad Sci U S A, 2003. **100**(14): p. 8424-9.

60. Yang, M., et al., *Mutations at codon 249 of p53 gene in human hepatocellular carcinomas from Tongan, China.* Mutat Res, 1997. **381**(1): p. 25-9.

61. Greenblatt, M.S., et al., *Mutations in the p53 tumor suppressor gene: clues to cancer etiology and molecular pathogenesis.* Cancer Res, 1994. **54**(18): p. 4855-78.

62. Hernandez-Boussard, T.M. and P. Hainaut, *A specific spectrum of p53 mutations in lung cancer from smokers: review of mutations compiled in the IARC p53 database.* Environ Health Perspect, 1998. **106**(7): p. 385-91.

63. Besaratinia, A. and G.P. Pfeifer, *Applications of the human p53 knock-in (Hupki) mouse model for human carcinogen testing.* FASEB J, 2010. **24**(8): p. 2612-9.

64. Shaulsky, G., N. Goldfinger, and V. Rotter, *Alterations in tumor development in vivo mediated by expression of wild type or mutant p53 proteins.* Cancer Res, 1991. **51**(19): p. 5232-7.

65. Dittmer, D., et al., *Gain of function mutations in p53.* Nat Genet, 1993. **4**(1): p. 42-6.

66. Olive, K.P., et al., *Mutant p53 gain of function in two mouse models of Li-Fraumeni syndrome.* Cell, 2004. **119**(6): p. 847-60.

67. Lang, G.A., et al., *Gain of function of a p53 hot spot mutation in a mouse model of Li-Fraumeni syndrome.* Cell, 2004. **119**(6): p. 861-72.

68. Wijnhoven, S.W., et al., *Mice expressing a mammary gland-specific R270H mutation in the p53 tumor suppressor gene mimic human breast cancer development.* Cancer Res, 2005. **65**(18): p. 8166-73.

69. Morton, J.P., et al., *Mutant p53 drives metastasis and overcomes growth arrest/senescence in pancreatic cancer.* Proc Natl Acad Sci U S A, 2010. **107**(1): p. 246-51.

70. Jackson, E.L., et al., *The differential effects of mutant p53 alleles on advanced murine lung cancer.* Cancer Res, 2005. **65**(22): p. 10280-8.

71. Acin, S., et al., *Gain-of-function mutant p53 but not p53 deletion promotes head and neck cancer progression in response to oncogenic K-ras.* J Pathol, 2011. **225**(4): p. 479-89.

72. Muller, P.A., et al., *Mutant p53 drives invasion by promoting integrin recycling.* Cell, 2009. **139**(7): p. 1327-41.

73. Caulin, C., et al., *An inducible mouse model for skin cancer reveals distinct roles for gain- and loss-of-function p53 mutations.* J Clin Invest, 2007. **117**(7): p. 1893-901.

74. Hanahan, D. and R.A. Weinberg, *Hallmarks of cancer: the next generation.* Cell, 2011. **144**(5): p. 646-74.

75. Lengauer, C., K.W. Kinzler, and B. Vogelstein, *Genetic instabilities in human cancers.* Nature, 1998. **396**(6712): p. 643-9.

76. Li, B., et al., *A transgenic mouse model for mammary carcinogenesis.* Oncogene, 1998. **16**(8): p. 997-1007.

77. Wang, X.J., et al., *Analysis of centrosome abnormalities and angiogenesis in epidermal-targeted p53172H mutant and p53-knockout mice after chemical carcinogenesis: evidence for a gain of function.* Mol Carcinog, 1998. **23**(3): p. 185-92.

78. Hingorani, S.R., et al., *Trp53R172H and KrasG12D cooperate to promote chromosomal instability and widely metastatic pancreatic ductal adenocarcinoma in mice.* Cancer Cell, 2005. **7**(5): p. 469-83.

79. Gualberto, A., et al., *An oncogenic form of p53 confers a dominant, gain-of-function phenotype that disrupts spindle checkpoint control.* Proc Natl Acad Sci U S A, 1998. **95**(9): p. 5166-71.

80. Murphy, K.L., A.P. Dennis, and J.M. Rosen, *A gain of function p53 mutant promotes both genomic instability and cell survival in a novel p53-null mammary epithelial cell model.* FASEB J, 2000. **14**(14): p. 2291-302.

81. Tarapore, P., et al., *Difference in the centrosome duplication regulatory activity among p53 'hot spot' mutants: potential role of Ser 315 phosphorylation-dependent centrosome binding of p53.* Oncogene, 2001. **20**(47): p. 6851-63.

82. Tomasini, R., et al., *TAp73 knockout shows genomic instability with infertility and tumor suppressor functions.* Genes Dev, 2008. **22**(19): p. 2677-91.

83. Jain, A.N., et al., *Quantitative analysis of chromosomal CGH in human breast tumors associates copy number abnormalities with p53 status and patient survival.* Proc Natl Acad Sci U S A, 2001. **98**(14): p. 7952-7.

84. Jong, Y.J., et al., *Chromosomal comparative genomic hybridization abnormalities in early- and late-onset human breast cancers: correlation with disease progression and TP53 mutations.* Cancer Genet Cytogenet, 2004. **148**(1): p. 55-65.

85. Borden, E.C., et al., *Soft tissue sarcomas of adults: state of the translational science.* Clin Cancer Res, 2003. **9**(6): p. 1941-56.

86. Overholtzer, M., et al., *The presence of p53 mutations in human osteosarcomas correlates with high levels of genomic instability.* Proc Natl Acad Sci U S A, 2003. **100**(20): p. 11547-52.

87. Jackson, S.P., *Sensing and repairing DNA double-strand breaks.* Carcinogenesis, 2002. **23**(5): p. 687-96.

88. Takata, M., et al., *Homologous recombination and non-homologous end-joining pathways of DNA double-strand break repair have overlapping roles in the maintenance of chromosomal integrity in vertebrate cells.* EMBO J, 1998. **17**(18): p. 5497-508.

89. Essers, J., et al., *Homologous and non-homologous recombination differentially affect DNA damage repair in mice.* EMBO J, 2000. **19**(7): p. 1703-10.

90. Zha, S., C. Boboila, and F.W. Alt, *Mre11: roles in DNA repair beyond homologous recombination.* Nat Struct Mol Biol, 2009. **16**(8): p. 798-800.

91. Song, H., M. Hollstein, and Y. Xu, *p53 gain-of-function cancer mutants induce genetic instability by inactivating ATM.* Nat Cell Biol, 2007. **9**(5): p. 573-80.

92. Buis, J., et al., *Mre11 nuclease activity has essential roles in DNA repair and genomic stability distinct from ATM activation.* Cell, 2008. **135**(1): p. 85-96.

93. Fedier, A., et al., *Loss of atm sensitises p53-deficient cells to topoisomerase poisons and antimetabolites.* Ann Oncol, 2003. **14**(6): p. 938-45.

94. Tutt, A., et al., *Cell cycle and genetic background dependence of the effect of loss of BRCA2 on ionizing radiation sensitivity.* Oncogene, 2003. **22**(19): p. 2926-31.

95. Blandino, G., A.J. Levine, and M. Oren, *Mutant p53 gain of function: differential effects of different p53 mutants on resistance of cultured cells to chemotherapy.* Oncogene, 1999. **18**(2): p. 477-85.

96. Bossi, G., et al., *Mutant p53 gain of function: reduction of tumor malignancy of human cancer cell lines through abrogation of mutant p53 expression.* Oncogene, 2006. **25**(2): p. 304-9.

97. Di Agostino, S., et al., *Gain of function of mutant p53: the mutant p53/NF-Y protein complex reveals an aberrant transcriptional mechanism of cell cycle regulation.* Cancer Cell, 2006. **10**(3): p. 191-202.

98. Li, Y. and C. Prives, *Are interactions with p63 and p73 involved in mutant p53 gain of oncogenic function?* Oncogene, 2007. **26**(15): p. 2220-5.

99. Rufini, A., et al., *p73 in Cancer.* Genes Cancer, 2011. **2**(4): p. 491-502.

100. Kaghad, M., et al., *Monoallelically expressed gene related to p53 at 1p36, a region frequently deleted in neuroblastoma and other human cancers.* Cell, 1997. **90**(4): p. 809-19.

101. Wu, G., et al., *DeltaNp63alpha and TAp63alpha regulate transcription of genes with distinct biological functions in cancer and development.* Cancer Res, 2003. **63**(10): p. 2351-7.

102. Lokshin, M., T. Tanaka, and C. Prives, *Transcriptional regulation by p53 and p73.* Cold Spring Harb Symp Quant Biol, 2005. **70**: p. 121-8.

103. Bergamaschi, D., et al., *p53 polymorphism influences response in cancer chemotherapy via modulation of p73-dependent apoptosis.* Cancer Cell, 2003. **3**(4): p. 387-402.

104. Irwin, M.S., et al., *Chemosensitivity linked to p73 function.* Cancer Cell, 2003. **3**(4): p. 403-10.

105. Schilling, T., et al., *Interference with the p53 family network contributes to the gain of oncogenic function of mutant p53 in hepatocellular carcinoma.* Biochem Biophys Res Commun, 2010. **394**(3): p. 817-23.

106. Bergers, G. and L.E. Benjamin, *Tumorigenesis and the angiogenic switch.* Nat Rev Cancer, 2003. **3**(6): p. 401-10.

107. Riedel, F., et al., *Vascular endothelial growth factor expression correlates with p53 mutation and angiogenesis in squamous cell carcinoma of the head and neck.* Acta Otolaryngol, 2000. **120**(1): p. 105-11.

108. Grant, S.W., et al., *Mutant p53 correlates with reduced expression of thrombospondin-1, increased angiogenesis, and metastatic progression in melanoma.* Cancer Detect Prev, 1998. **22**(3): p. 185-94.

109. Fontemaggi, G., et al., *The execution of the transcriptional axis mutant p53, E2F1 and ID4 promotes tumor neo-angiogenesis.* Nat Struct Mol Biol, 2009. **16**(10): p. 1086-93.

110. Adorno, M., et al., *A Mutant-p53/Smad complex opposes p63 to empower TGFbeta-induced metastasis.* Cell, 2009. **137**(1): p. 87-98.

111. Girardini, J.E., et al., *A Pin1/mutant p53 axis promotes aggressiveness in breast cancer.* Cancer Cell, 2011. **20**(1): p. 79-91.

112. Marin, M.C., et al., *A common polymorphism acts as an intragenic modifier of mutant p53 behaviour.* Nat Genet, 2000. **25**(1): p. 47-54.

113. Luo, J.L., et al., *Knock-in mice with a chimeric human/murine p53 gene develop normally and show wild-type p53 responses to DNA damaging agents: a new biomedical research tool.* Oncogene, 2001. **20**(3): p. 320-8.

114. Dudgeon, C., et al., *Tumor susceptibility and apoptosis defect in a mouse strain expressing a human p53 transgene.* Cancer Res, 2006. **66**(6): p. 2928-36.

115. Liu, D.P., H. Song, and Y. Xu, *A common gain of function of p53 cancer mutants in inducing genetic instability.* Oncogene, 2010. **29**(7): p. 949-56.

116. Bertout, J.A., et al., *Heterozygosity for hypoxia inducible factor 1alpha decreases the incidence of thymic lymphomas in a p53 mutant mouse model.* Cancer Res, 2009. **69**(7): p. 3213-20.

117. Bougeard, G., et al., *Molecular basis of the Li-Fraumeni syndrome: an update from the French LFS families.* J Med Genet, 2008. **45**(8): p. 535-8.

118. Birch, J.M., et al., *Cancer phenotype correlates with constitutional TP53 genotype in families with the Li-Fraumeni syndrome.* Oncogene, 1998. **17**(9): p. 1061-8.

119. Petitjean, A., et al., *Impact of mutant p53 functional properties on TP53 mutation patterns and tumor phenotype: lessons from recent developments in the IARC TP53 database.* Hum Mutat, 2007. **28**(6): p. 622-9.

120. Li, M., et al., *The ATM-p53 pathway suppresses aneuploidy-induced tumorigenesis.* Proc Natl Acad Sci U S A, 2010. **107**(32): p. 14188-93.

121. Westphal, C.H., et al., *atm and p53 cooperate in apoptosis and suppression of tumorigenesis, but not in resistance to acute radiation toxicity.* Nat Genet, 1997. **16**(4): p. 397-401.

122. Celeste, A., et al., *H2AX haploinsufficiency modifies genomic stability and tumor susceptibility.* Cell, 2003. **114**(3): p. 371-83.

123. Hanel, W. and U.M. Moll, *Links between mutant p53 and genomic instability.* J Cell Biochem, 2012. **113**(2): p. 433-9.

124. Torchia, E.C., et al., *Myc, Aurora Kinase A, and mutant p53(R172H) co-operate in a mouse model of metastatic skin carcinoma.* Oncogene, 2011.

125. Hsiao, M., et al., *Gain-of-function mutations of the p53 gene induce lymphohematopoietic metastatic potential and tissue invasiveness.* Am J Pathol, 1994. **145**(3): p. 702-14.

126. Haines, B.B., et al., *Block of T cell development in P53-deficient mice accelerates development of lymphomas with characteristic RAG-dependent cytogenetic alterations.* Cancer Cell, 2006. **9**(2): p. 109-20.

127. Charytonowicz, E., et al., *Alveolar rhabdomyosarcoma: is the cell of origin a mesenchymal stem cell?* Cancer letters, 2009. **279**(2): p. 126-36.

128. Terzian, T., et al., *The inherent instability of mutant p53 is alleviated by Mdm2 or p16INK4a loss.* Genes Dev, 2008. **22**(10): p. 1337-44.

129. Kikushige, Y., et al., *Self-renewing hematopoietic stem cell is the primary target in pathogenesis of human chronic lymphocytic leukemia.* Cancer Cell, 2011. **20**(2): p. 246-59.

130. de Boer, J., et al., *Transgenic mice with hematopoietic and lymphoid specific expression of Cre.* Eur J Immunol, 2003. **33**(2): p. 314-25.

131. Yoshikawa, K., et al., *Mutant p53 R248Q but not R248W enhances in vitro invasiveness of human lung cancer NCI-H1299 cells.* Biomed Res, 2010. **31**(6): p. 401-11.

132. Torchia, E.C., et al., *Myc, Aurora Kinase A, and mutant p53(R172H) co-operate in a mouse model of metastatic skin carcinoma.* Oncogene, 2012. **31**(21): p. 2680-90.

133. Difilippantonio, M.J., et al., *Evidence for replicative repair of DNA double-strand breaks leading to oncogenic translocation and gene amplification.* J Exp Med, 2002. **196**(4): p. 469-80.

134. Nemajerova, A., et al., *Targeted deletion of p73 in mice reveals its role in T cell development and lymphomagenesis.* PLoS One, 2009. **4**(11): p. e7784.

135. Li, T., et al., *Tumor Suppression in the Absence of p53-Mediated Cell-Cycle Arrest, Apoptosis, and Senescence.* Cell, 2012. **149**(6): p. 1269-83.

136. de Vries, A., et al., *Targeted point mutations of p53 lead to dominant-negative inhibition of wild-type p53 function.* Proc Natl Acad Sci U S A, 2002. **99**(5): p. 2948-53.

137. Lee, M.K. and K. Sabapathy, *The R246S hot-spot p53 mutant exerts dominant-negative effects in embryonic stem cells in vitro and in vivo.* J Cell Sci, 2008. **121**(Pt 11): p. 1899-906.

138. Morse, H.C., 3rd, et al., *Bethesda proposals for classification of lymphoid neoplasms in mice.* Blood, 2002. **100**(1): p. 246-58.

139. Kogan, S.C., et al., *Bethesda proposals for classification of nonlymphoid hematopoietic neoplasms in mice.* Blood, 2002. **100**(1): p. 238-45.

140. Cowell, J.K., et al., *Application of bacterial artificial chromosome array-based comparative genomic hybridization and spectral karyotyping to the analysis of glioblastoma multiforme.* Cancer Genet Cytogenet, 2004. **151**(1): p. 36-51.

141. Petrenko, O., et al., *The molecular characterization of the fetal stem cell marker AA4.* Immunity, 1999. **10**(6): p. 691-700.

Appendix

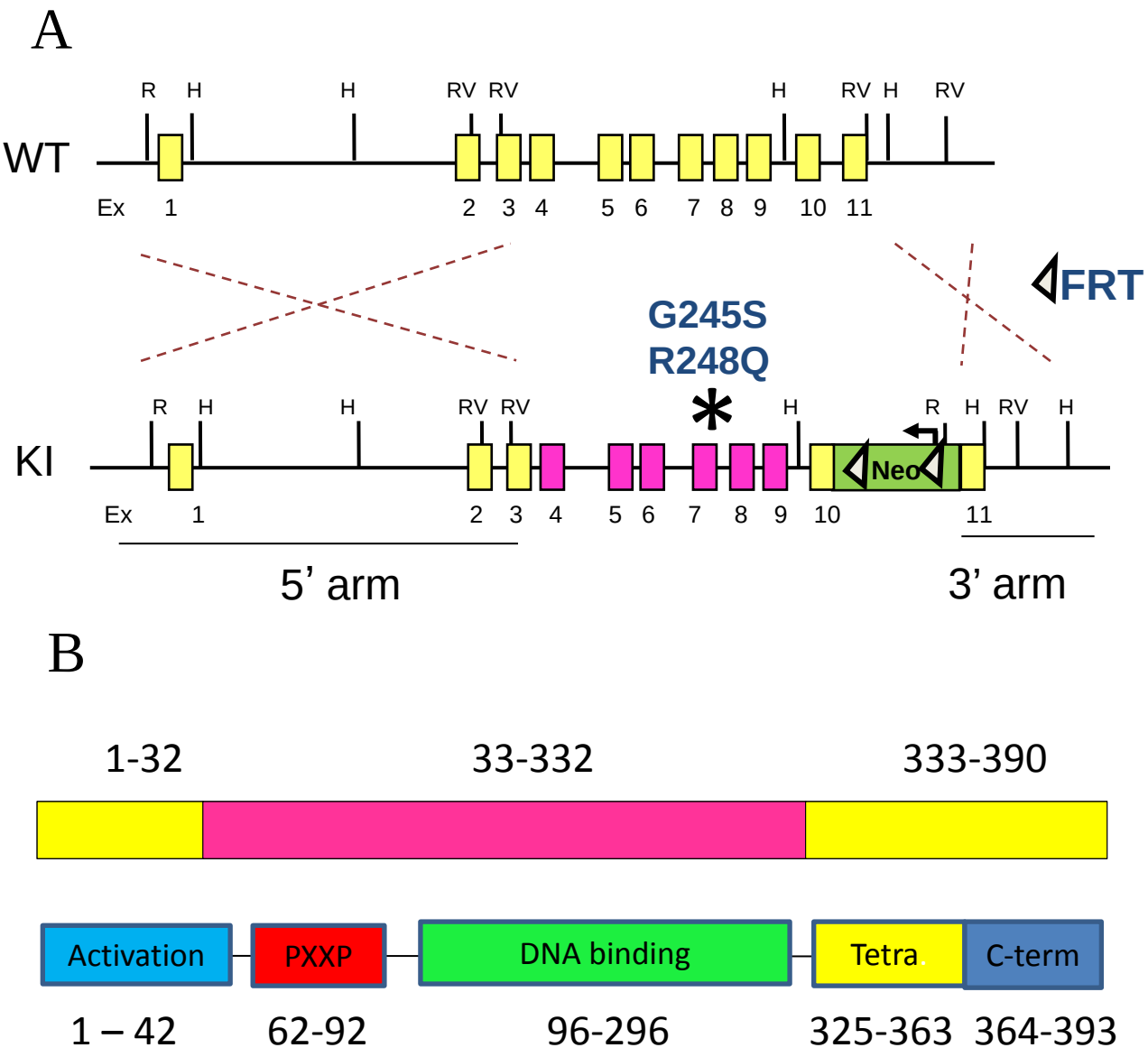

Figure 1. Construction of HUPKI mouse models.

A. Diagram of the mutp53 HUPKI targeting vectors. Mouse genomic region spanning Ex4-9 was replaced with human genomic region Ex4-9 (HUPKI) containing either a p53 R248Q or G245S mutation (marked by *). This generates a chimeric p53 protein of mouse aa 1-32, human aa 33-332, mouse aa 333-390. A deletable Neo selection box flanked by FRT sites was inserted downstream of mouse Ex10. Yellow boxes represent mouse exons and pink boxes represent human exons. Restriction enzyme sites are indicated. H: HindIII; R: EcoRI; RV: EcoRV.

B. Diagram outlining the specific amino acid sequences swapped in the HUPKI chimeric protein, along with p53's domain diagram for reference.

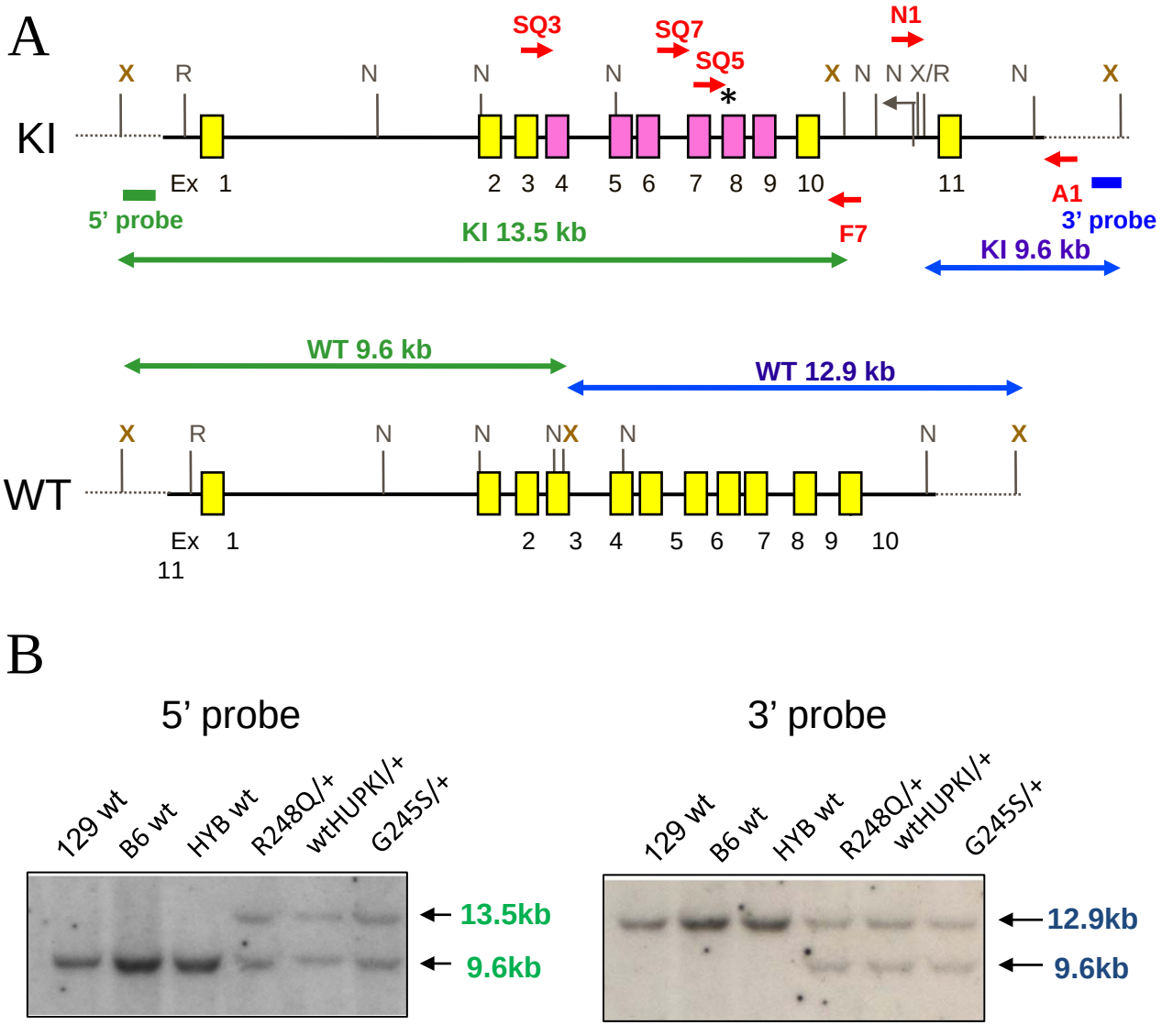

Figure 2. Verification of insertion of HUPKI construct into ES cells

A. Diagram of the knocked-in germline configuration of the two mutp53 HUPKI alleles. Primers F7/SQ7, F7/SQ5 and F7/SQ3 were used to amplify the mutated regions for sequence confirmation (in red). The neomycin resistance cassette was deleted by transfecting recombinant ES lines with *flp* recombinase; deletion was confirmed by PCR. Southern blot probes are indicated.

B. Southern blot confirmation of neo-deleted recombinant ES clones. XbaI digestion was used for 5' and 3' probes. The expected band sizes for the 3' probe are WT ~12.9kb; KI 9.6 kb. For the 5' probe expected band sizes are WT 9.6 kb; KI 13.5 kb. The untargeted ES line was a 129:B6 hybrid (HYB).

A

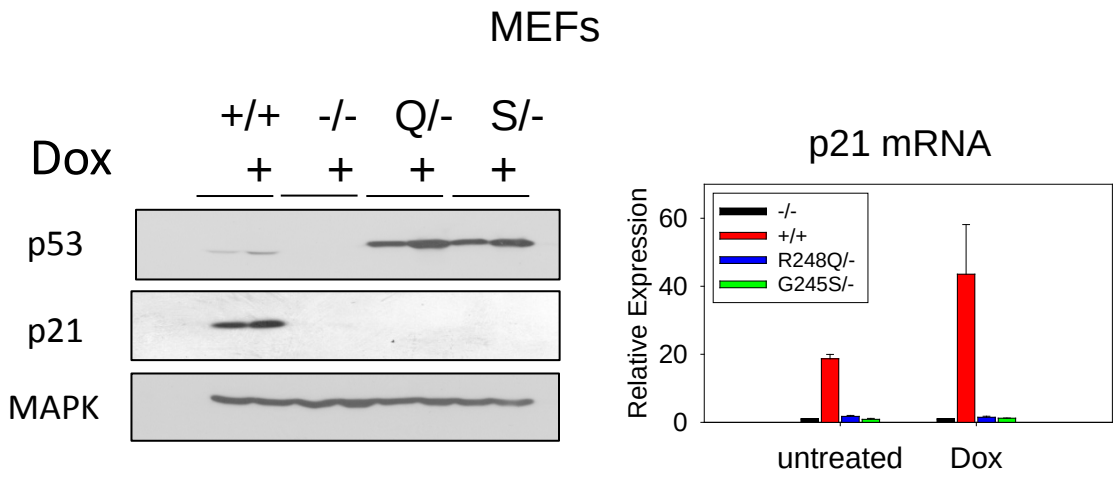

B

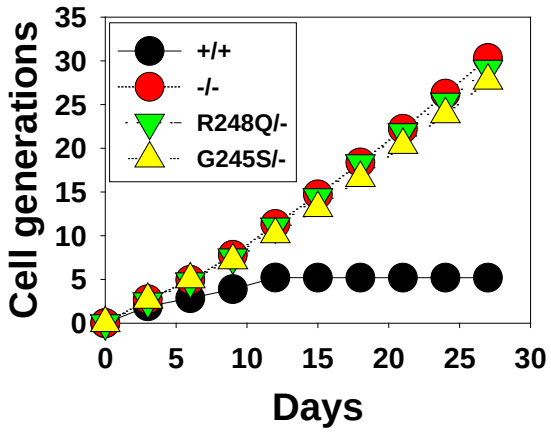

Figure 3. Both R248Q and G245S lack wtp53 functional activity in MEFs
A. Early passage MEFs of the indicated genotypes were treated with 250 nM Doxorubicin for 24 hrs. Cells were harvested and protein and RNA prepared. (Left) Lysates were blotted for p53, p21 and MAPK (loading control). An antibody directed against a peptide sequence surrounding mouse p53 Serine 20 (clone 1C12), present as mouse sequence in both the wildtype (wt) and HUPKI configurations, is used to compare p53 levels. There is a slight reduction in mobility of HUPKI proteins compared to mouse wtp53 due to the higher molecular weight of the HUPKI proteins. *Right*, p21 mRNA levels determined by qRT-PCR.
B. Early passage MEFs of the indicated genotypes were passaged every three days at a density of 4 x 10^5 per 10 cm dish. The total number of cell generations over 27 days was determined. Results are representative of two independent MEF preparations per genotype.

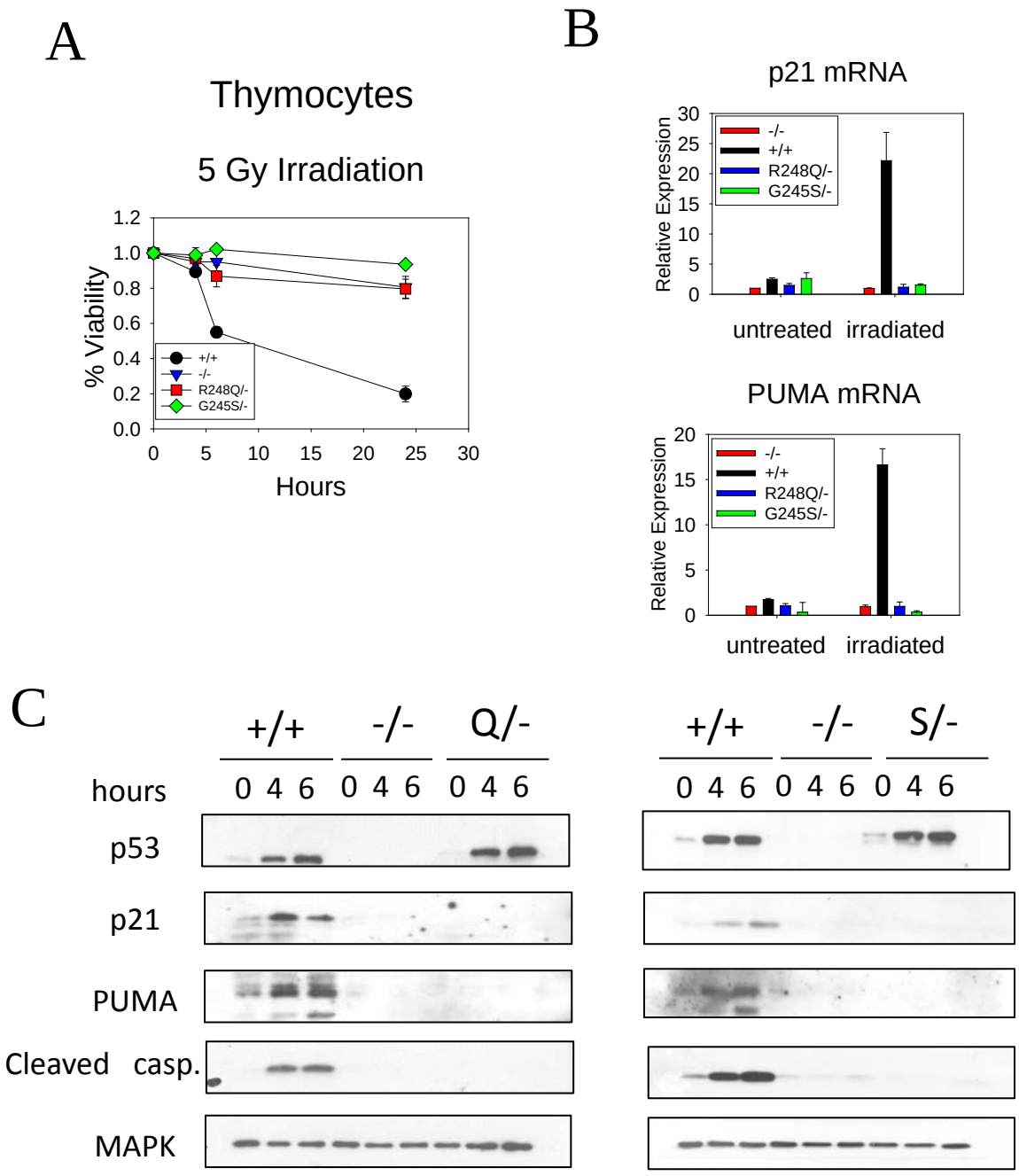

Figure 4. Both R248Q and G245S lack wtp53 functional activity in thymocytes
A. Thymocytes of the indicated genotypes were freshly isolated from 4-week old mice and gamma irradiated (5 Gy). *Left* Cell viability was determined by AnnexinV/PI staining at 0, 4, 6, and 24 hrs. Percent viable cells in treated samples were normalized to untreated samples; n=3 mice per genotype.
B. qRT-PCR of p21 and Puma mRNA from thymocytes 6 hrs after irradiation.
C. Immunoblot analysis for p53, p21, PUMA, cleaved caspase and MAPK (loading control) from irradiated thymocytes at the indicated time points.

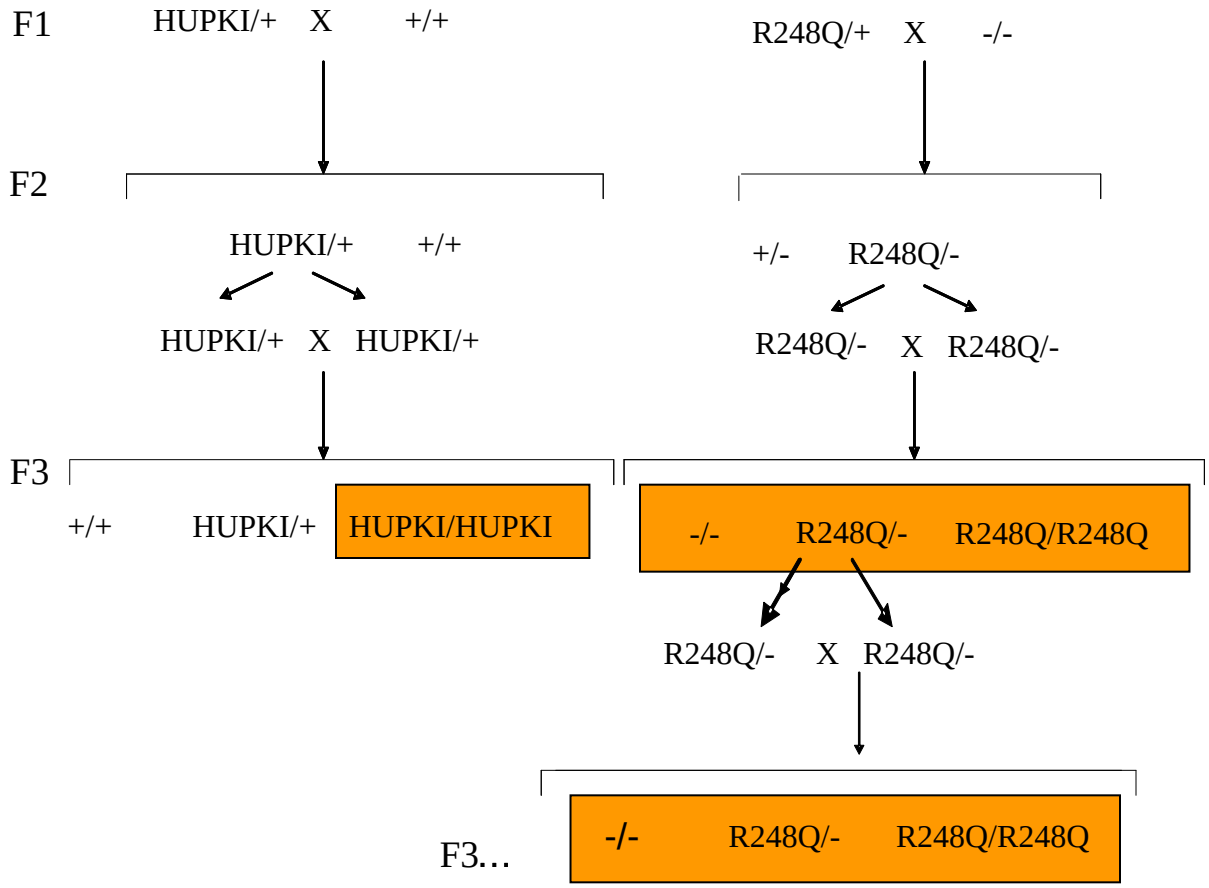

Figure 5. Breeding scheme for generation of mouse cohorts for tumorigenesis study. F0 chimeric mice (C57BL/6/129SvEv) were bred to wild type C57BL/6 mice to confirm germline transmission of the HUPKI alleles. *Left, F1* wtHUPKI/+ mice were crossed to 129S1/SvImJ mice to obtain F2 wtHUPKI/+ breeding pairs which were intercrossed to yield F3 wtHUPKI/wtHUPKI mice. *Right,* F1 R248Q/+ mice were bred to p53-/- mice to obtain heterozygous F2 mut/- mice, which were then intercrossed to yield -/-, mut/-, and mut/mut mice. F3 Mut/- mice used in brother-sister matings to obtain the desired amount of mice in the cohorts.

A

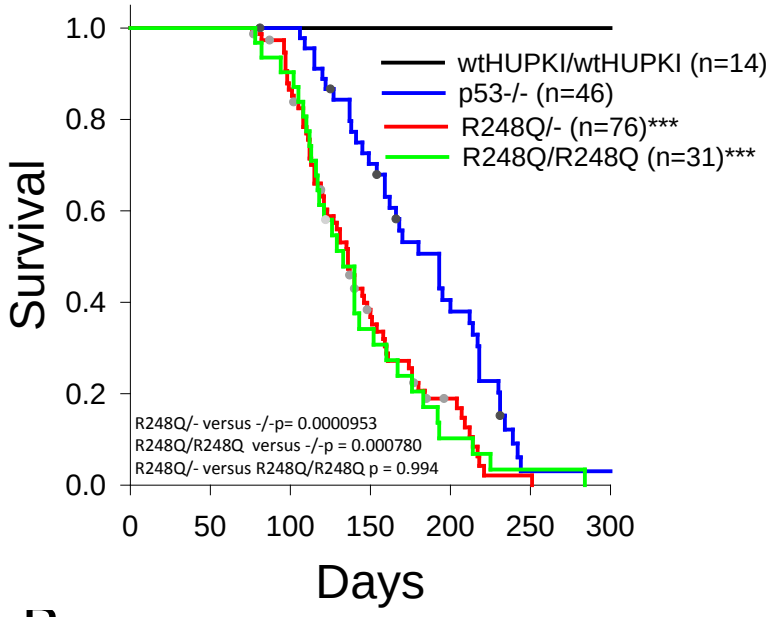

C

Accelerated tumor onset in R248Q mice

	Q/-	Q/Q	combined
All tumors	<0.001	0.001	<0.001
T-cell	0.009	0.118	0.013
B-cell	0.004	0.037	0.002
Solid tumors	0.061	0.075	0.031

B

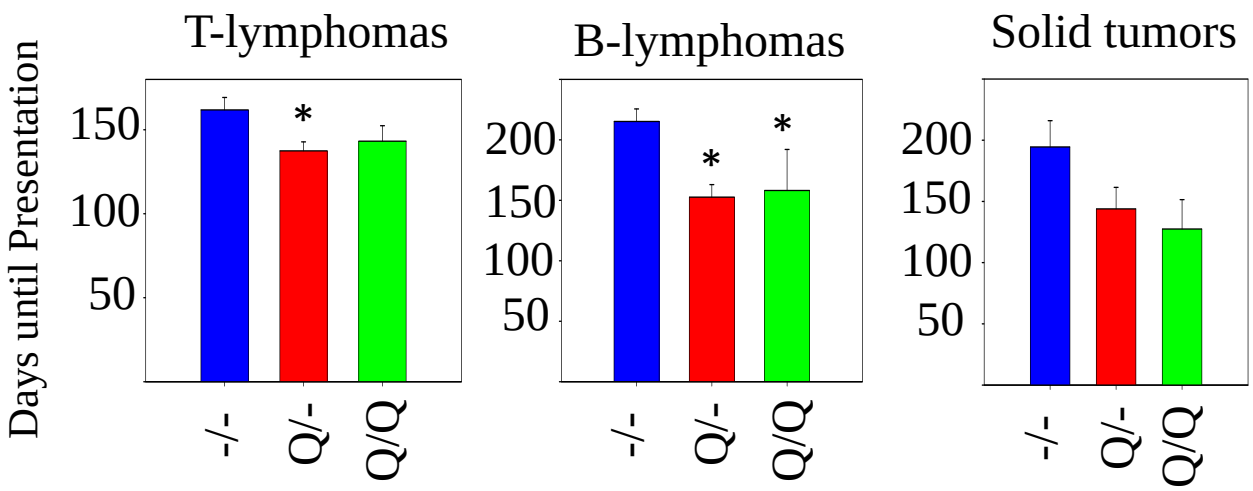

Figure 6. Expression of the mutant p53 R248Q allele results in accelerated tumor onset and shorter survival compared to the p53 null allele.

A. Tumor-specific survival curves for mice of the indicated genotypes. Dots on the curves represent mice that were censored due to deaths from non-tumor related causes (p53 -/-, n=6, R248Q/-, n=11, R248Q/R248Q, n=1, wtHUPKI/wtHUPKI, n=1). ***p<.0001 compared to null mice, log-rank analysis.

B. Mean days until presentation of the main tumor types. Error bars indicate SE. *p<.05 compared to null mice.

C. Table summarizing p-values compared to null mice for Q/-, Q/Q, and a combination of Q/- and Q/Q into a single data set.

A

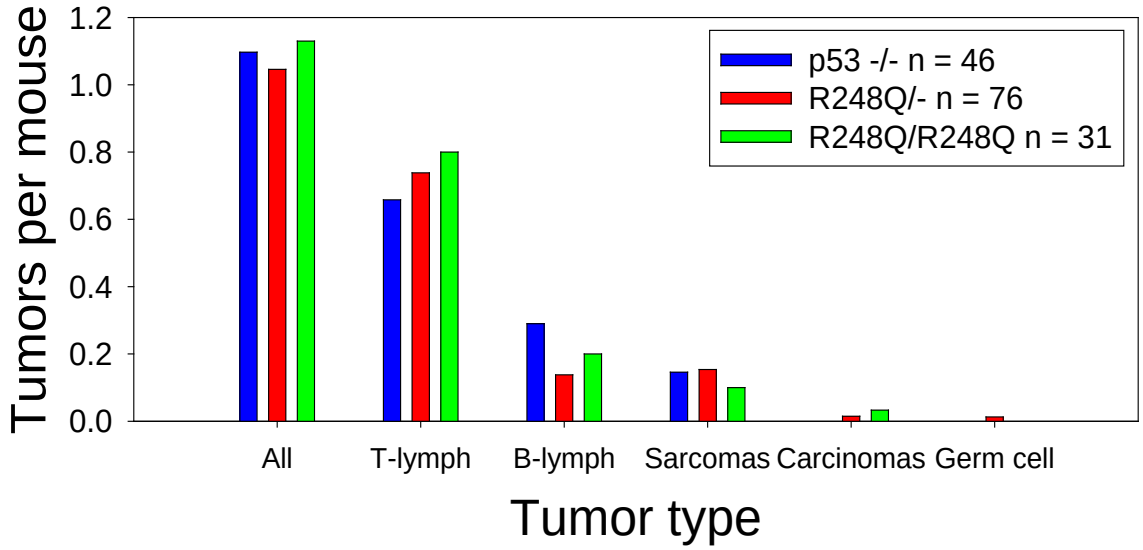

B

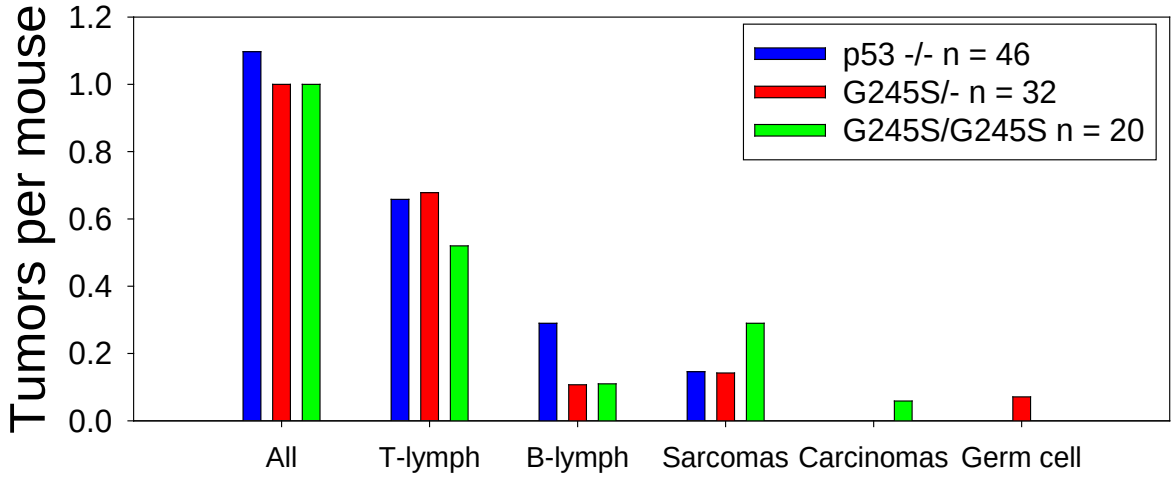

Figure 7. R248Q and G245S display a modest broadening of tumor spectrum compared to p53 null mice.

Tumors per mouse of the indicated tumor subtypes. **A,** null, R248Q/-, and R248Q/R248Q mice and **B,** null, G245S/-, and G245S/G245S mice.

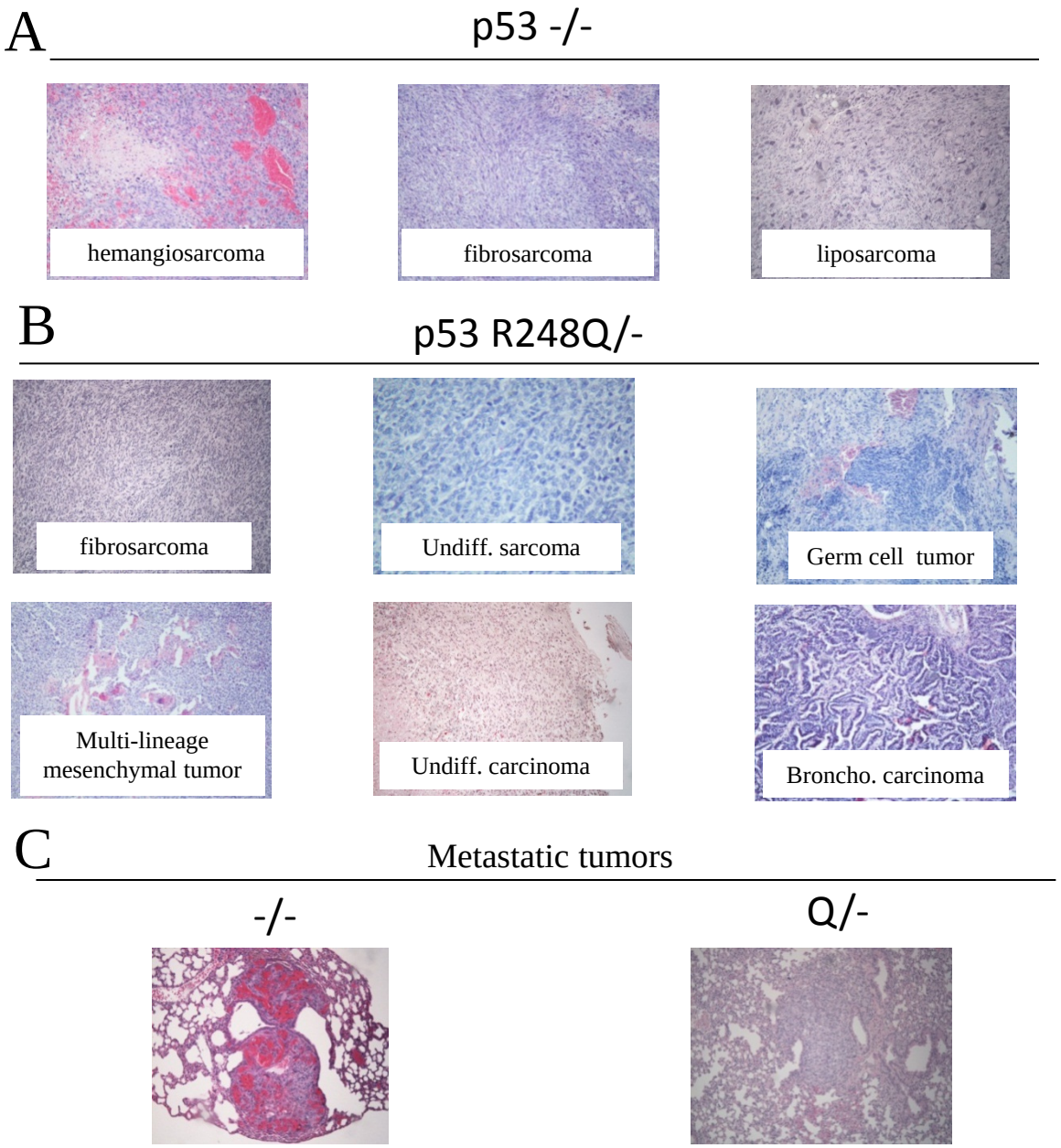

Figure 8. Expression of R248Q results in a broader histological spectrum of tumor types
A. p53-null mice developed hemangiosarcoma, fibrosarcoma and liposarcoma.
B. p53R248Q/- mice developed fibrosarcoma, undifferentiated sarcoma, abdominal germ cell tumor,
multi-lineage mesenchymal tumor with areas of osteoid and pericyte differentiation, undifferentiated carcinoma with areas of glandular differentiation, and bronchoalveolar carcinoma of the lung.
C. Left, One p53 null mouse developed a large diffuse hemangiosarcoma of the heart that had seeded multiple tumor emboli to the lung. Right, One R248Q/- mouse developed a large fibrosarcoma in the abdomen that generated multiple
distant true metastases into the lungs and numerous subcutaneous nodules on the back.

-/-	Q/-	Q/Q	S/-	S/S
Hemangiosarcoma (3/6) Fibrosarcoma (2/6) Liposarcoma (1/6)	Fibrosarcoma (3/12) Hemangiosarcoma (2/12) Undiff. Sarcoma (2/12) Germ Cell tumor (1/12) Mutlilineage mesenchym. tumor (1/12) Lung carcinoma (1/12) Undiff. Carcinoma (1/12)	Fibrosarcoma (3/4) Undiff.carcinoma (1/4)	Fibrosarcoma (2/6) Hemangiosarcoma (1/6) Germ cell tumor (2/6) Undiff. Carcinoma (1/6)	Fibrosarcoma (3/6) Undiff. Sarcoma (1/6) Hemangiosarcoma (1/6) Eccrine carcinoma (1/6)

Figure 9. Histological types of all solid tumors that arose in the indicated genotypes.

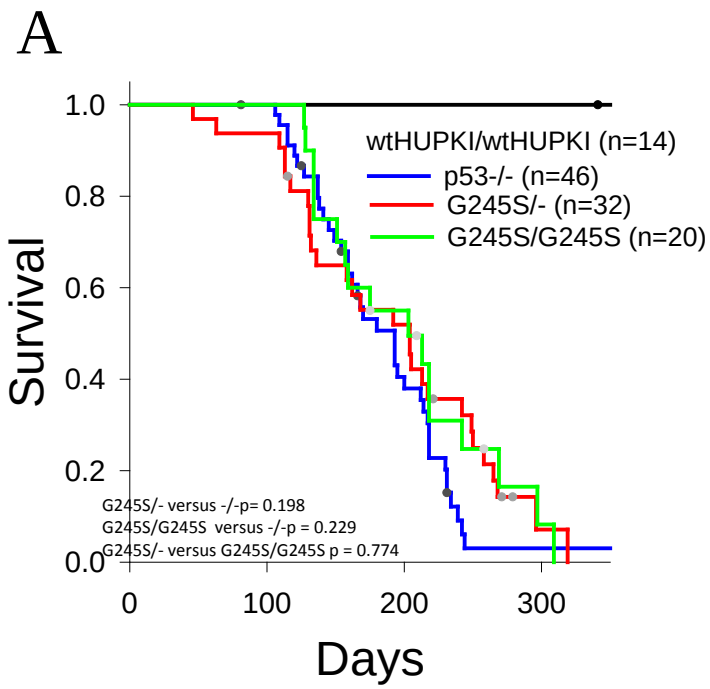

C

No difference in tumor onset in G245S mice

	S/-	S/S	combined
All	0.560	0.362	0.386
T-cell	0.248	0.562	0.488
B-cell	0.359	0.358	0.209
Solid tumors	0.901	0.232	0.410

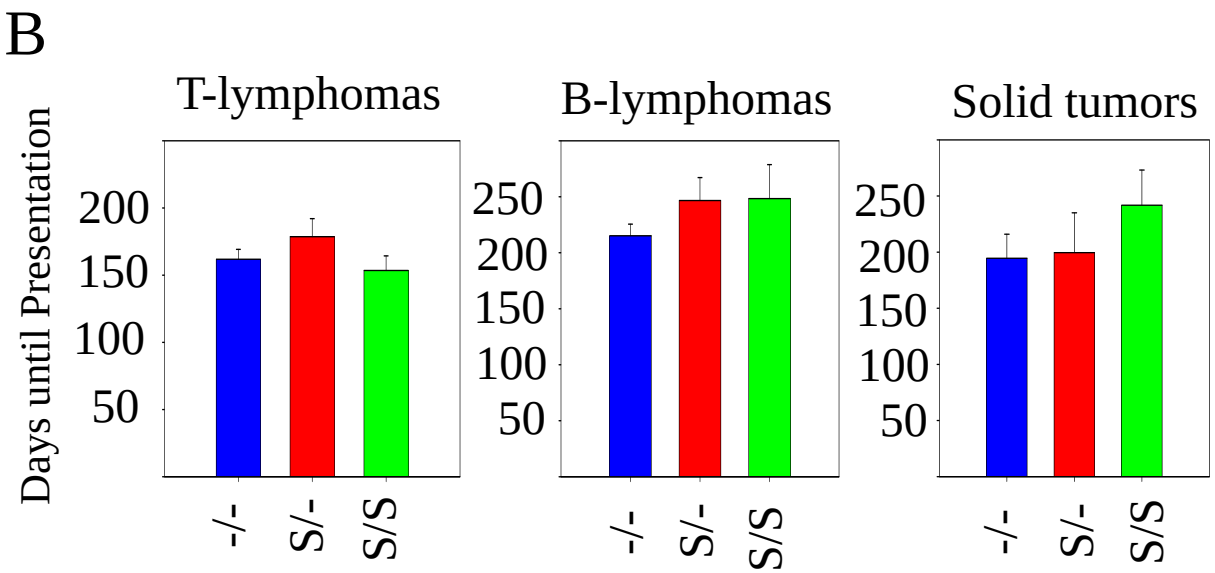

Figure 10. Expression of the mutant p53 G245S allele results in no difference in tumor onset compared to the p53 null allele.

A. Tumor-specific survival curves for mice of the indicated genotypes. Dots on the curves represent mice that were censored due to deaths from non-tumor related causes (p53 -/-, n=6, G245S/-, n=4, G245S/G245S, n=3, wtHUPKI/wtHUPKI, n=1).

B. Mean days until presentation of the main tumor types. Error bars indicate SE.

C. Table summarizing p-values compared to null mice for S/-, S/S, and a combination of S/- and S/S in a single data set.

A

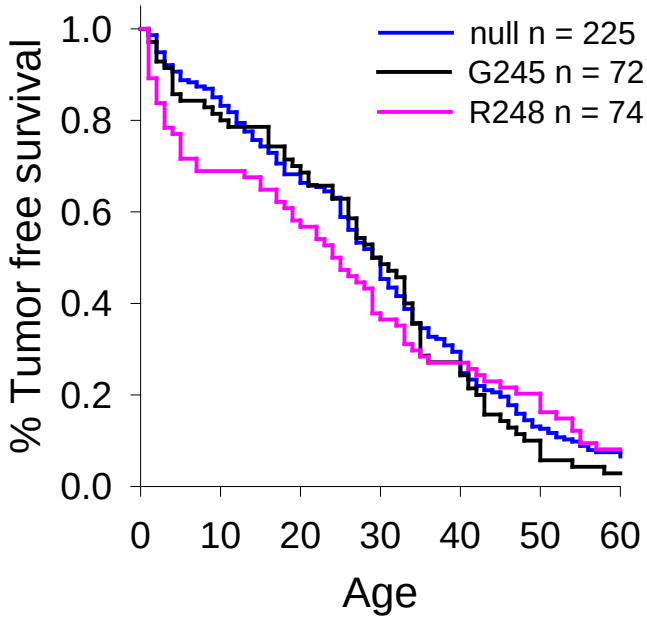

Li-Fraumeni carriers

group	p-value
null vs R248	0.097
null vs G245	0.956
R248 vs G245	0.174

B

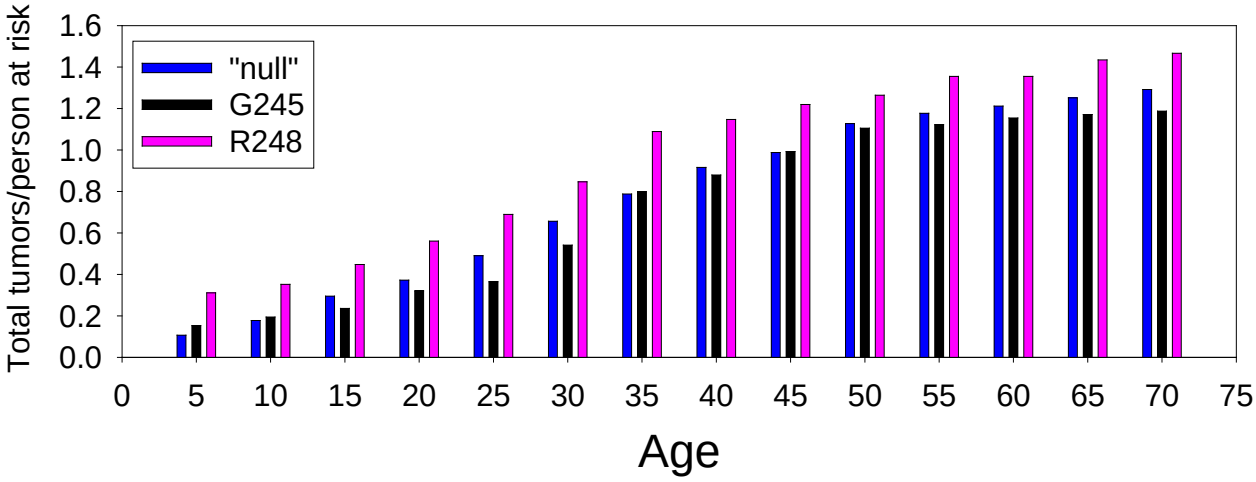

Figure 11. Human persons harboring mutations in codon 248 show a decreased time to first tumor presentation compared to persons with p53 null or codon G245 mutations.
A. *Left*, Kaplan-Meier survival analysis showing the percent of patients remaining tumor-free versus age in years. *Right*, p-values (ranked sum) comparing the median time to first tumor presentation between the three different genotypes.
B. Total number of tumors per persons at risk as a function of age in years. Persons reported to have died of tumors were censored at the time of death.

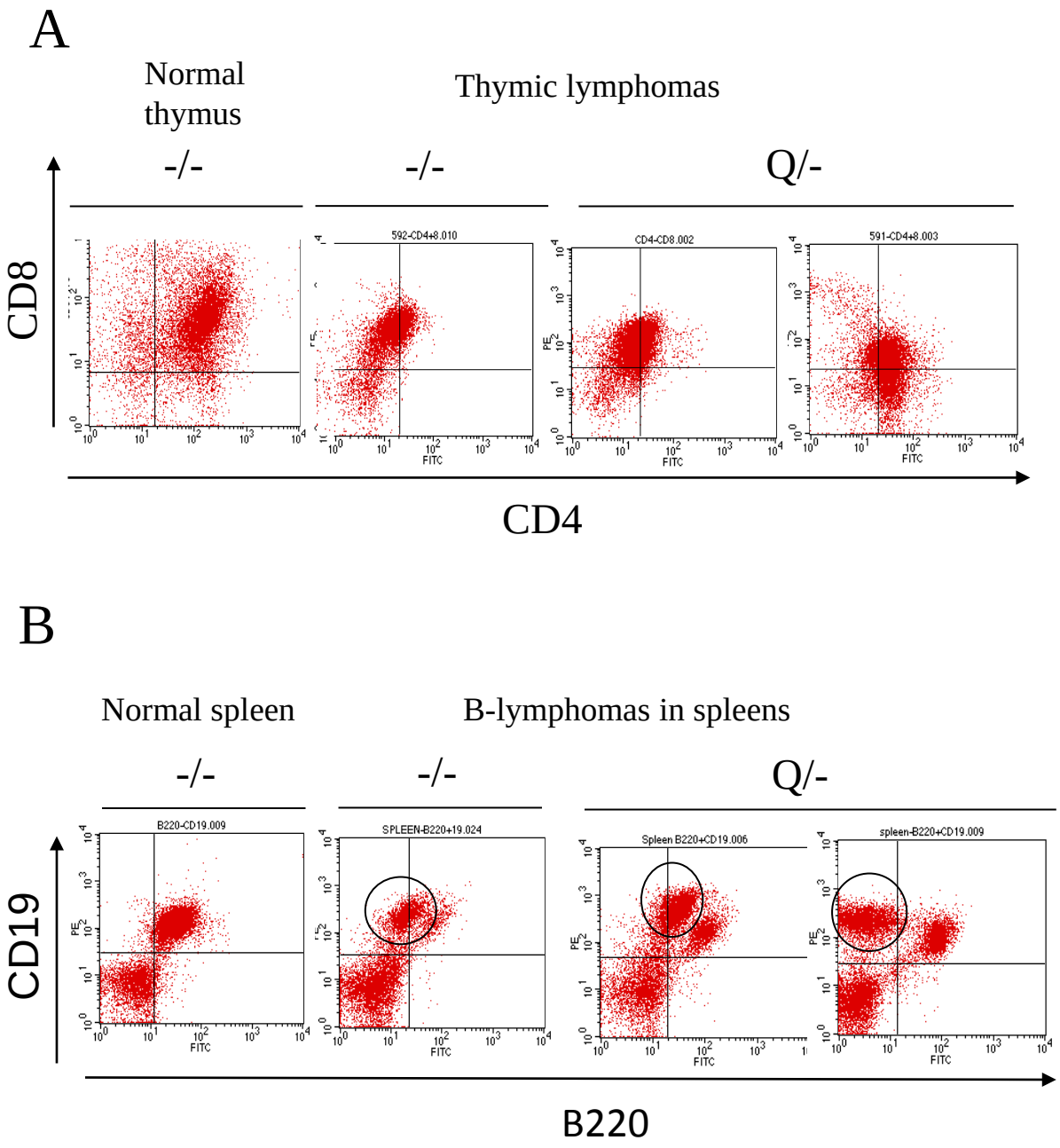

Figure 12. p53 -/- and R248Q/- T and B-cell lymphomas display similar surface phenotypes

A. *Left*, Normal thymus and *Right* T-lymphomas from p53 -/- and R248Q/- mice,

B. *Left*, Normal spleen and *Right* B-lymphomas from p53 -/- and R248Q/- mice, with leukemic populations

Circled.

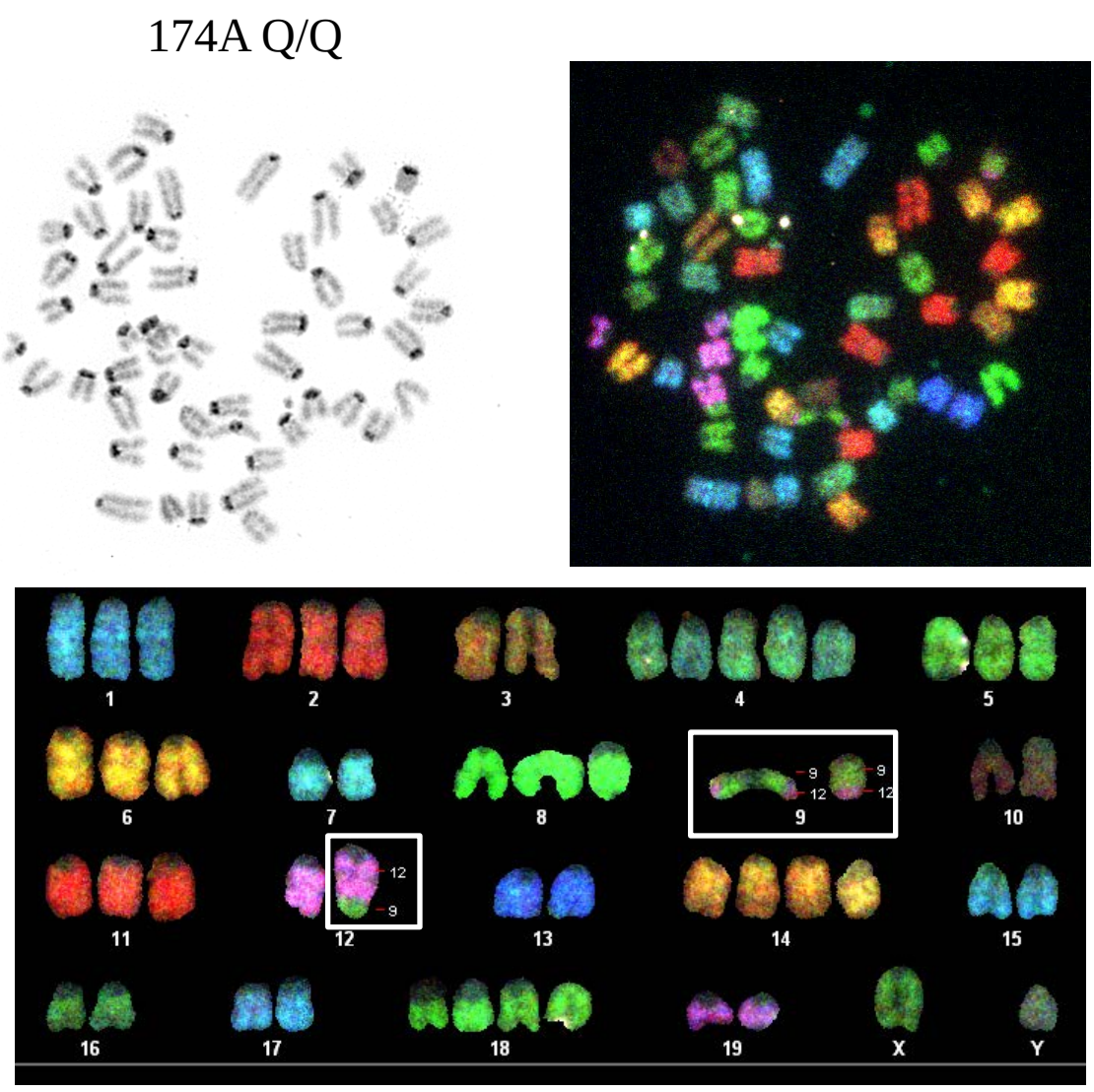

Figure 13. p53R248Q/R248Q T-lymphoma displaying extensive aneuploidy and a clonal translocation.
Metaphases from a homozygous R248Q/R248Q cell line at early passage exhibiting extensive aneuploidy and a 9:12 translocation (boxed) *Upper left* Giemsa staining, *upper right* and *bottom* SKY analysis.

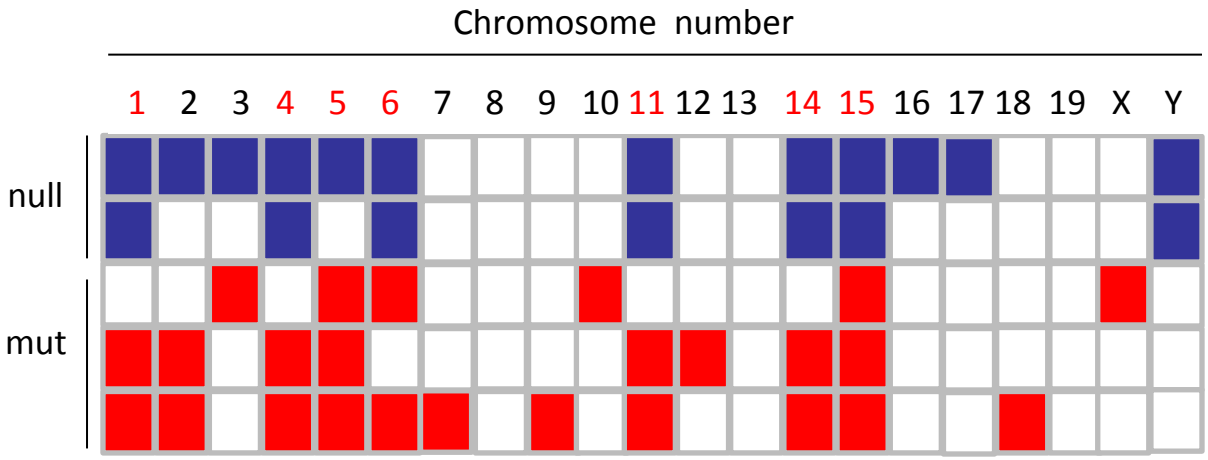

Chromosomal structural abnormalities

-/-	Q/-	Q/Q
(Y;1)- (11/20) Deletion(del16) (11/20) t(2;X)- (18/20) t(14;X)- (20/20)	del(3)-(25/30) der(3)t(3;19)-(13/30) t(4;16)-(17/20)	(9:12)- (14/20)

Figure 14. R248Q expressing T-lymphomas and p53 null T-lymphomas both display extensive aneuploidy and contain clonal translocations.
Top, Chromosomes displaying aneuploidy in >50% of metaphases analyzed from two p53 null cell lines (blue) and three R248Q cell lines (red). *Bottom*, Specific clonal translocations found within the cell lines analyzed. In parenthesis is the number of metaphases displaying the translocation over total number of metaphases analyzed for that cell line.

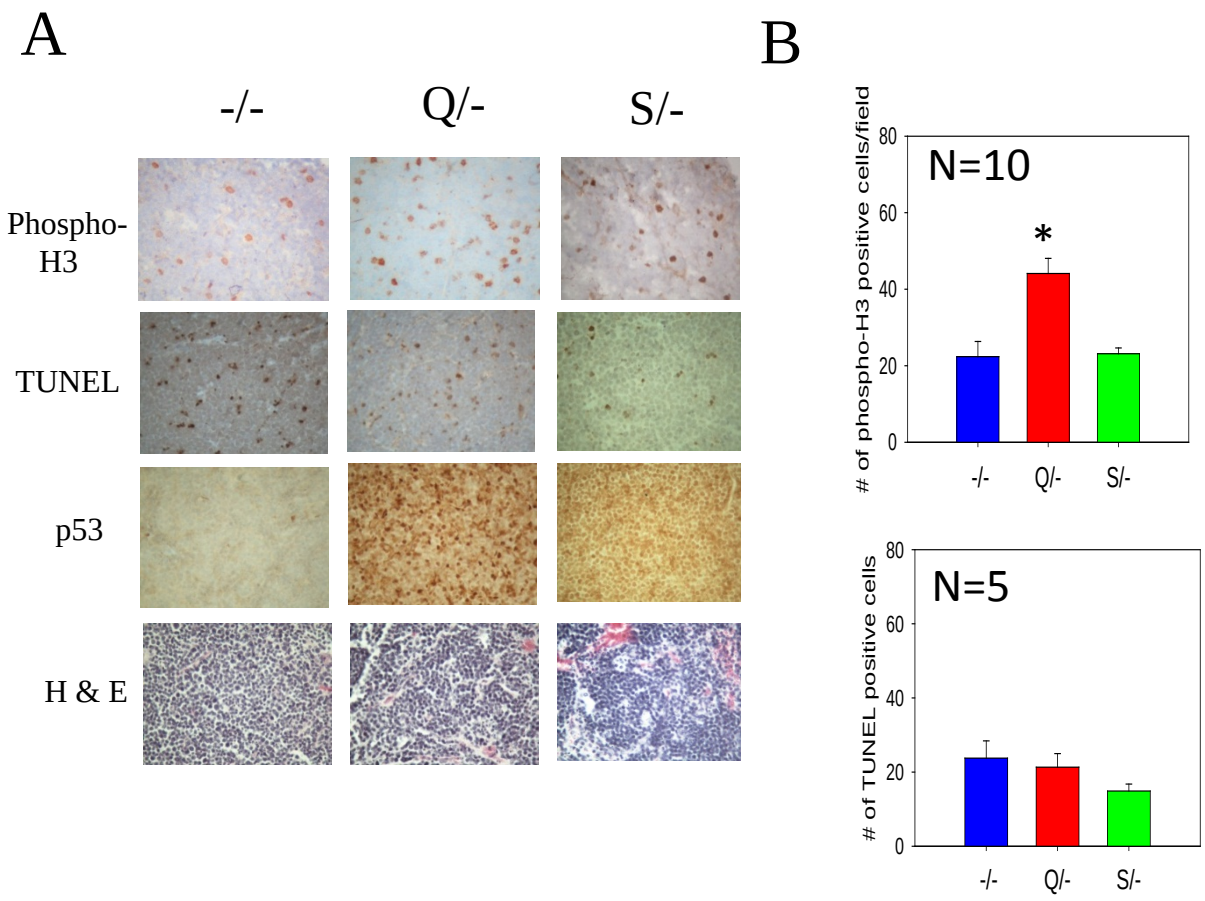

Figure 15 . R248Q/- T-lymphomas show higher cell division *in vivo* compared to null or G245S/- lymphomas

A. Phospho-H3, TUNEL, p53 , and H & E stainings were perfomed on T-lymphomas of null, R248Q/-, and G245S/- mice.

B. Positive nuclei were counted in ten random fields per lymphoma. The mean of these averages for 10 (phospho-H3)
or 5 (TUNEL) lymphomas are shown +/- SE.

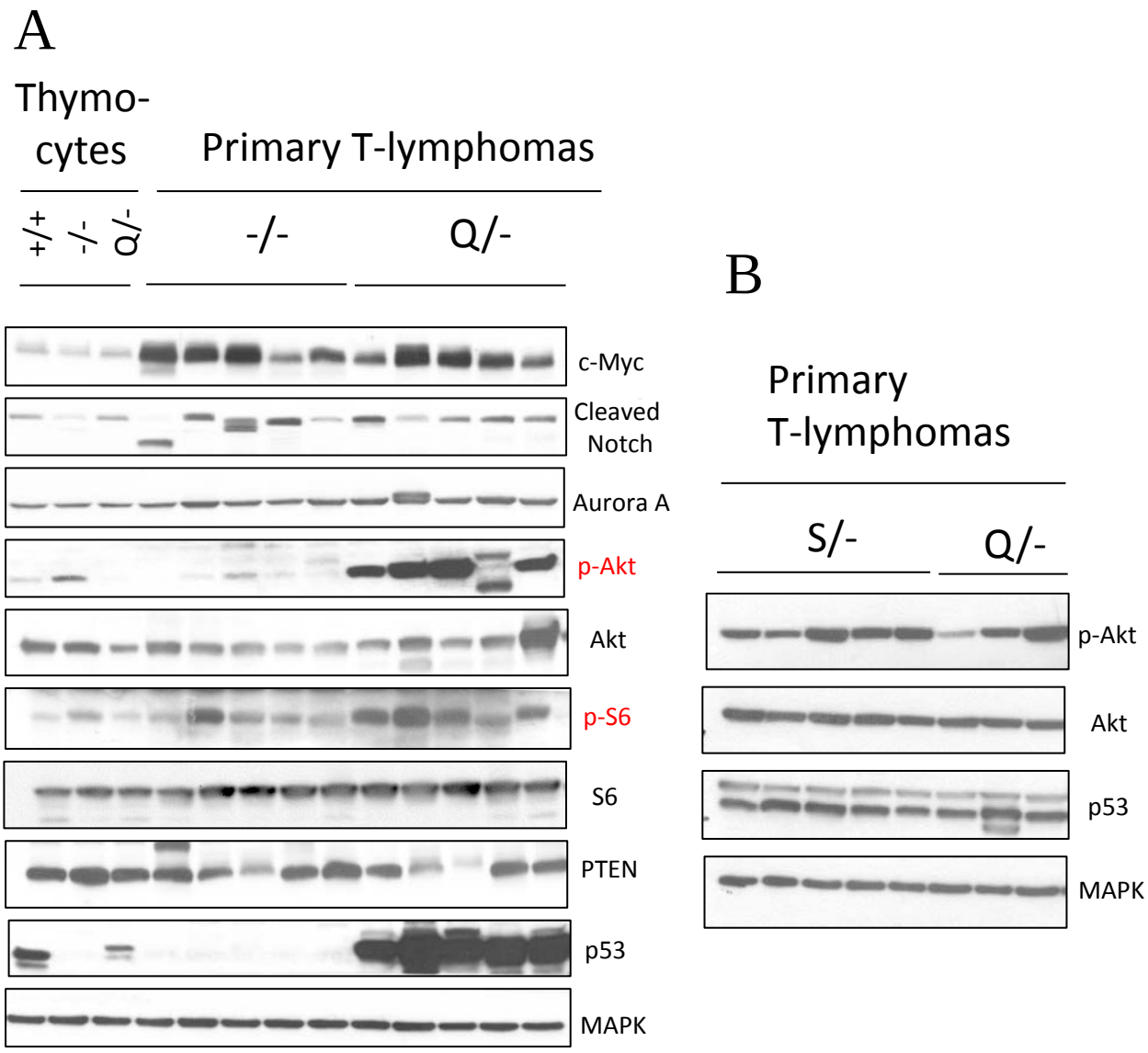

Figure 16 . Both R248Q/- and G245S/- T-lymphomas show higher signaling through the Akt pathway.
A. Thymocytes from 4 week old +/+. -/-, and Q/- thymocytes and primary T-lymphomas from -/- and Q/- lymphomas were blotted for various signaling pathway intermediates.
B. Primary T-lymphomas from S/- and Q/- were blotted for p-Akt, Akt, p53, and MAPK.

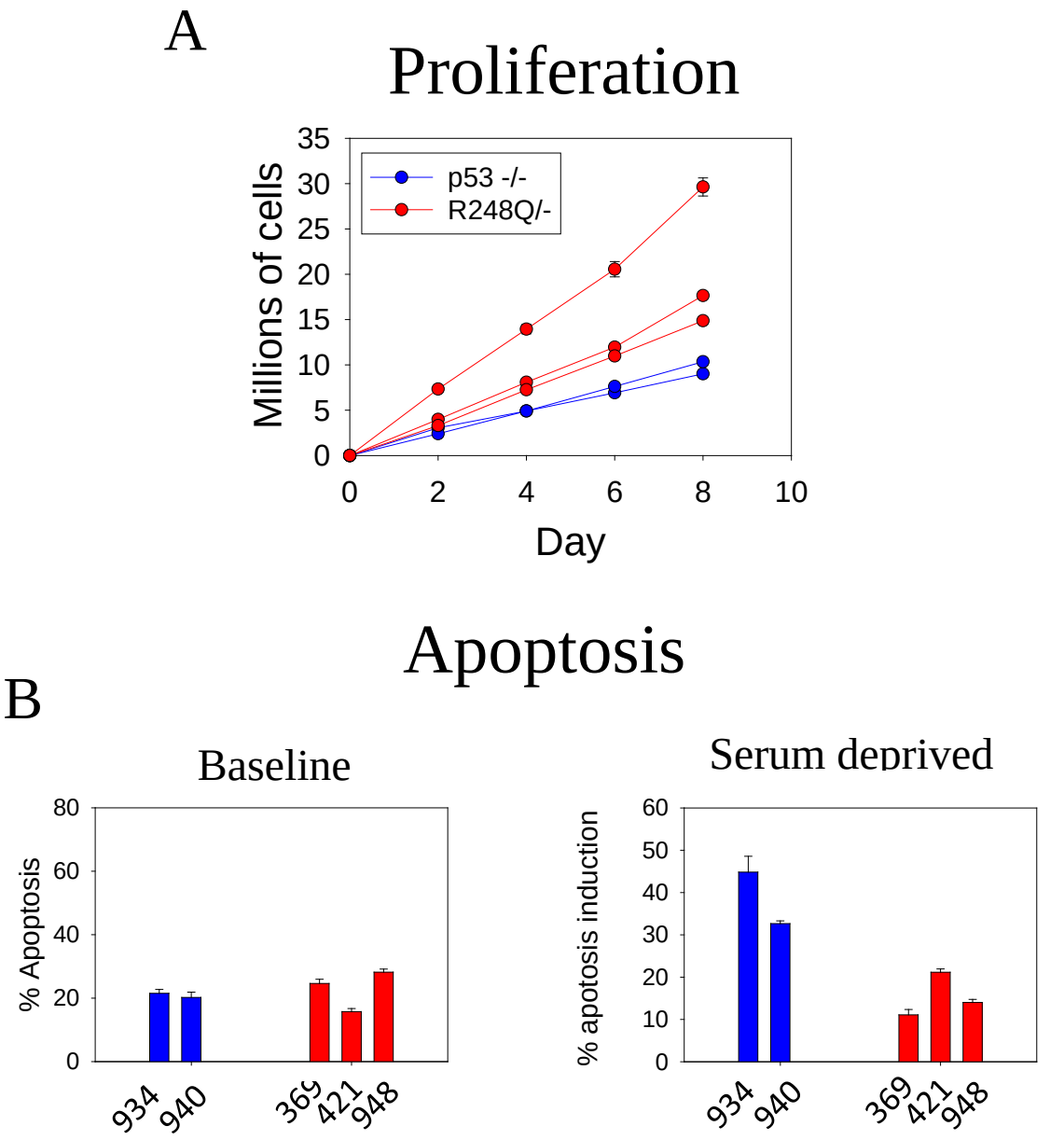

Figure 17. Cell lines derived from Q/- lymphomas show enhance d proliferation and reduce apoptosis *in vitro.*

A. Two p53 null and three R248Q/- cell lines were passaged in culture every 2 days at a density of 2.5 X 10^5 cells per mL and the total number of cells accumulated at each time point was summed. The mean +/- S.E. of three cultures for each cell line is shown.

B. *Left*, The percent of apoptotic cells at base line and *Right*, amount of apoptosis induced after 24 hours of serum starvation. Bars indicate average +/- SE for three replicate experiments per cell line.

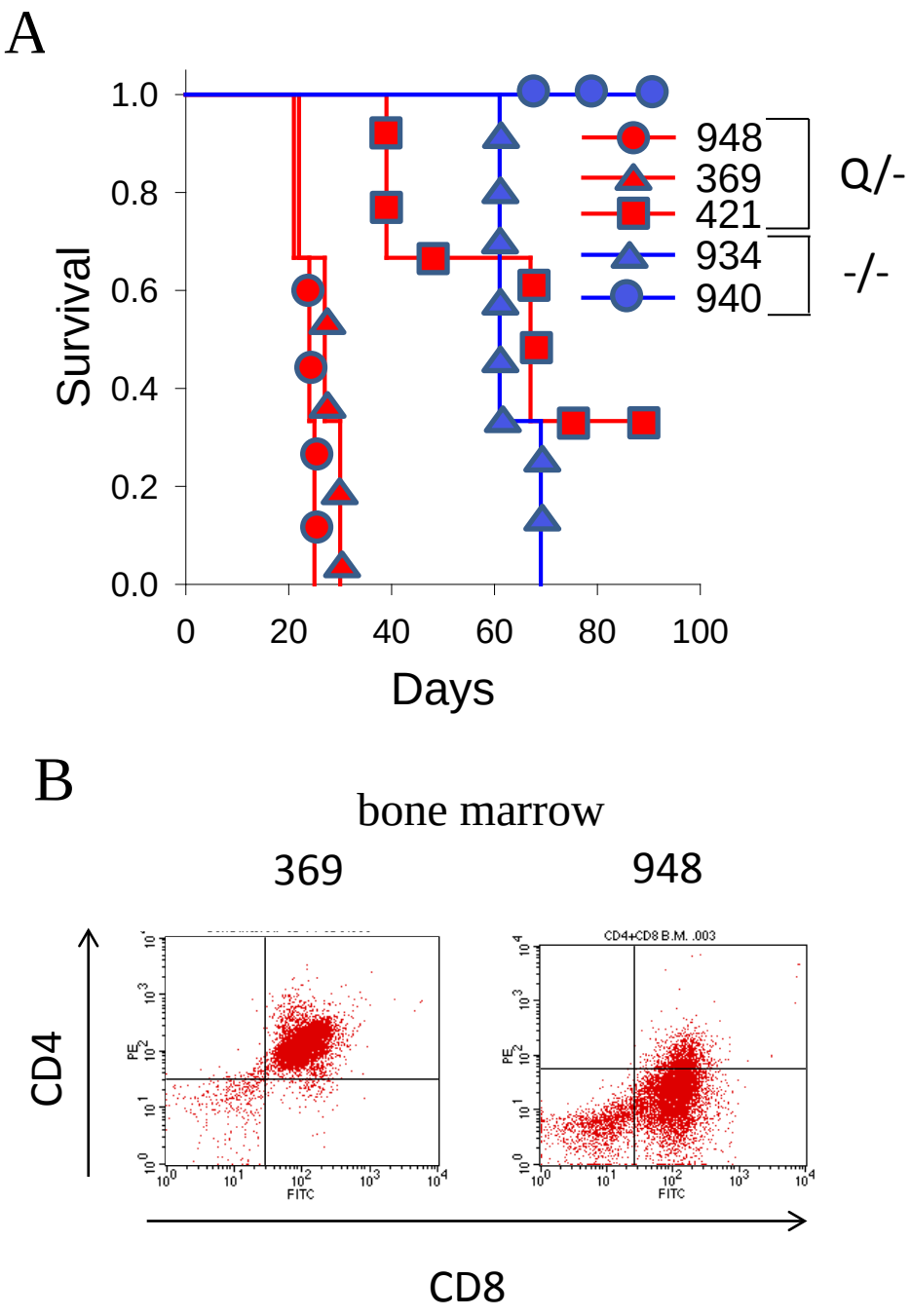

Figure 18. Injection of Q/- lymphomas into nude mice results in aggressive leukemia formation *in vivo.*

A. 1 X 10^5 cells were injected into the tail vein of nude mice. Mice were sacrificed when moribund and each curve represents three injections per cell line from the indicated genotypes.

B. Bone marrow was harvested and analyzed for the presence of leukemic (CD4+CD8+) cells.

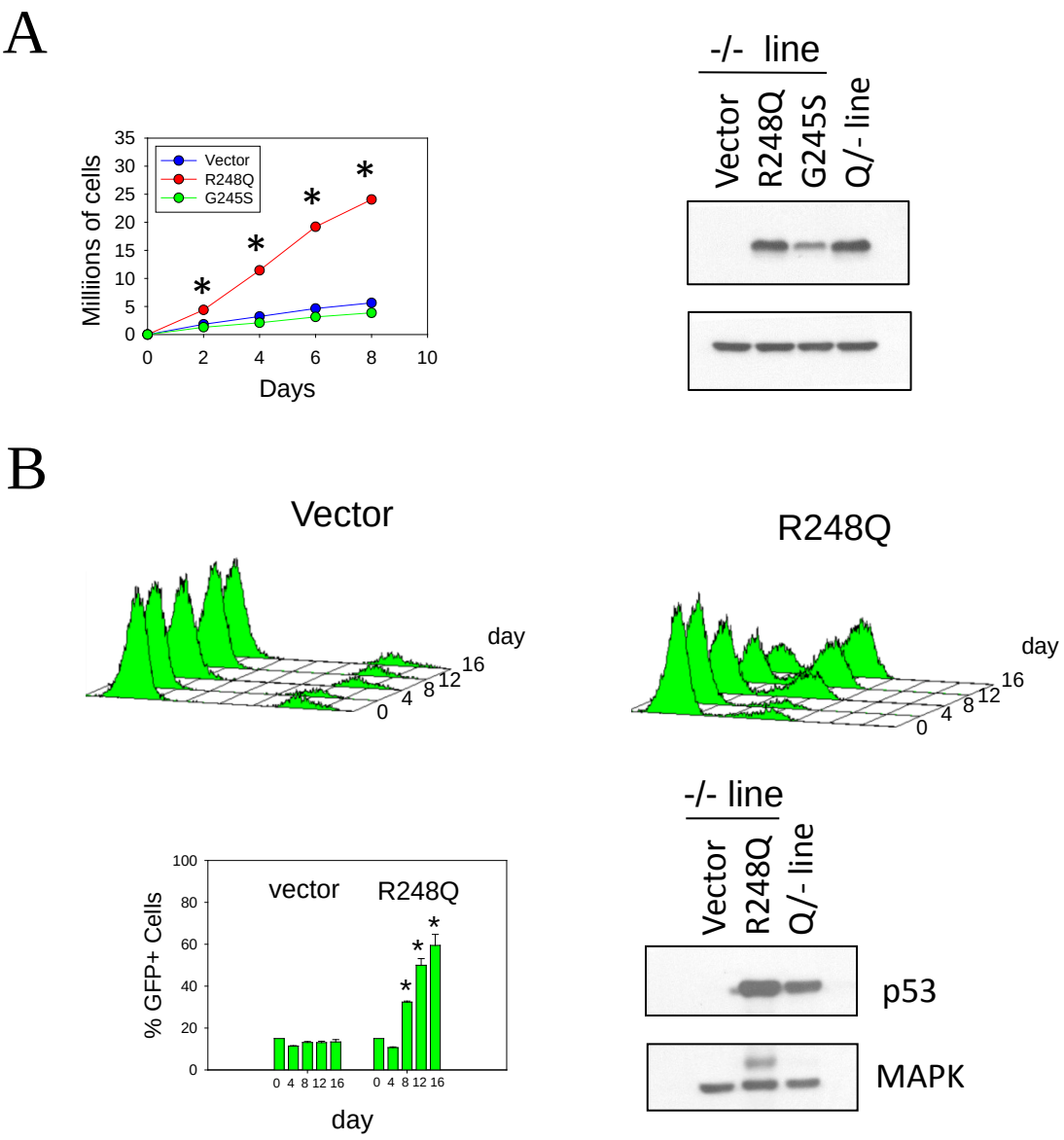

Figure 19. Ectopic expression of mutant p53R248Q increases the growth rate of p53 null T-lymphoma cells in vitro.

A. *Left*, p53 R248Q and G245S was introduced retrovirally into a p53 null T-lymphoma cell line. Cells were plated in triplicate at a density of 5.0 X 10^5 cells and the total cell number was quantified each day and presented as the average+/- SE of three repeat experiments. *Right*, Western blot showing levels of ectopic mutant compared to the endogenous mutant p53 R248Q present in a mutant p53 line.

B. *Top*, p53 null lymphoma cell line (#934) expressing a retroviral vector-IRES-GFP or R248Q-IRES-GFP were added to the original uninfected p53 null line at a ratio of 15% GFP+ cells to 85% GFP- cells. Aliquots from three independent cultures were analyzed for the percent of GFP+ cells by FACS over 16 days. *Bottom*, The average percent of GFP+ cells is shown for each time point from three independent cultures. Error bars represent +/- SE.

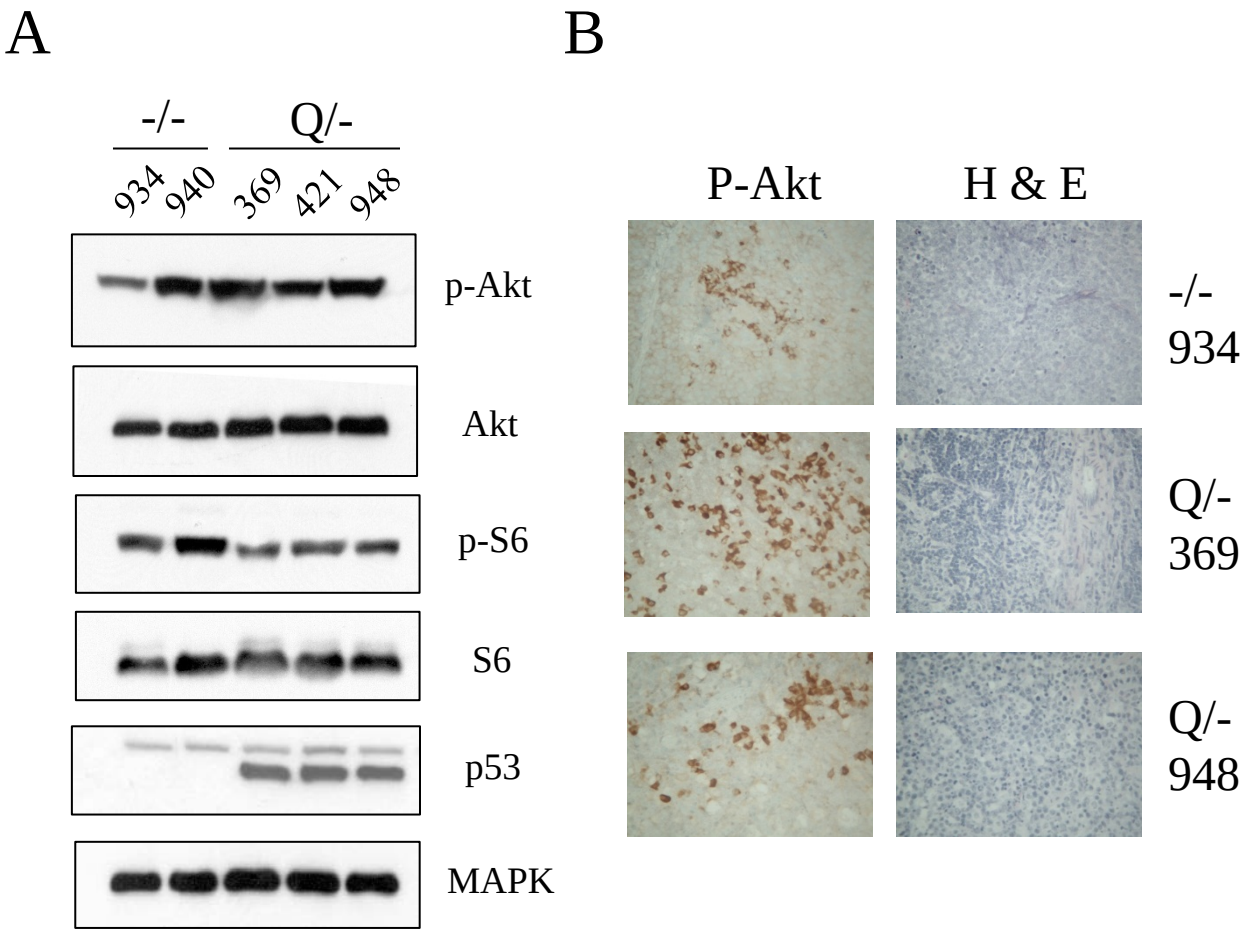

Figure 20. T-lymphoma cell lines derived from -/- and Q/- mice display similar signaling through the Akt pathway.

A. Protein lysates from T-lymphoma cell lines in tissue culture from -/- and Q/- mice were blotted for p-Akt, total Akt, p-S6, total S-6, and MAPK.

B. Tissue section of T-lymphoma infiltrates in the spleen from cell lines 934 (-/-), 369 (Q/-), and 948 (Q/-) injected into nude mice were stained for p-Akt.

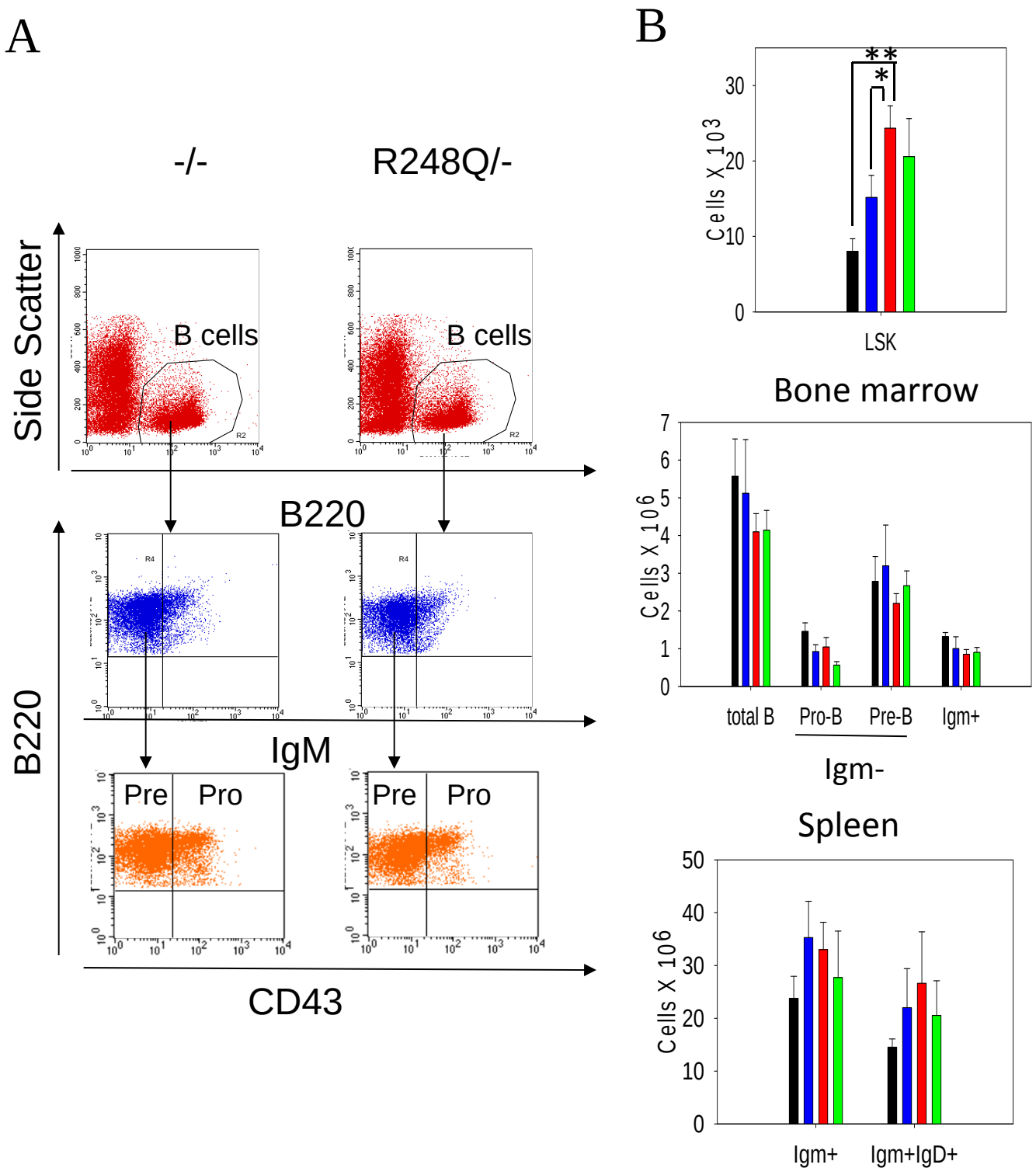

Figure 21. Expression of R248Q results in expansion of LSK cells but does not perturb B-cell development..

A. Gating strategy for analysis of B-cell subpopulations from bone marrow.

B. Quantitation of LSK (Lin-Sca1+c-kit+) and B-cell subpopulations from wild type(n=6), null(n=6), R248Q/-(n=6) and G245S/- mice. Averages +/- SE is shown for each cell population, * p<.05 ** p<.01.

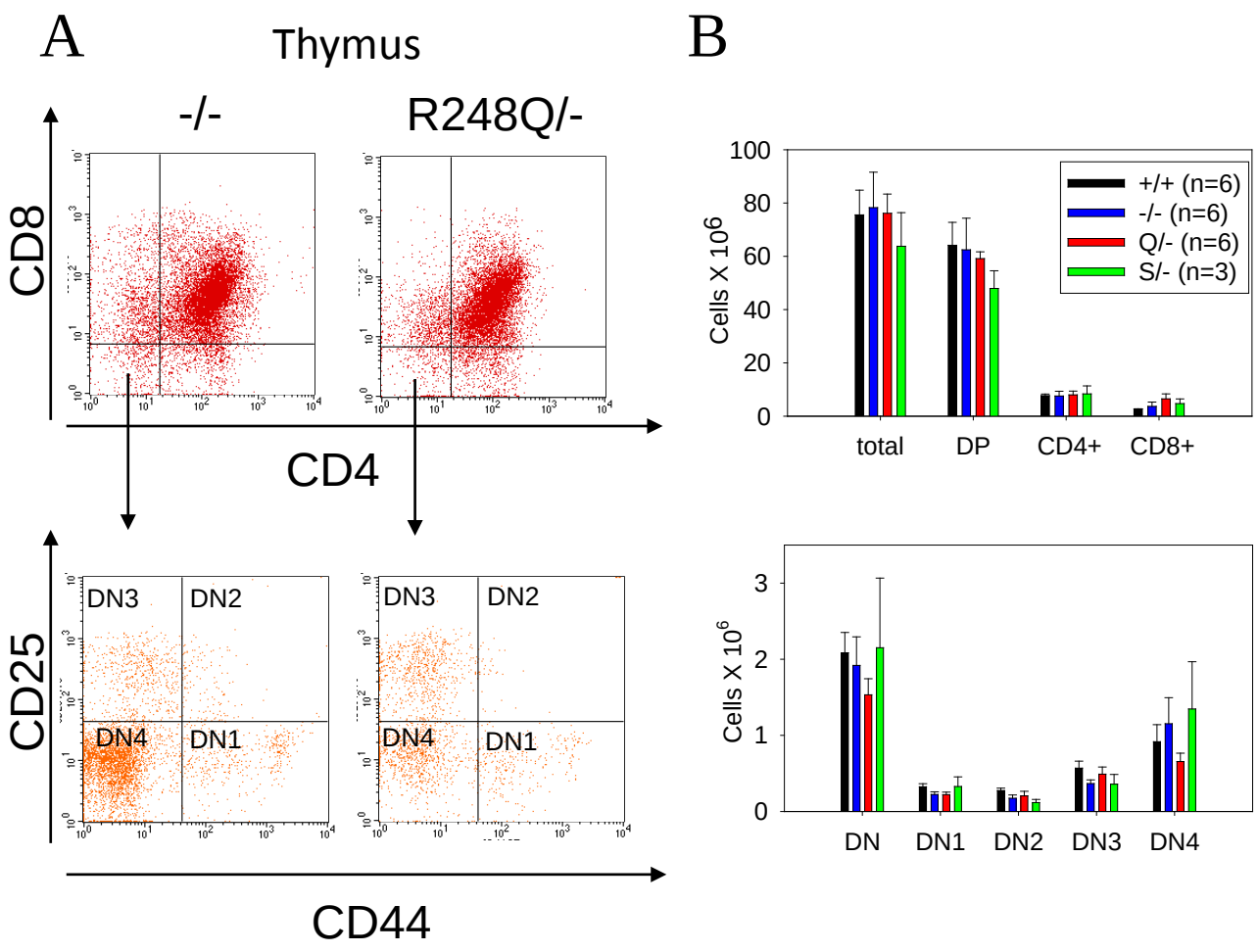

Figure 22. p53R248Q and G245S do not perturb T-cell development.
A. Gating strategy for analysis of t-cell subpopulations from thymus.
B. Quanitations of T-cell subpopulations from wild type(n=6), null(n=6), R248Q/-(n=6) and G245S/- mice. Averages +/- SE is shown for each cell population.

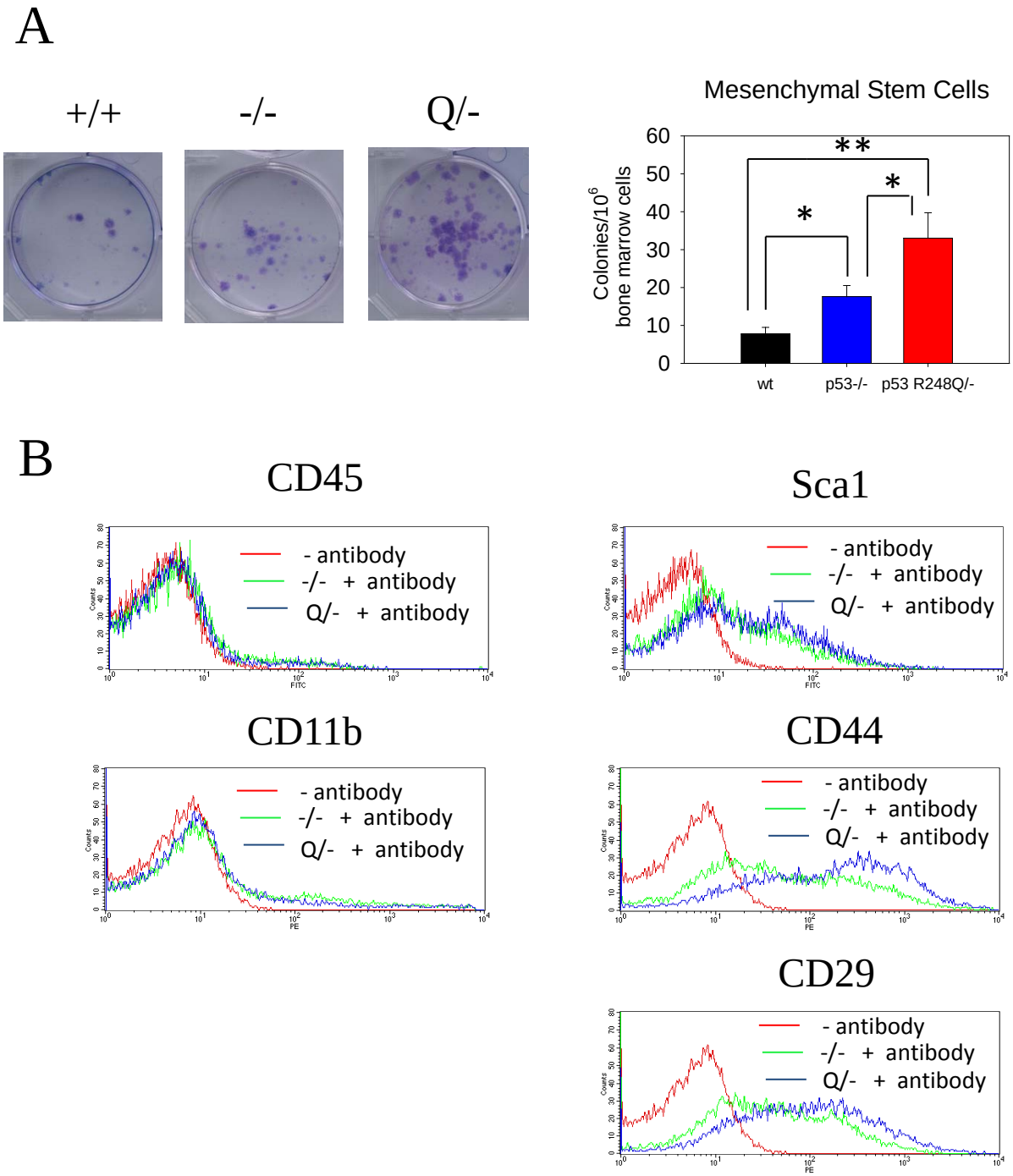

Figure 23. Expression of mutp53 R248Q results in expansion of mesenchymal stem cells and have expression of MSC markers.

A. Bone marrow cells of -/- and Q/- were plated at 1 X 10^6 cells and at the end of two weeks, the number of adherent fibroblast colonies were enumerated.

B. Adherent fibroblast colonies from the bone marrow -/- and Q/- mice were probed for *left*, expression of CD45 and CD11b (hematopoetic markers) and right, expression of Sca1, CD44, and CD29.

.

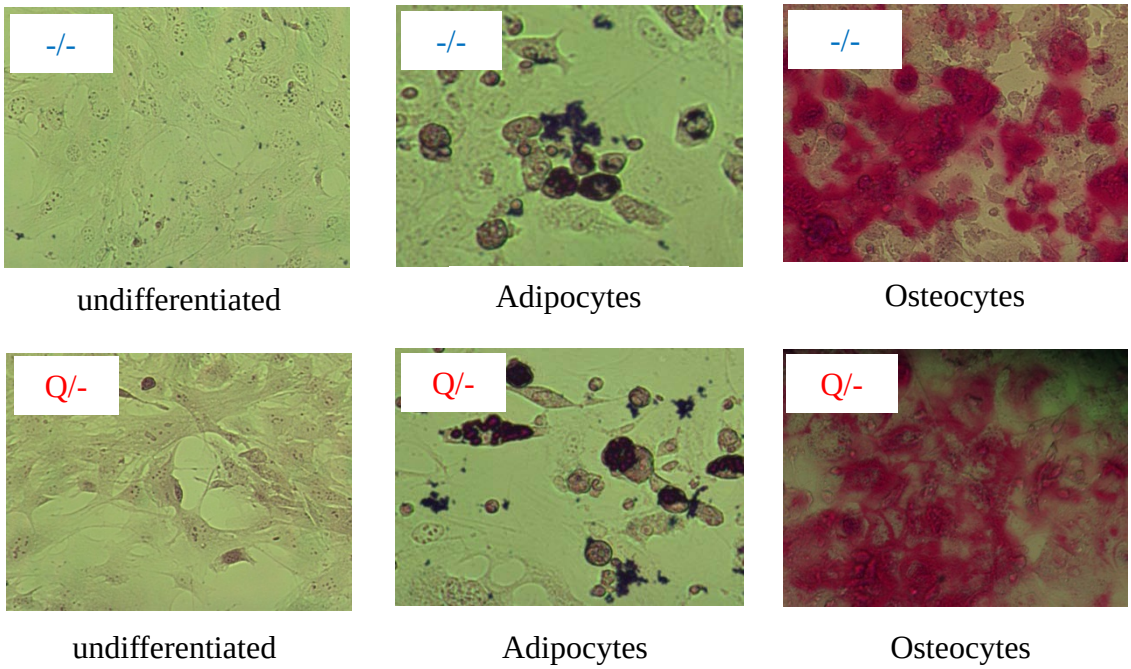

Figure 24. -/- and Q/- MSCs show similar differentiation into adipocytes and osteocytes.
MSC colonies from -/- and Q/- mice were plated in *left*, expansion media, *middle*, adipocyte differentiation media, and *right*, osteocyte differentiation media. At the end of two weeks, adipocytes and osteocytes were stained with oil Red O and Alizarin Red S, respectively. Wild type MSCs underwent senesence after two weeks and could not be differentiatied.

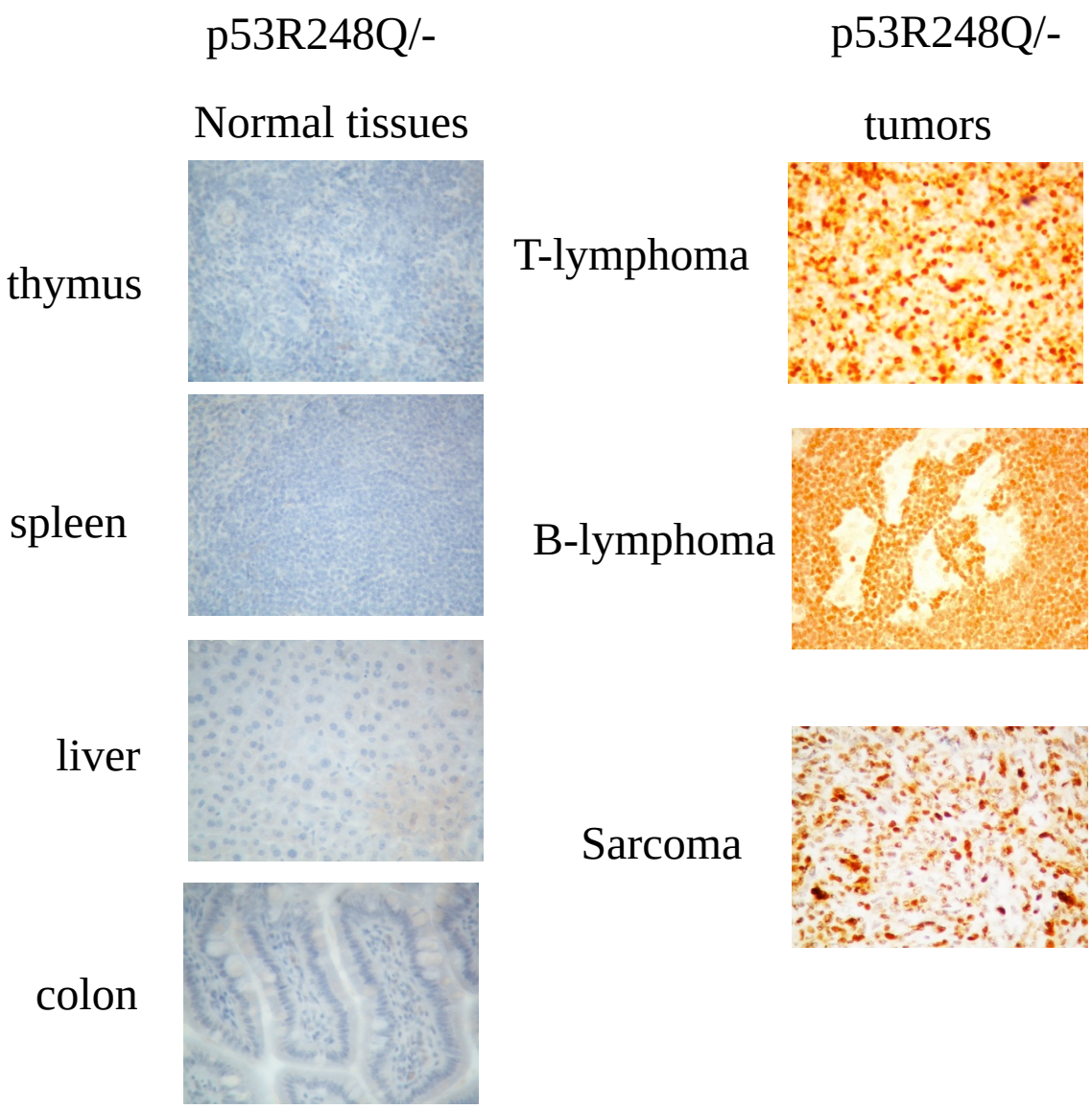

Figure 25. The mutp53 R248Q protein becomes stabilized only in tumor tissues but not in normal tissues.
Normal tissues *left* and different tumors *right* from R248Q/- mice were stained for the presence of stabilized p53 protein. Identical results were seen for G245S/- mice.

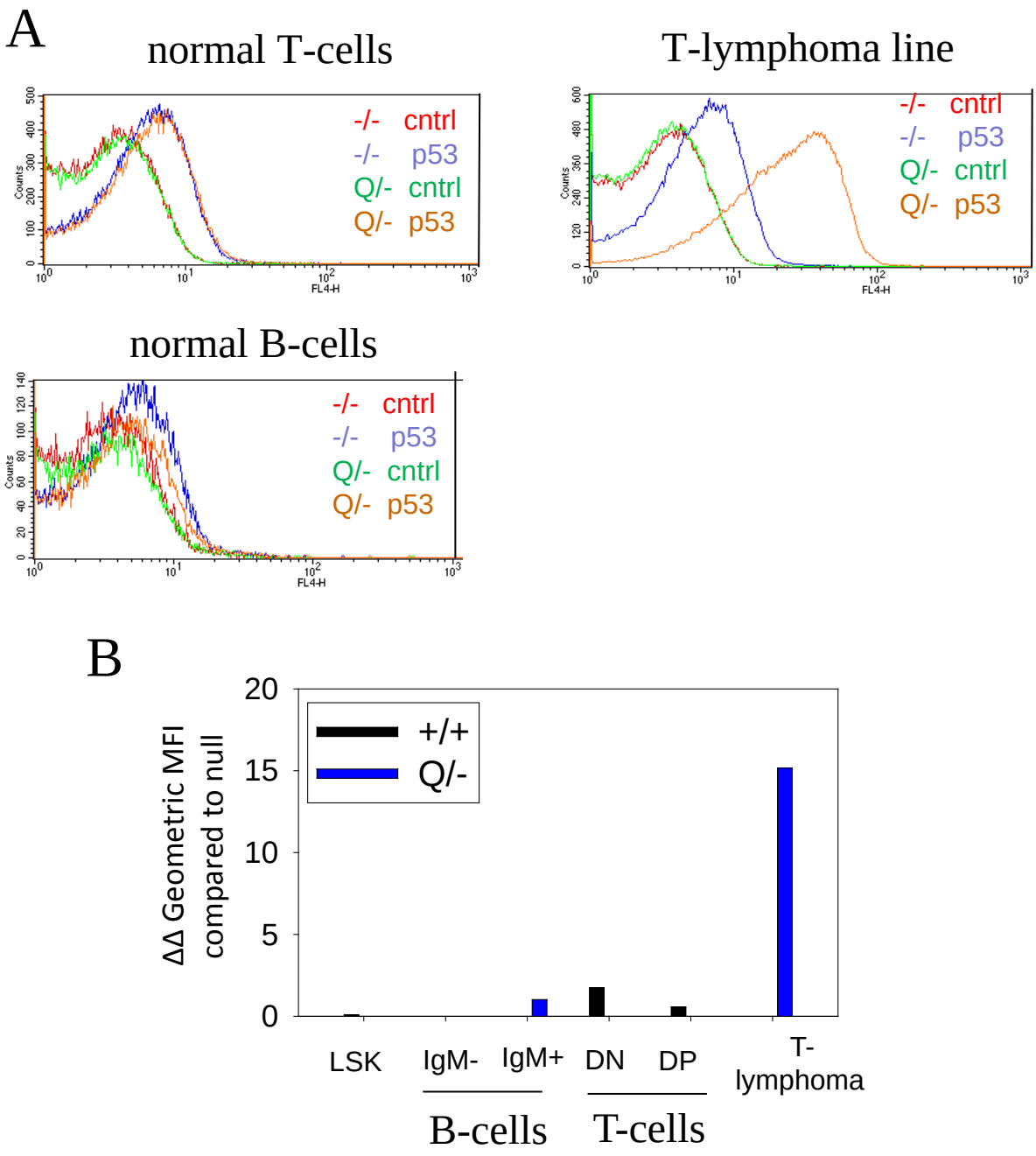

Figure 26. The mutp53 R248Q protein becomes stabilized only in tumor tissues but not in normal tissues.

A. Histograms of p53 -/- and R248Q/- normal B-lymphocytes, T-lymphocytes and malignant T- lymphoma cells with and without intracellular staining for p53 by FACS analysis. Normal wild type cells were also measured for p53 levels (not shown) for quantification in **B**.

B. Quantification of the changes in geometric mean flourescence intensity (MFI) measured in **A** for individual cell populations after correction for background staining of -/- cells.

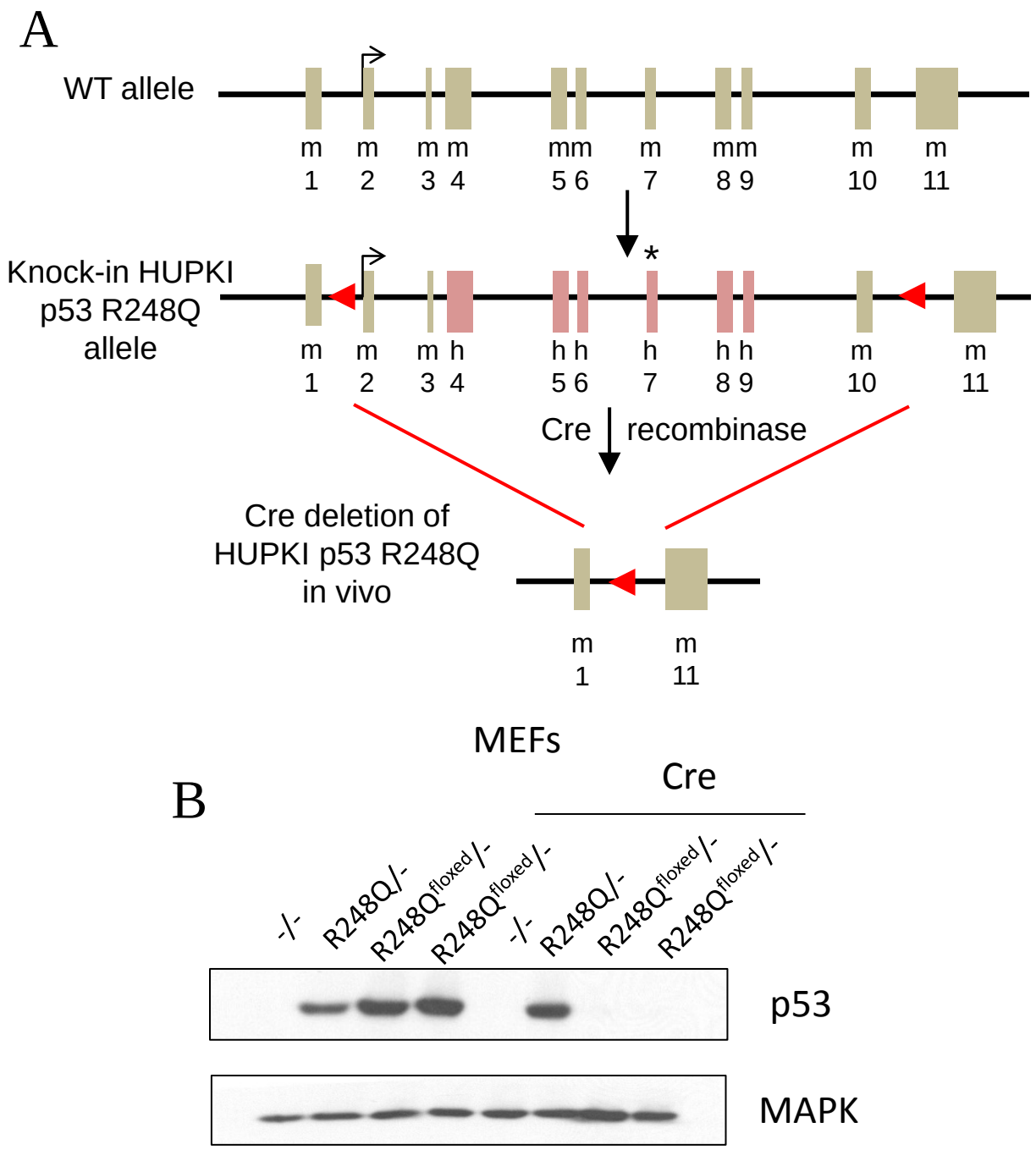

Figure 27. Mutp53R248Q can be removed using a Cre-loxed based approach.
A. *Top*, wt allele in germline configuration. *Middle* , Configuration of the R248Q^{floxed} mice in the absence of Cre. Bottom, R248Q^{floxed} allele configuration in the presence of Cre expression. m, mouse, h, human, Red triangles, loxP sites.
B. MEFs were derived from p53 -/-, R248Q/-, and R248Q^{floxed} /- mice , and infected with Cre. Lysates were prepared and probed for p53 and MAPK (loading control).

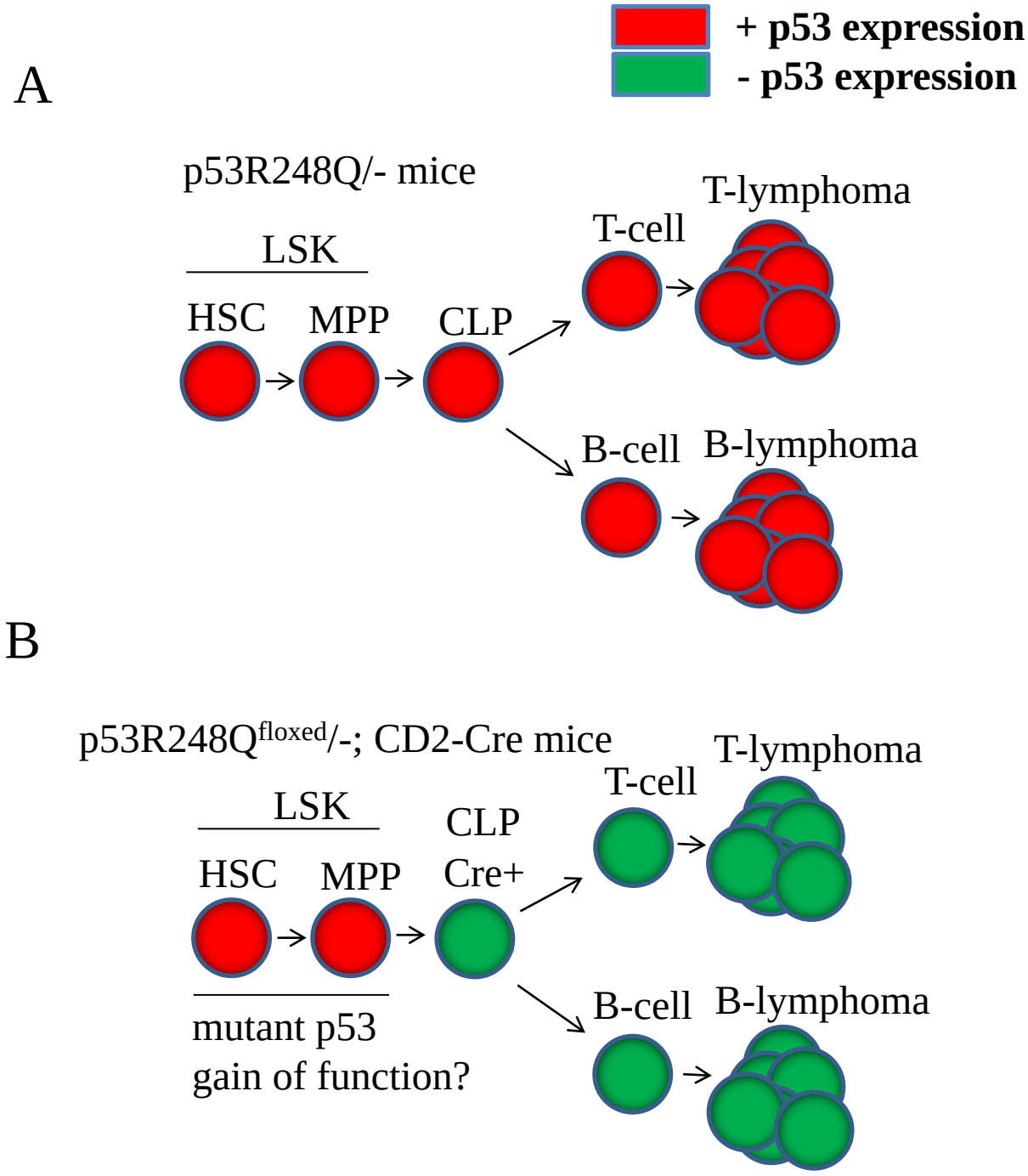

Figure 28. mutp53R248Q can be expressed in LSK cells and removed from B and T cells.

A. p53 expression in T and B cell populations in the p53R248Q/- mouse model.

B. p53 expression in T and B cell populations in the p53 R248Q^{floxed} /-; CD2-Cre mouse model.

p21

5’-CCTGGTGATGTCCGACCTG-3’

5’-CGGGACCGAAGAGACAACG-3’

PUMA

5’-AGCAGCACTTAGAGTCGCC-3’

5’-CCTGGGTAAGGGGAGGAGT-3’

HPRT

5'-GGGGGCTATAAGTTCTTTGC-3'

5'-TCCAACACTTCGAGAGGTCC-3'

Figure 29. Primers used in real-time PCR experiments.

Thymocyte stain	cell populations
1. CD4-PE CD8-FITC TER119-APC B220-APC Mac1-APC	**DP** APC-, PE+, FITC+ **DN** APC-, PE-, FITC-
2. CD4-APC CD8-APC TER119-APC B220-APC Mac-1-APC CD25-FITC CD44-PE	**DN1** APC-, PE+, FITC- **DN2** APC-, PE+ FITC+ **DN3** APC-, PE-, FITC+ **DN4** APC-, PE-, FITC-
Bone marrow stain	
1. B220-PE Mac1-PE Gr1-PE CD3-PE TER119-PE c-kit-APC Sca1-FITC	**LSK** PE-, APC + FITC +
2. B220-PE CD43-APC IgM-FITC	**Total B-cells**- PE+ **Pro-** PE+, APC+, FITC- **Pre**- PE+, APC-, FITC- **Immature**- PE+, FITC- **Mature-** PE+, FITC+
Spleen stain	
1. B220-PE CD43-APC IgM-FITC	**Total B-cells**- PE+ **Pro-** PE+, APC+, FITC- **Pre**- PE+, APC-, FITC- **Immature**- PE+, FITC+ **Mature-** PE+, FITC-
2. IgM-FITC IgD- PE	**Igm+,IgD+** FITC+, PE+

p53 intracellular stainings

Thymocyte stain	cell populations
1. CD4-PE CD8-FITC p53- Alexa R-647	**DP** PE+, FITC+ **DN** PE-, FITC-
Bone marrow stain	
1. B220-PE Mac1-PE Gr1-PE CD3-PE TER119-PE c-kit-PerCP-eFluor710 Sca1-FITC p53- Alexa R-647	**LSK** PE-, APC + FITC +
2. B220-PE IgM-FITC p53- Alexa R-647	**Total B-cells**- PE+ **Immature**- PE+, FITC- **Mature**- PE+, FITC+

Figure 30. Listing of antibodies and gating for indicated subpopulations in development experiments.